UNIVERSIDAD DE CANTABRIA

Departamento de Ciencias y Técnicas
del Agua y del Medio Ambiente

Numerical modeling of the global wave climate variability and associated environmental and technological risks

A Doctoral Thesis by: Borja González Reguero

Advisors: Iñigo J. Losada and Fernando J. Méndez

Santander, December, 2012

Chapter 5
Environmental Risks

"Sometimes it takes a natural disaster to reveal a social disaster"

Jim Wallis, evangelical writer and political activist

5.1 Introduction

Coastal zones face nowadays different problems and impacts both from anthropogenic and climatic stressors. Changes in wave climate and rising sea-levels may result in coastal impacts such as erosion and flooding, exacerbating current vulnerability. Prediction of shoreline erosion and storm-surge flooding is essential for coastal planning and management.

Sea-Level Rise (SLR) is one of the greatest drivers of impacts of climate change in coastal zones. The panorama described in recent studies is not particularly optimistic about SLR this century (e.g., [Meehl et al., 2007, Pfeffer et al., 2008, Vermeer and Rahmstorf, 2009, Woodworth et al., 2009, Church and White, 2011]). SLR is not however the only climatic factor with potential impact in coastal zones. Changes in the wave climate together with extreme total sea levels may induce coastal impacts which must be taken into account ([IPCC, 2007a, Nicholls, 2011]).

On a global context, the coastal management practices are shifting towards using a risk based approach for managing coastal inundation and beach erosion hazards. Therefore, it has become increasingly important to include probability in assessing the coastal socioeconomic and environmental impacts of increased risk of flooding and changes in storm severity, frequency and tracking, which in an end induce changes in the wave climate. In this work, a new approach is developed for assessing risk due to climate change in coastal areas. The method is tested and applied along a highly variable (over 72,000 km) reach of the Latin America and the Caribbean coast.

Consequently, the focus of this chapter lies on an assessment of the coastal flooding and erosion risks for the region of Latin America and the Caribbean, a region which presents several characteristics which make it particularly vulnerable. Before proceeding to the evaluation of the impacts and risks, a brief overview on the importance of the coastal zones, the impacts associated with a changing climate and the particularities of the LAC region are provided. Some of the main impacts of a changing wave climate and rising sea-levels upon the LAC coastal region will also be described and studied in detail in section 5.2 which, combined with the vulnerability and exposure of the coast, provides a holistic vision of the coastal zone problems. Section 5.3 builds on the latter to evaluate the risks, and finally, section 5.4 outlines the main conclusions and results.

5.1.1 What is the Coastal Zone?

The coastal zone, where land meets ocean, is one of the most dynamic natural systems. Here, the three main components of our planet—the hydrosphere, the lithosphere, and the atmosphere—meet and interact, forming interconnected systems. According to the IPCC-AR4, "coastal systems are considered as the interacting low-lying areas and shallow coastal waters, including their human components. This includes adjoining coastal lowlands, which have often developed through sedimentation during the Holocene (past 10,000 years), but excludes the continental shelf and ocean margins (and inland seas)".

Coastal systems are also part of the larger marine ecosystems that include coasts and open ocean areas. They are of great ecological and socioeconomic importance since they sustain economies and provide livelihoods through fisheries, ports, tourism, and other industries. They also provide ecosystem services such as regulating atmospheric composition, cycling of nutrients and water, and waste removal. These areas have also been centers of human settlement since perhaps the dawn of civilization, and have cultural and aesthetic values as well.

Coastlines are also among the most populated regions. Nearly half of the world's major cities are located within 50 km from the coast, and coastal population densities are 2.6 times greater than those of inland areas.

The continuous area along the coast that is less than 10 meters above sea level represents 2% of the world's land area but contains 10% of its total population (i.e. over 600 million people) and 13% of its urban population (around 360 million people). Almost two-thirds of the world's cities with more than 5 million inhabitants fall in this zone, partly at least. Besides, low-income and lower-middle-income nations have a higher proportion of their urban population in this zone than high-income nations. Additionally, the least developed nations, on average, have nearly twice the proportion of their urban population in this zone, compared to high-income nations ([McGranahan and Anderson, 2007, Satterthwaite et al., 2009]).

5.1.2 The coastal zones in a changing climate

The Intergovernmental Panel on Climate Change (IPCC) in their fourth assessment report (AR4) states: *"...coasts are projected to be exposed to increasing risks, including coastal erosion, due to climate change and sea level rise. The effect will be exacerbated by increasing human-induced pressures on coastal areas" (very high confidence). "Many millions of people are projected* *to be flooded every year due to sea-level rise by the 2080s. Those densely-populated and low-lying areas where adaptive capacity is relatively low, and which already face other challenges such as tropical storms or local coastal subsidence, are especially at risk. The numbers affected will be largest in the mega-deltas of Asia and Africa while small islands are especially vulnerable" (very high confidence).*

The IPCC Working Group II summary noted the following with very high confidence: *"Small islands have characteristics which make them especially vulnerable to the effects of climate change, sea level rise and extreme events".* And also awares: *"Sea-level rise is expected to exacerbate inundation, storm surge, erosion and other coastal hazards, thus threatening vital infrastructure, settlements and facilities that support the livelihood of island communities".*

Finally, let consider that: *"Tourism is the major contributor to GDP and employment in many small islands. Sea-level rise and increased sea water temperature will cause accelerated beach erosion, degradation of coral reefs and bleaching. In addition, loss of cultural heritage from inundation and flooding reduces the amenity value for coastal users. Whereas a warmer climate could reduce the number of people visiting small islands in low latitudes, it could have the reverse effect in middle and high latitude islands. However, water shortages and increased incidence of vector-borne diseases may also deter tourists"* ([IPCC, 2007b]).

Under this scenario, climate change is one of the greatest threats to human lives and livelihoods in coastal regions all over the world. Coastal areas figure among the most vulnerable of all environments to global climate change. Projected impacts from global warming include rising sea-levels, stronger tropical cyclones, larger storm surges, increasing sea surface temperatures, and as the oceans absorb more of the carbon dioxide from human activities, growing acidification of surface waters. For coastal ecosystems and communities, the repercussions could be considerable, thereby threatening the livelihoods, health, and welfare of millions of people.

More frequent and severe storms can inundate low-lying coastal zones, destroying infrastructure and displacing populations. Higher water levels and larger wave surges can contribute to accelerated shoreline erosion and retreat. Mounting sea levels can also exacerbate saltwater intrusion into the rivers and aquifers that furnish freshwater. Warmer water temperatures and acidifying oceans can degrade the ecology of coral reefs and threaten the artisanal and commercial fisheries that nourish many seaboard communities. Finally, the climate threats to coastal regions also reverberate well beyond the shoreline.

Countering such risks will present both opportunities for international cooperation and possibilities for international conflict. Many of the coastal countries most vulnerable to global warming have contributed little to world emissions of greenhouse gases, and many possess limited capacity and few resources to counter or cope with prospective climate damages. These nations will require international assistance, technical, financial, and institutional, to enable them to adapt to and rebound from the looming greenhouse impacts that they cannot avoid.

It is difficult to estimate with any precision how many people are at risk from the increased frequency and intensity of extreme-weather events and the sea-level rise (SLR) that climate change will bring. The first detailed analysis on the number and proportion of urban dwellers (and total population) living in the low-elevation coastal zone was published recently in [McGranahan and Anderson, 2007]. One estimate has suggested that 10 million people are currently affected each year by coastal flooding and that such figures will increase under all climate-change scenarios ([Nicholls, 2004]). The problems with coastal flooding will obviously be much more serious if certain potentially catastrophic events, whose probability is uncertain, were to happen, for instance the accelerated melting of Greenland's ice sheet or the collapse of the West Antarctic's one.

Many small islands are at risk from extreme weather events and a range of other environmental hazards, independent of climate change, but which are likely to be exacerbated by climate change. Many small islands are at risk from coastal, river and rain-induced flooding, tropical cyclones and storm surges ([Tompkins et al., 2005]). Small islands, by definition, have limited physical size and much of their land area close to coasts. This usually means limits for adaptation options, for instance by developing new activities or moving vulnerable settlements away from coasts. Many small islands also have high levels of natural-resource exploitation and urbanization occurring in zones at high risk from disasters. Often coastal development increases risks, by way of example as mangroves and wetlands are displaced by residential or tourist developments. Many of the larger-population small island nations also have cities with a significant proportion of their population living in informal or illegal settlements, often on sites at risk from flooding or landslides. Many are already facing serious freshwater shortages, and climate change may exacerbate this situation.

Finally, studies of the cost of SLR on coasts have been based mainly on the economic loss to the areas flooded ([Yohe et al., 1999]), but it has been shown that this cost might be underestimated because it fails to take account for the damage associated with coastal flooding affecting properties not flooded permanently above sea-level ([West et al., 2001, Michael, 2007]). SLR will increase the risk of temporary flooding to properties a priori at sufficient elevation for them to be affected nowadays. Changes in the wave climate and the storm surges will also contribute to higher flooding and erosion rates. This makes a quantitative assessment of the potential impacts in coastal areas increasingly important.

5.1.3 Coastal areas of Latin America and the Caribbean, development and adaptation to climate change

Urban settlements are not only growing sources of greenhouse gases but are also hotspots of vulnerability to floods, heat waves, and other hazards that climate change is expected to aggravate ([Hardoy and Pandiella, 2009, Satterthwaite et al., 2009, Martine, 2009, Hardoy and Lankao, 2011]). These roles create unique challenges and opportunities for urban mitigation and adaptation responses, and for mainstreaming them with development goals ([Hardoy and Pandiella, 2009, Satterthwaite et al., 2009]). The region of LAC presents specific features in this regard.

Urban and demographic development conditions vulnerability and the capacity to adapt to the impacts of climate change in general and in particular on coasts. In the region of Latin America and the Caribbean (LAC), the population grew by 7% between 2006 and 2012, 4% on the Caribbean islands and, moreover, the growth rate is expected to hold between 0.7 and 0.9% per annum in the coming decades. Should that be the case, the region's population would rise by 21.8%, 12.3% in the Caribbean, by the year 2040 ([ECLAC, 2011]). Population concentration in urban areas is also expected to increase, shifting capacity to adapt. The urban population rose from 79.6 to 81.5% between 2005 and 2010 and is forecasted to reach 86.9% by 2040. Particularly in the Caribbean, it will rise from 69.3 to 79.1% to the same horizon, with a faster acceleration than in the rest of the region. Greater population density will cause higher risks to the populations of the region because of the lack of infrastructures, services and appropriate institutional frameworks ([Dodman, 2009]). The situation is aggravated by high levels of poverty ([Smolka, 2008]) and the regional economy's heavy dependence on natural resources and tourism ([Magrin et al., 2007]). These characteristics make this region especially sensitive to meteorological and environmental changes and stresses ([Dodman, 2009, Smolka, 2008, Hardoy and Pandiella, 2009, Hardoy and Lankao, 2011, ECLAC, 2011]).

In Latin America, the coastal plain of north-east South America is very low-lying, generating risks for major settlements from north-east Brazil to Venezuela. The coastal zone of Guyana holds 90% of national population and 75% of the national economy; its highest point is 1.5 meters above sea-level with much residential land, including the capital Georgetown, below high-water sea level. In many Caribbean states, between 20 and 50% of the population resides within the low-elevation coastal zone ([Satterthwaite et al., 2009]). Although calculations of costs are controversial, the impacts of hurricanes, floods, extreme temperatures, landslides and other hydrometeorological disasters can exceed the Gross Domestic Product in more than 50% in less developed and more natural resource dependent regions as in LAC ([Dodman and Satterthwaite, 2009]).

In particular, many small island nations in the Caribbean face high risks from cyclones. Many of them also have a high proportion of their economy and urban population in urban centers on the coast – for instance, close to two-thirds of the population in the Caribbean lives in urban areas. Most of these small islands have economies and much of their populations' livelihoods at risk from the disruptions that extreme-weather events bring, including a reliance on imports for many essential goods. Many also rely heavily on international tourism ([Satterthwaite et al., 2009]).

Although some LAC countries and regions are taking actions to adapt, including policies to control settlement in dangerous locations, many places continue to have difficulties. Among other needs, and especially from a management point of view, it has been made clear that there is a lack of information and data on hazards, locations at risk and the most exposed and vulnerable populations ([Hardoy and Lankao, 2011]). Coastal impacts often affect low-income groups living in high-risk zones with fewer protective infrastructures ([Hardoy and Lankao, 2011] and references therein). Coastal zones are therefore critical for population settlement.

This work tends to rise awareness about the critical areas and the risks associated with changes in the wave climate and sea-levels. It aims a pioneer definition of some coastal impacts in the region by identifying the areas most likely to be affected, through an analysis of risks which would ultimately provide an initial diagnosis of such problems in a consistent and homogeneous way for the entire region. These risks are analyzed using a methodology which integrates the probability of occurrence and the consequences for various levels of impact on coasts. The following risks are analyzed: (1) to population and infrastructures from rising sea-levels, both under continuous currently detected variability and for a 1 m SLR scenario, (2) storm-related coastal flooding, taking account of the different sea-level components and (3) beach erosion from changes in both sea-levels and changing wave directions, from the standpoint of two beach functions: as a coastal protection infrastructure and as a major tourist asset.

5.2 Impacts in the coastal zones of Latin America and the Caribbean

5.2.1 Identifying the hazards

Erosion is a global problem for coasts and human settlements. It is estimated that at least 70% of the world's fine-sediment beaches are receding ([Bird, 1985]). There are both short-term and long-term causes of shoreline erosion. It may be natural or human-induced. The most common type of short-term erosion is provoked by storms which can produce rapid and dramatic erosion. Natural causes of erosion are in the short-term: storm waves, storm surge, overwash, flooding, rip currents, etc. Long-term erosion may be less noticeable, but may ultimately have more sever consequences. In the long-term, factors that may induce long-term erosion are: sea-level rise, decreased sediment supply, littoral transport lost, sustained changes in waves intensity and direction, flooding or subsidence, among others. Anthropogenic causes are often related with navigation inlets, coastal structures, dams, aquifer exploitation and dune destabilization. [USACE, 2002] can be consulted for further explanation on these and other coastal problems.

Because of the concentration of population and infrastructures in the planet's coastal zones, possible accelerating SLR and changes in wave climate will make beach erosion a further problem to be dealt with ([Nicholls, 1998]) and that surely should be managed. Coastal erosion affects not just beaches but also infrastructures like roads or railroads built near the coast. It has already been shown that, in the LAC region, part of the coastal express highways connecting the Rio de la Plata with the tourist resorts is in danger of flooding from SLR ([Fiore et al., 2009]).

Wind-driven waves and storms are seen as the primary drivers of short-term coastal processes on many European coasts ([Smith, 2001]). Higher waves and increased storm-surge elevations would have important potential consequences, such as enhanced erosion and flooding in estuaries, deltas and embayments ([Flather and Williams, 2000, Lionello et al., 2002, Tsimplis et al., 2005, Woth, 2005]).

Sea-Level Rise (SLR) has promoted erosive tendency for coasts, widely observed worldwide ([Bird, 1985, Bird, 2000]). But a sea-level change is not the unique factor affecting coastal erosion. Beaches in New South Wales, Australia, has been shown to rotate induced by a shift in wave energy direction with the ENSO phenomenon ([Ranasinghe et al., 2004]). Also, erosion in Northwest USA has been detected associated to this climatic pattern, but in this case the responsibility lies on the increase of the mean sea-level during El-Niño events ([Komar et al., 2000, Allan and Komar, 2006]) rather in the affection to the wave climate (as can be seen in Chapter 3). A dual dimension of the problem arises since both climatic variability and long-term changes coexist and more than one variable, sea-level and wave climate in this case, contribute, with different relative importance, to the final impact.

For an early but clarifying study on the engineering impacts of SLR, [CEI-RMSL, 1987] can be consulted. It provides an useful basis for design calculations and policy decisions that must take changes in water levels into account, examining: (1) shoreline responses, (2) consequences for engineering works and built facilities, (3) methods for protecting structures from erosion and flooding, and adapting to shoreline retreat, and (4) the need of new technologies for mitigation.

Global mean sea-level has risen at an average rate of 1.7 ± 0.5 mm/yr during the twentieth century ([IPCC, 2007a]). Subsequent to the IPCC AR4 report in 2007, there have been several research estimating SLR from 1.9±0.4 mm/yr ([Church and White, 2011]) to 3.2±0.4 mm/yr ([Merrifield, 2009]). Whether an acceleration is occurring or not is an issue under current research (e.g., [Douglas, 1992, Cazenave, 2008, Church et al., 2010, Rignott, 2011, Houston and Dean, 2011, Rahmstorf and Vermeer, 2011, De Santis et al., 2012]. For the coming future, several studies have proposed estimates of SLR for the end of the present century ([IPCC, 2007a, Rahmstorf, 2007, Pfeffer et al., 2008, Horton et al., 2008, Vermeer and Rahmstorf, 2009, Jevrejeva et al., 2010]). Other researchers defend that global SLR is accelerating in a way strongly correlated with global temperature ([Rahmstorf, 2007, Vermeer and Rahmstorf, 2009]) and the future figures could easily exceed the AR4 scenarios. Although the different authors use different physical bases, a rise greater than 2 m seems to be not feasible.

On the other hand, the sometimes devastating impact of extreme sea-levels heighten awareness property damage and loss of life from coastal inundation. North Sea, coast of Bangladesh or the Gulf of Mexico with hurricanes Rita and Katrina are examples of coastal regions where extensive damage to infrastructure and environment have occurred.

Low-lying areas are already dependent on flood risk strategies of some type such as flood defenses, drainage or construction planning. Hurricane Katrina showed in New Orleans, in 2005, the devastating effect of failure in flood defenses (see images in Figure 5.1). Rising mean sea-level and changes in storminess are well accepted that will exacerbate these risks, but the actual consequences of SLR remain uncertain and contested despite the threats ([Nicholls, 2011]).

Figure 5.1: New Orleans in 2005 after the hurricane Katrina. Source: Wikipedia.

Flooding is, however, a common effect of coastal storms due to a combination of tides, mean water levels, storm surge and waves setup. Low-lying coastal areas are of special concern for this type of impact. Coastal flooding is also intimately related with storm erosion. It is a factor contributing to erosion but many coastal sections are protected against flooding by elements under erosion. Such are the cases of beach/dunes systems or sand barriers that if resulted in breaching, most severe flooding can occur behind them.

Episodic events of flooding, associated with extreme water levels, differ from permanent flooding, commonly known as *inundation* or *submergence*, where the responsible is the rising sea-level. The time scale of occurrence is of longer-term in this case. Climate patterns can also affect mean sea-level and cause, although not permanently, a sustained rise in sea-level for long periods (months to years).

5.2.2 Defining the hazard and the vulnerability in Latin America and the Caribbean

5.2.2.1 Hazards

In this chapter the analysis focuses on the following hazards:

1. *Coastal inundation*: the permanent flooding of the coast from SLR.
2. *Flooding*: temporary coastal flooding events, generally associated with storm events, and that are caused by the joint effect of the different sea level components: Mean Sea-Level (MSL), Sea-Level Rise (SLR) in the long-term, astronomical tide (AT), storm surge (SS) and wave set-up.
3. *Coastal erosion*: particularly beach erosion due to SLR and changes in the dominant wave energy direction.

The methods for the calculation of the probability of the hazard varies according to the type of impact studied, in this work determined by:

1. Extrapolation of past long-term trends: for erosion and flooding to the target year 2040 upon the assumption that changes observed in recent decades may continue in the foreseeable future preserving the statistical uncertainty for future values.
2. Extreme analysis: obtaining the variation of probability of exceeding a given return period, in the case of extreme flooding events associated with the 50 year value.
3. Assumption of a given a priori scenario, for a case which is deterministic and spatially homogenous (i.e. without considering its probability of occurrence), associated with a given SLR of 1 m.

Table 5.1 sets out the dynamics involved for each coastal impact, the impacts considered and the techniques used to evaluate the probability in each case. More trends and impacts for the region can be found in [CEPAL, 2012b] and [CEPAL, 2012a].

HAZARD	DYNAMICS	HAZARD PROBABILITY METHOD
Inundation (permanent flooding)	SLR & 1 m SLR scenario	Trend extrapolation
Flooding (temporal events)	SLR + AT + SS + Wave set-up	Extreme analysis (50 yr return period)
Beach Erosion Changes in wave direction	SLR	Past long-term trend extrapolation to 2040

Table 5.1: Description of the coastal hazards or impacts dealt with in this work, changes in the dynamics generating them, and the method for calculating the probability of the hazard for each case

DATA	SOURCE OF INFORMATION
Land uses	Land Cover & Global Cover
Population density	CIESIN
Roads and railways	Digital Chart of the World
Beach typology	Google Earth Images ©
Urban coastline	Google Earth Images ©
River outlets	Google Earth Images ©

Table 5.2: Vulnerability data analyzed to evaluate risk of flooding and erosion and the associated sources of information.

5.2.2.2 Vulnerability

The vulnerability and exposure of the region under study is described using various data sources (Table 5.2). The geo-referenced data are analyzed using Geographical Information Systems (GIS), specifically the "ArcGis 9.2" software © and its extensions "Spatial Analyst" and "3D Analyst".

Geospatial analysis of the data for processing and calculating vulnerability has taken the following steps:

1. Preprocessing of the base data; clipping the information to the coastal strip and re-projecting all the data layers to a common projection that conserves distances and area.

2. Delimitation and drawing of the coastal area to be evaluated, and definition of an overall line of coast for the area of study.

3. Creation of analysis units from the target coastline (henceforth referred to as study units), forming the basic unit where results are obtained for hazards, vulnerability and risks.

4. To obtain the flooding masks from 1 to 10 m of elevation in each unit of study, using the Digital Terrain Model (DTM).

5. To compute the spatial distribution of variables.

6. Calculation of the area affected for each variable at the various possible flooding levels (1 to 10 m heights).

Variables	Time span	Time resolution	Spatial Resolution	Data source
Mean Sea Level (MSL)	1950-2009	monthly	Global, 1°	CSIRO
	Variable	hourly	Global, variable	Tidal Gauges (UHSLC)
Astronomic Tide (AT)	Harmonic constants	hourly	Global, 0.25°	TPXO
Storm Surge (SS)	1948-2008	hourly	LAC, 0.25°	Numerical Reanalysis
	variable	hourly	Buoys OPPE, NDBC-NOAA	
Waves	Variable	variable	variable	Sat. altimetry CSIRO
	1948-2008	hourly	Global and LAC, 0.5° to 0.25°)	Numerical Reanalysis

Table 5.3: The variables considered, temporal coverage, space-time resolution and source of information.

As seen, the risk evaluation requires discretization of the coast into sections or units of study to evaluate the terms of hazard, vulnerability and exposure. In line with the information available and the spatial scope of study, a working scale has been adopted of approximately 5 km on the coastline. Impact and risk calculations are thus representative of 5 km of coastline and 20 km landward. However, to show the results spatially, the 5 km units are aggregated at a 50 km scale. These study units have been generated in three stages:

1. The LAC coastline is divided into 5 km sections;
2. Once the 14,494 segments have been obtained, polygons are generated automatically which delimited the initial and final vertices of the line, covering 20 km landward;
3. Finally, the creation of the polygons is supervised using topological rules, to check possible errors in complex areas.

5.2.3 Data

5.2.3.1 Hazards

A wide variety of sources of information have been used, both instrumental and numerically modeled, to assess the diverse sea-level components and the wave climate n the LAC region. Table 5.3 summarizes the variables considered, the original sources and their spatial and temporal resolution. More trends for other variables in the region and further details can be found in [CEPAL, 2012b].

Sea-level data were taken from the Commonwealth Scientific and Industrial Research Organization (CSIRO) at `http://www.cmar.csiro.au/sealevel/sl_data_cmar.html`. These data provide monthly mean sea-level series in a mesh of spatial resolution 1° x 1° (longitude x latitude) between 65°S and 65°N, in the period from 1950 to present, although in this study 2008 is the last year considered in the analysis. Sea-level data between 1950 and 2001 were reconstructed using tidal gauges ([Church et al., 2004]), and for the period 1993-2009 the data come from altimetry from the TOPEX/Poseidon, Jason-1 and Jason-2/OSTM missions. The data are deseasonalized and the inverse barometer correction included, following the glacial isostatic adjustment correction.

Tidal data were obtained from the University of Hawaii's Sea Level Center (UHSLC) and used to compare the results of the AT and SS time series. These data are available on the Internet at `http://ilikai.soest.hawaii.edu/uhslc/rqds.html`. The data series are in hourly time resolution and the length of the register is variable, depending on each tide gauges station.

The astronomic tide data were generated on the LAC coast using the harmonic constants from the TPXO global tide model (version 7) developed by Oregon State University ([Egbert and Erofeeva, 2002]). The TPXO model assimilates data from the TOPEX/Poseidon missions and from tide gauges ([Ardalan and Hashemi-Farahani, 2007]) and is one of the most accurate global tide models (`http://www.esr.org/polar_tide_models/Model_TPXO71.html`). The database includes eight primary harmonic constants (M2, S2, N2, K2, K1, O1, P1, Q1) and two long- period (Mf and Mm), provided in a global mesh of 1,440 x 721 points, with 0.25° spatial resolution (`http://volkov.oce.orst.edu/tides/global.html`). These components were used to reconstruct the hourly astronomic tide series since 1948. The results were checked against the tide gauges in the zone; absolute errors were in any event less than 10 cm, so that the reconstruction of the astronomical tide is adequate for offshore depths. The distribution of astronomical tides reveals a large spatial variation in the region, from micro-tidal regimes in tropical latitudes to macro-tidal in the south of the continent (see [CEPAL, 2012b] for more information).

The meteorological tide, or Storm Surge (SS), was obtained numerically using the Regional Ocean Modeling System (ROMS; [Shchepetkin and MacWilliams, 2003]) at 0.25°x0.25° resolution, in a grid covering from 125°W to 20°W longitude and 61°S to 40°N latitude. The inverse barometer condition was used for the simulation. The atmospheric forcing (pressure and wind data) correspond to the NCEP/NCAR reanalysis. The results are hourly time series of storm surge in the period from 1948 to 2008, which were validated with instrumental tidal gauge data. Figure 5.2 shows the results of the validation for several tidal gauges in the zone. A good fit for both the statistical distribution and surge time series (not shown) is obtained. [Losada et al., 2012] or [Reguero et al., 2011]) can be consulted for further validation. It must be noted that the numerical modeling does not include hurricanes defining the SS extremes tail because the wind and pressure force from NCEP/NCAR reanalysis is insufficient to define them properly.

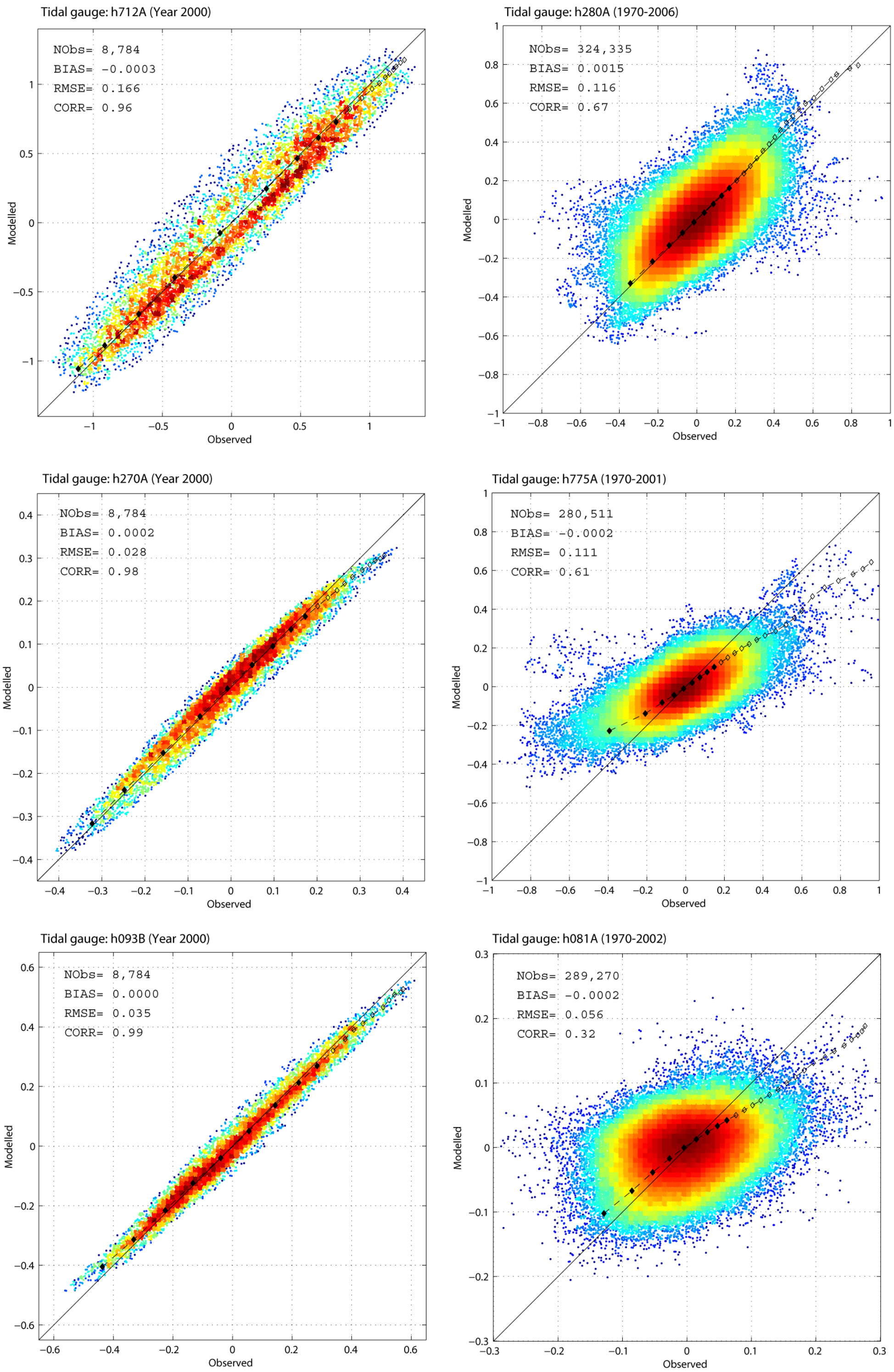

Figure 5.2: Validation of the reconstruction of the Astronomical Tide (left) and the modeled Storm Surge (right) with various regional tidal gauges in the study area. Scatter data and quantile distribution are shown. Values expressed in meters.

The wave heights measurements used for the analysis include altimeter data covering from the end of 1992 to 2009, with variable spatial and temporal resolution. They have been obtained from AVISO (`http://www.aviso.oceanobs.com/`) and corrected according to [Hemer et al., 2010]. Buoy data used comes from two sources: Puertos del Estado - Gobierno de España (`http://www.puertos.es/es/index.html`) and the NOAA agency National Data Buoy Center (`http://www.ndbc.noaa.gov/`).

Observations are complemented with numerical results. NCEP-NCAR reanalysis wind and ice cover fields ([Kalnay et al., 1996]) is used to make global waves simulations since 1948, with the Wavewatch III model ([Tolman, 2002a, Tolman, 2002b]) of resolution 1.5° longitude and 1° latitude (i.e. GOW wave reanalysis, see Chapter 2). Domains of greater spatial resolution were nested to the global grid design for the LAC region, with a total of three more detailed computational grids: two of spatial resolution 0.5ºx0.5º (longitude x latitude) for the Atlantic and the Pacific and one of 0.25°x0.25° for the Caribbean region. The results of the reanalysis are hourly time series of various statistical wave parameters. The numerical wave simulations were subsequently compared with buoy and satellite data. The numerical data were corrected with satellite data using the method of [Mínguez et al., 2011]. More details of results, validation and the corrections applied to this reanalysis can be found in [Reguero et al., 2012b] or in Chapter 2 of the present thesis.

5.2.3.2 Vulnerability and physical exposure

The area delimited by the units of study was used to find the Digital Terrain Model (DTM) of the coastal strip of interest. Using a DTM that covered the area of study continuously and uniformly was a key aspect. For this reason, the data employed were the Shuttle Radar Topography Mission (STRM v4), with 90 m horizontal resolution and 1 m vertically ([Farr et al., 2007]). The DTM reference is not uniform throughout the domain because zero height cannot be the same in micro and macro tidal zones where the tidal range may affect heights from 0 to 3 m (0 m taken as mean sea-level). It was thus considered that the zero topographical reference could be assumed to be that corresponding to percentile 95% of the AT series at each point.

Population density was taken from "Gridded Population of the World and the Global Rural-Urban Mapping Project" (GRUMP), with 1,000 m resolution and referenced to year 2000 ([CIESIN, 2005]). These data were analyzed at each elevation level to obtain the population distribution along the coasts studied. To define the uses of the land affected, data from the following sources were employed: (1) Global Land Cover ([Bartholome and Belward, 2005]) of the National Mapping Organizations (GLCNMO) and (2) GlobCover, with 250 m spatial resolution. Figure 5.3 shows the urban area distribution approximately every 50 km along the coasts of LAC to a height of 10 m.

Maps of road and rail networks were obtained from the Digital Chart of the World data base (DCW; `http://statisk.umb.no/ikf/gis/dcw/`) at 1:1,000,000 scale. This digital terrestrial map is a GIS global database with data of roads and rail lines among other and which is updated to 1992 (Figure 5.4).

Vulnerability data sources are outlined in Table 5.2. More information on the vulnerability

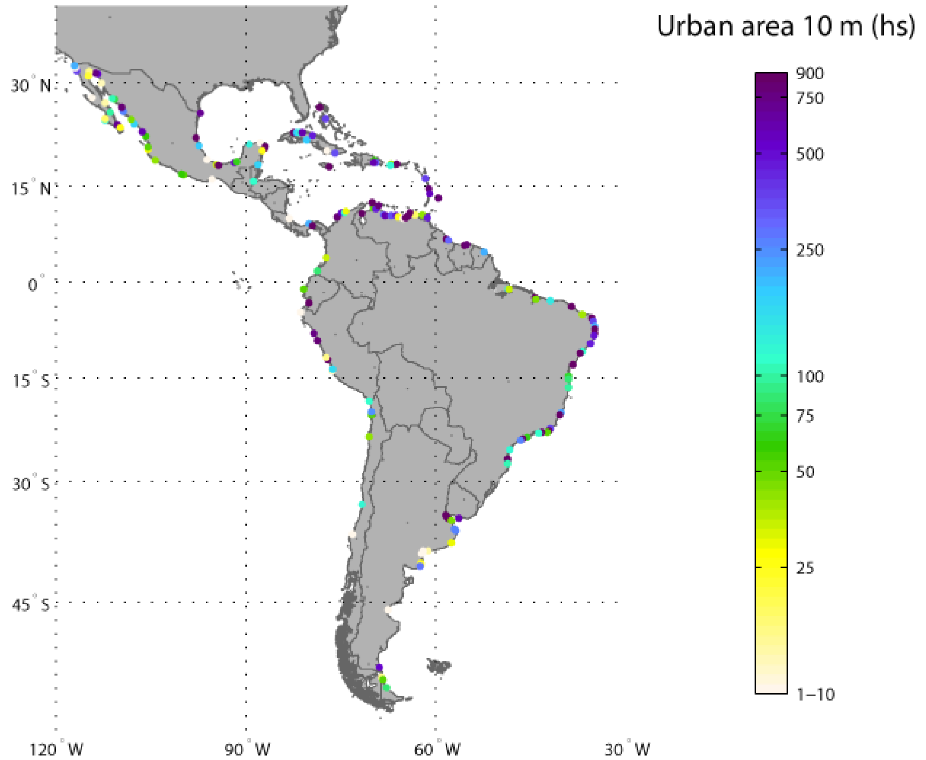

Figure 5.3: Urban area distribution in Latin America and the Caribbean from 0 to 10 m (results are expressed in hectares and representative of 50 km study units).

and exposure of the region can be found in [CEPAL, 2012c].

A particular feature of the coastal zones is its exposure to marine hazards, which is characterized by a wide diversity of configurations of the coastlines, such as river outlets, urban fronts, beaches, cliffs, estuaries or human infrastructure. Because of the lack of data in this regard for erosion and flooding studies, it was necessary to first gather information on various characteristics of the coast at approximately 15,000 study units from satellite images based on Google Earth software ©. Information was classified in: (1) beach size and type, distinguishing between (a) pocket beaches, (b) with strict outlines, (c) if adjacent to a river mouth or (d) unlimited so that it could be considered rectilinear, on the grounds that each type of beach performs differently in terms of sediment transport; (2) the length of the consolidated urban frontage adjacent to the coastline (i.e. the distance built beside the sea line) to identify areas of urban development making up the sea front; (3) the length of urban frontage where the coastline is formed by beaches (i.e. in such a case an urban beach acts as a protective element for the city's coastal frontage), and (4) the length and location of protective sea dikes. In quantitative terms, these data are of sufficient quality given the scale of the study (5 km). It was possible, using this information, to roughly categorize the different types of coasts by country, as shown, by way of an example, in Figure 5.5 for the coasts of Brazil.

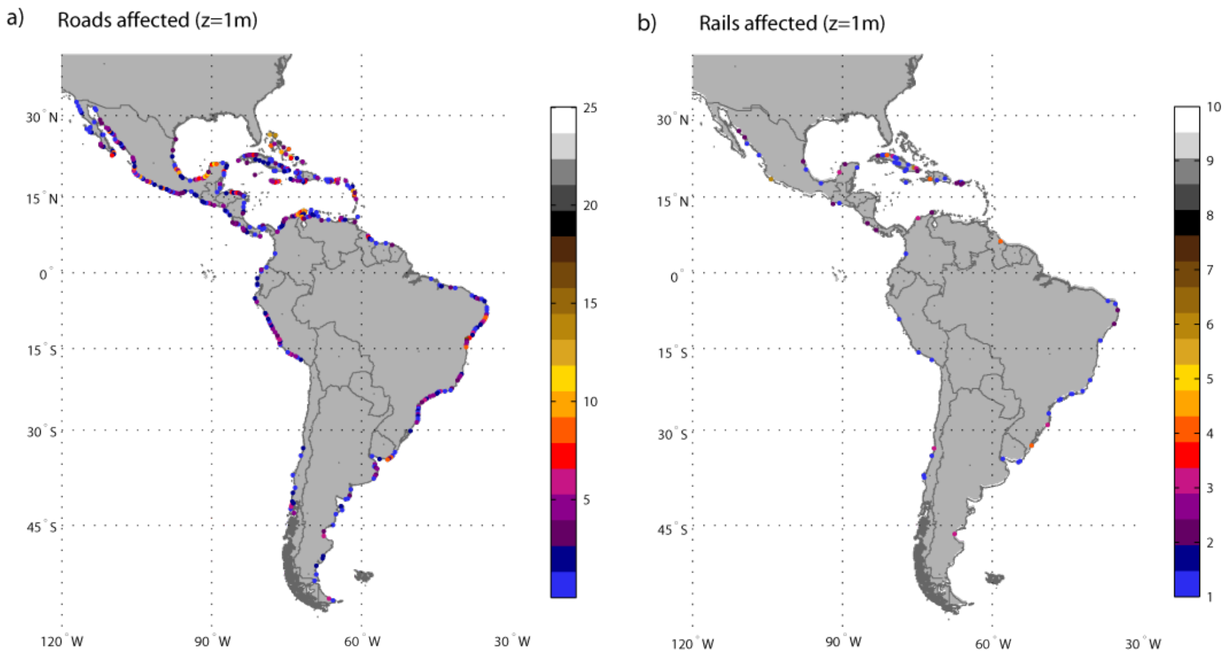

Figure 5.4: Infrastructures: roads (a) and rails (b) below 1 m height (number of study units affected).

Beach type was classified into rectilinear and pocket beaches, among other types, in order to determine the proportion of beaches that could be susceptible of being subjected to rotation due to changes in the mean direction of the incident wave energy flux. Figure 5.6 represents the proportion of both types in sections of 50 km.

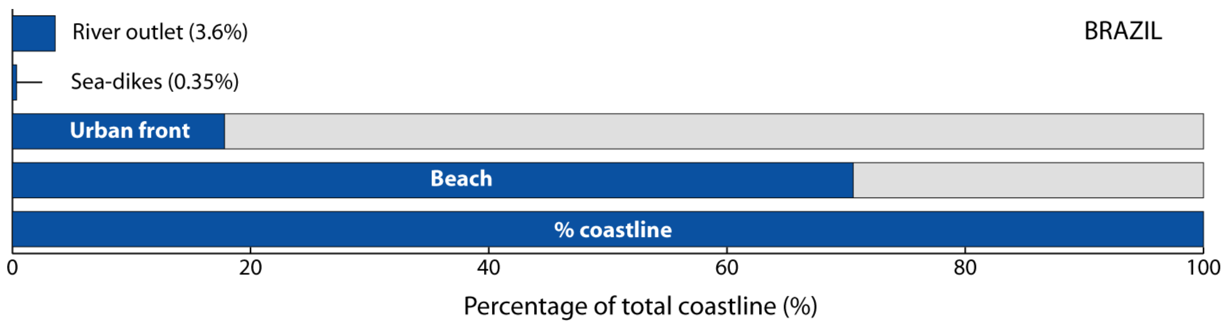

Figure 5.5: Coastal typology classification, identifying percentage of coastline with beach front, urban front, sea-dikes and river outlets. Example for the Brazilian coastline.

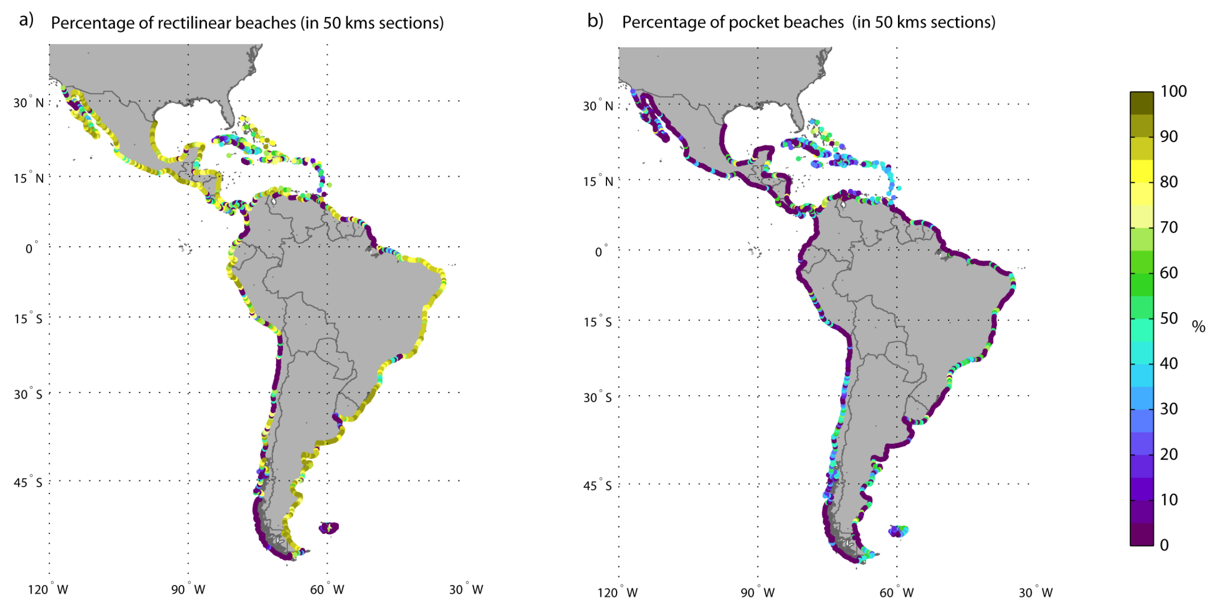

Figure 5.6: Coastal typology analysis, percentage (over sections of 50 km) of coastline with rectilinear (a) and pocket beaches (b).

5.2.4 Long-term trends and climate variability in the region marine dynamics

The study of the wave climate and its variability is addressed specifically in Chapter 3 for a global scale. However, for coastal impacts, other dynamics, such as the different components contributing to the sea-level are also necessary. In the following, a brief overview on the main past changes in the region of LAC is given. In the interest of concision, only changes in SLR and in the storm surges will be outlined herein.

SLR has been reported to increase in the last decades (e.g., [Church and White, 2011]). In this work, local linear regression and Trend-EOF techniques (see annex for description of techniques) have been used to detect the long-term trends in the sea-level database. Figure 5.7 shows the global trend detected, in agreement with previous findings. Comparing both techniques, it can be stated that Trend-EOF is less influenced by the ENSO phenomenon and other local influencing factors thus providing a trend with higher spatial continuity, of about 2 mm/yr, as seen in Figure 5.8.

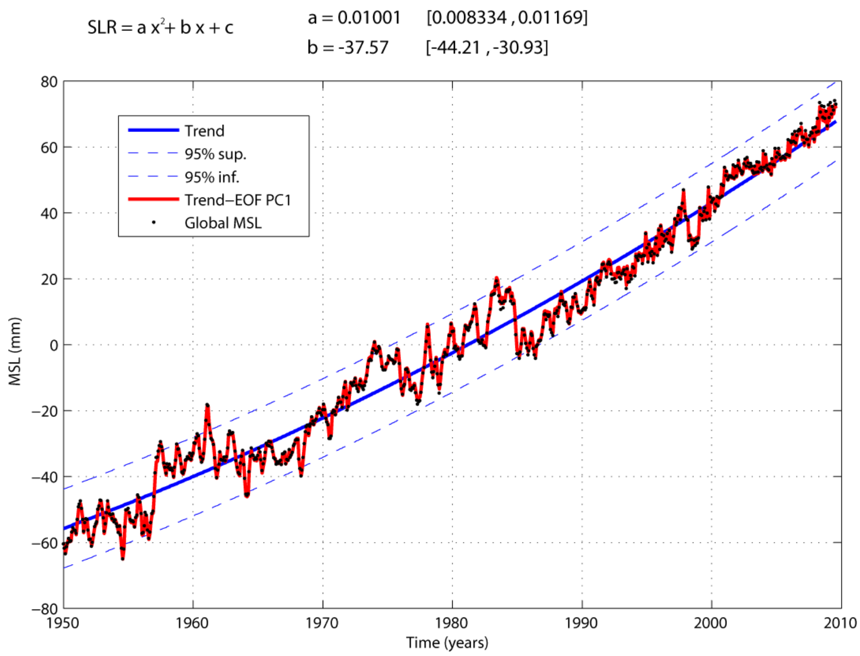

Figure 5.7: Global Sea-Level Rise showing long-term trend computing with Trend-EOF and linear regression and showing the 95% confidence bounds. Latitudinal weighting has been considered in the computation.

Different SLR time series and the detected trends are shown in Figure 5.9 showing a clear area of ENSO influence in the equatorial Pacific area. Trends computed with Trend-EOF technique is not affected by those outliers and provides an adequate estimate of the long-term trend. It can also be checked that in that particular area, the range of variation due to El Niño events is of the order of magnitude of the past changes in SLR. This fact is important to be considered in the coastal risk management in the area, like in other areas of the globe such as California or Australia.

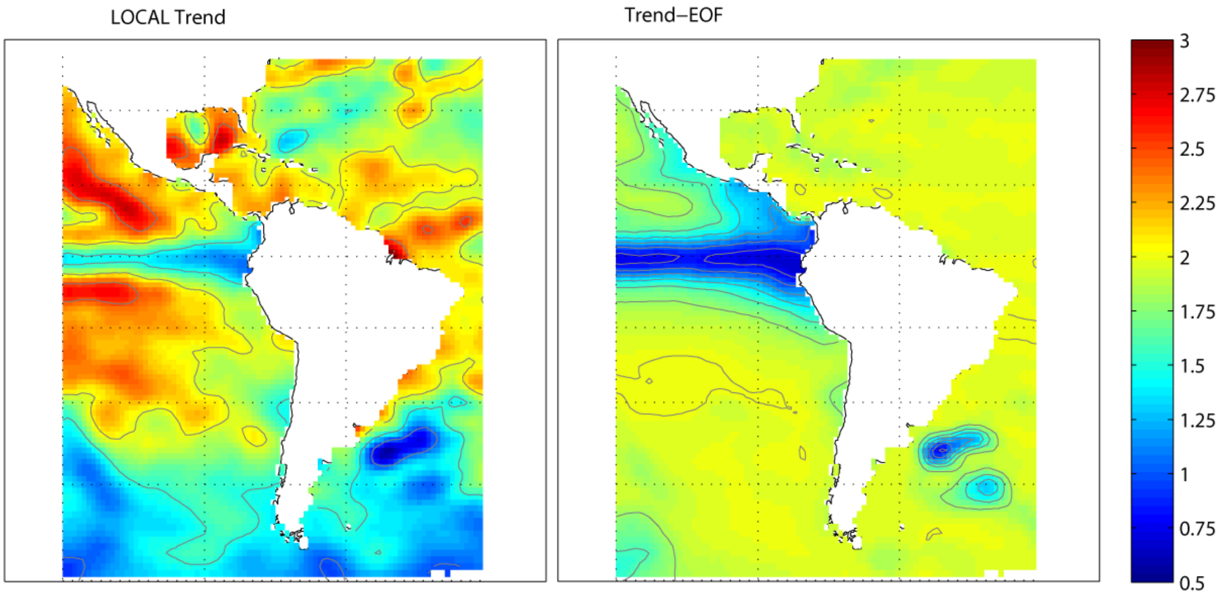

Figure 5.8: Average linear long-term trend of Sea-Level Rise in Latin America and the Caribbean from Local linear regression (left panel) and Trend-EOF (right panel) analysis, in mm/yr.

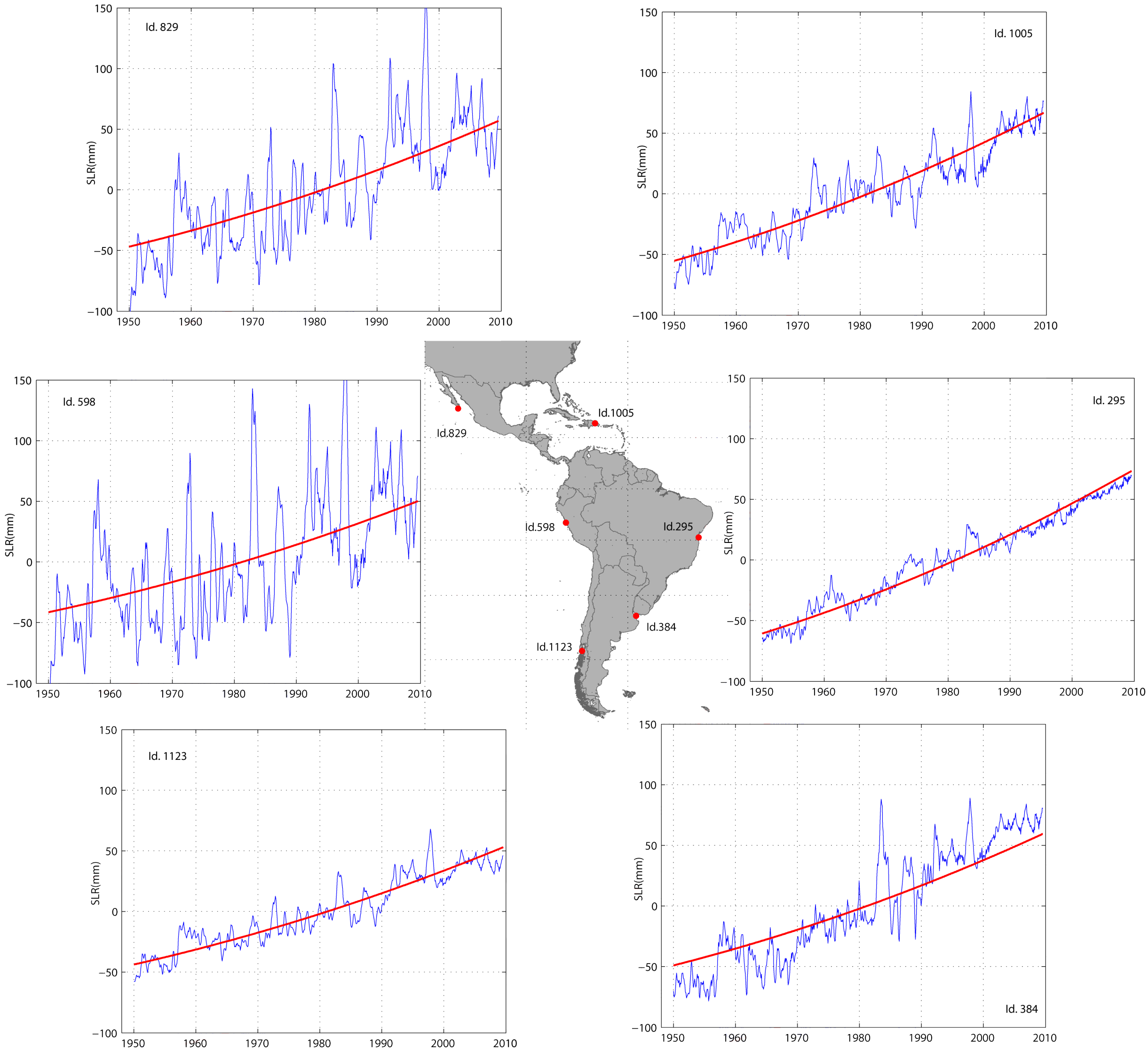

Figure 5.9: Time series of Sea-Level Rise and detected long-term trends for several representative points along the Latin America and the Caribbean coast.

Nevertheless, SLR is not the unique factor that must be considered in a coastal hazard analysis. Storm surges (i.e. elevation of sea-level due to the combined effect of atmospheric pressure and wind, usually associated to storm events) also suppose a main agent affecting the coastal areas which may be responsible for coastal flooding. The annual long-term trend identified in the extremes of the Storm Surge (SS) are shown in Figure 5.10 along with the seasonal trends at five representative points. The computation was performed based on a non-stationary analysis of extreme values (see annex), in an analogous manner to the study of wave heights extremes shown in Chapter 3. Largest increases are occurring in the Rio de la Plata area and the California Bay, precisely at the areas more affected by SS. Where the trends in SS extreme events are significant, they are in the order of SLR changes, about 4 to 5 mm/yr maintained along the year in the Rio de la Plata. In the case of California Bay, decreases of 3 mm/yr are found indicating that the effect of SLR can be offset by SS at the storm events. The combination of these two factors, alongside with the statistic behavior of the rest of sea-level components (i.e. astronomic tide, mean sea-level and waves set-up) should be considered for coastal flooding analysis.

As seen for SLR time series in Figure 5.9, SS is also strongly affected by El Niño events and other inter-annual variability factors. To reflect this influence in the storm surges Figure 5.11 displays the correlation pattern with the monthly mean sea-level (left panel) and with the 95% percentile of monthly mean SS. It has been made clear that the influence of the inter-annual variability should be of concern for the statistical analysis of coastal flooding.

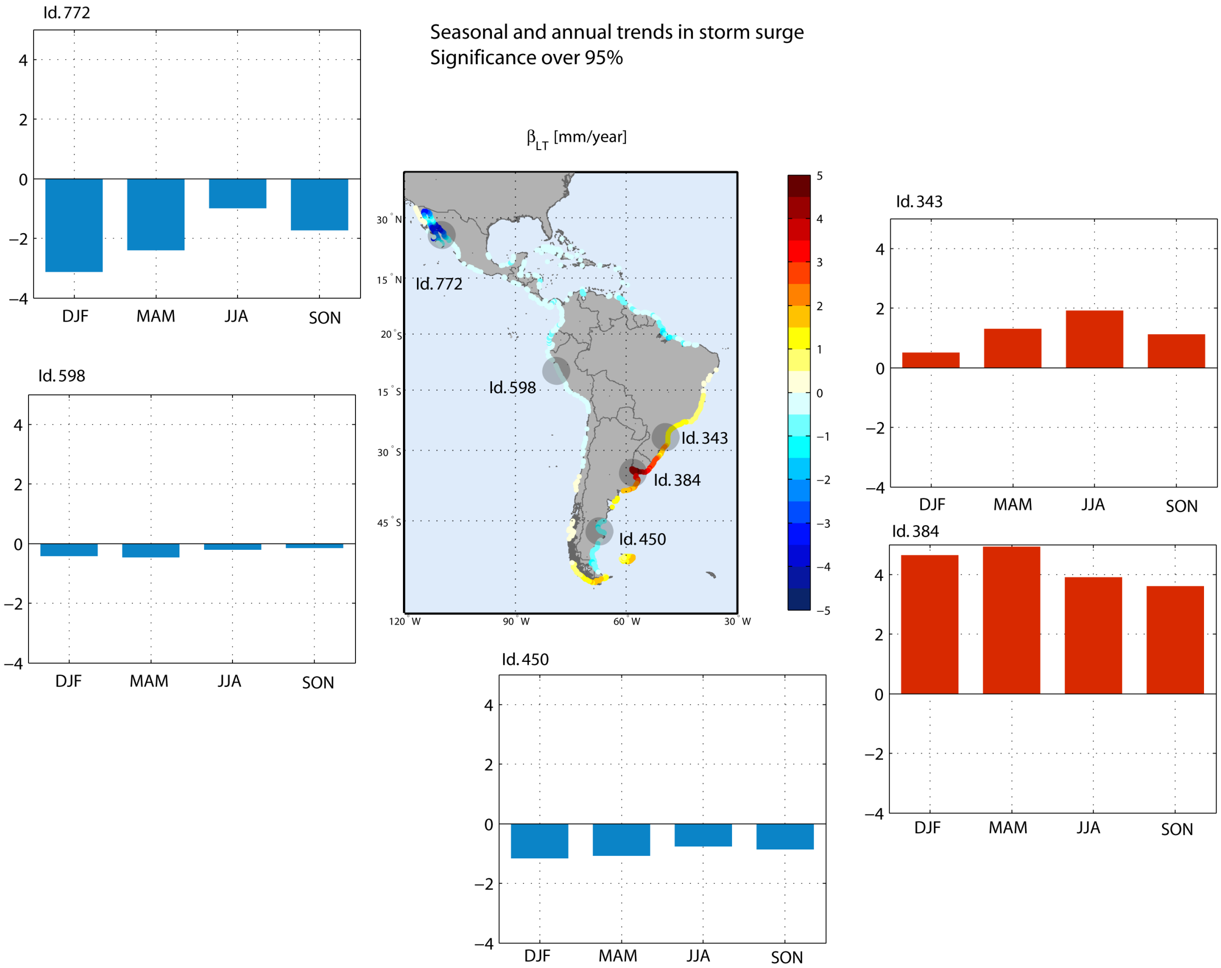

Figure 5.10: Annual long-term trend in extreme storm surges (central panel) and seasonal trends for five representative points (obtained from Global Ocean Surges database, from 1948 to 2008).

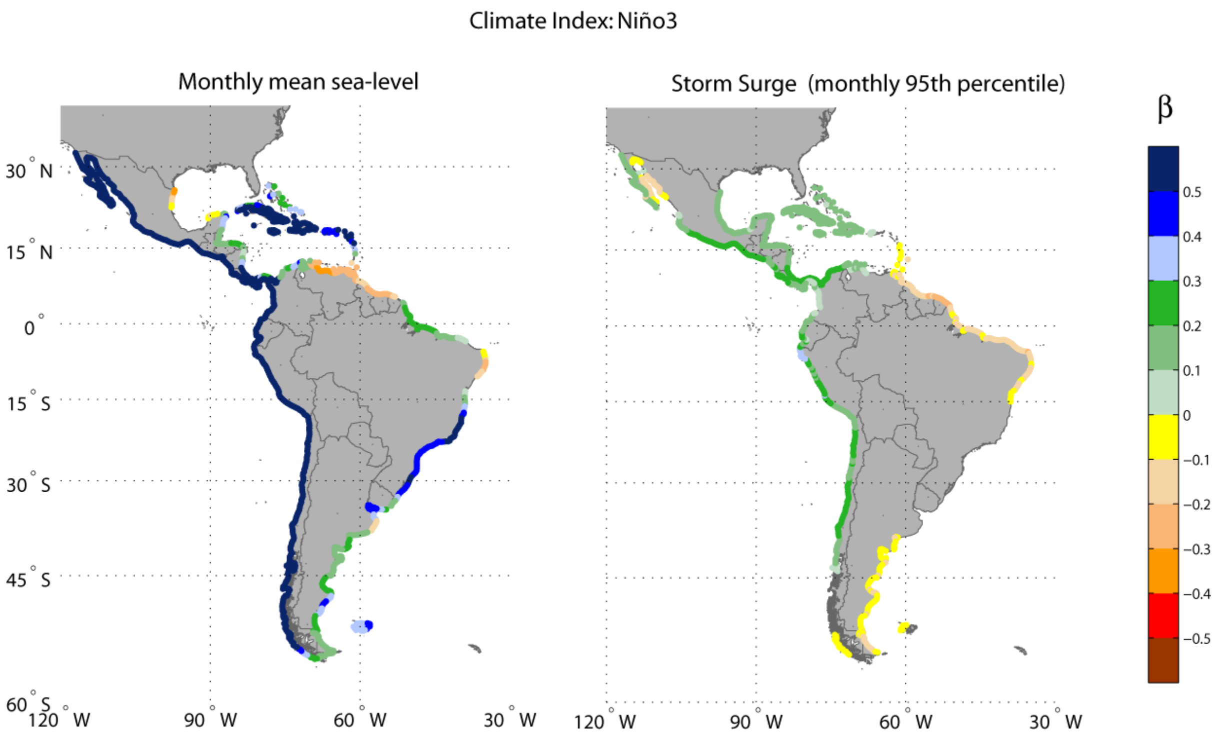

Figure 5.11: Correlation patterns of Niño3 index with the monthly mean sea-level (left panel) and the monthly 95% percentile of storm surge (right panel).

5.2.5 Inundation

Mean global sea-level rose 17 cm in the twentieth century, faster than the previous century ([Woodworth et al., 2009, Church and White, 2011]). Recent studies of SLR estimates in the twenty-first century show that the projections of the IPCC in the AR4, of 0.26-0.59 m global SLR by 2100 in an A1F1 scenario ([Meehl et al., 2007]) may be exceeded and sea-level may approach or even exceed 1 m by the end of the century ([Pfeffer et al., 2008, Vermeer and Rahmstorf, 2009]).

Both approaches, past trends and SLR estimates for the end of the century, are considered herein. On the one hand considering the extrapolation of past changes detected in the mean sea-level for 2040 from the work of [Losada et al., 2012], and on the other considering a uniform scenario of 1 m of SLR.

As a vulnerability term for the definition of the risk (equation 1.4) the population affected, up to the flooding level, is used. Figure 5.12 shows the population distribution by heights (between 1 and 3 m) for various units of study in the region. Population distribution varies depending on the coasts. Increased vulnerability can be seen in urban zones like Vila Velha (Brazil), Alvarado or Veracruz (Mexico).

5.2.6 Flooding level trends and scenarios

While SLR is one of the most significant impacts that coastal zones will experience in the future, temporary flooding events, from the combined action of tides and rising sea-levels, added to the effects caused by wind, pressure and waves, must also be taken into account as a factor of greater relative importance on some coasts ([Michael, 2007, Nicholls, 2011]).

Such events are episodic and are associated with unexpectedly high seas caused by the combined effect of winds, pressure and waves, generally associated with storm episodes. The results shown here do not include flooding caused by hurricanes due to lack of resolution in the numerical generation, a feature configuring the greatest damage in tropical zones.

To study coastal flooding events, the time series for Flooding Height (FH) were obtained by aggregating the different sea components:

$$FH = MSL + SLR + AT + SS + waveSetup \tag{5.1}$$

where FH denotes the total flooding height, MSL the mean sea-level, AT the astronomic tide and SS the storm surge.

These temporal series are analyzed with a specific model for extremes (see annex for description) to isolate the monthly maxima for the analysis of the frequency and intensity of extreme flooding events on the LAC coast. Significant changes have been found in the extreme distribution for flooding levels. The evolution of the probability density functions (pdf) is represented in Figure 5.13 for five representative points along with the long-term trend in the location parameter that represents the mean displacement rate of the distribution. Values around 10 mm/yr

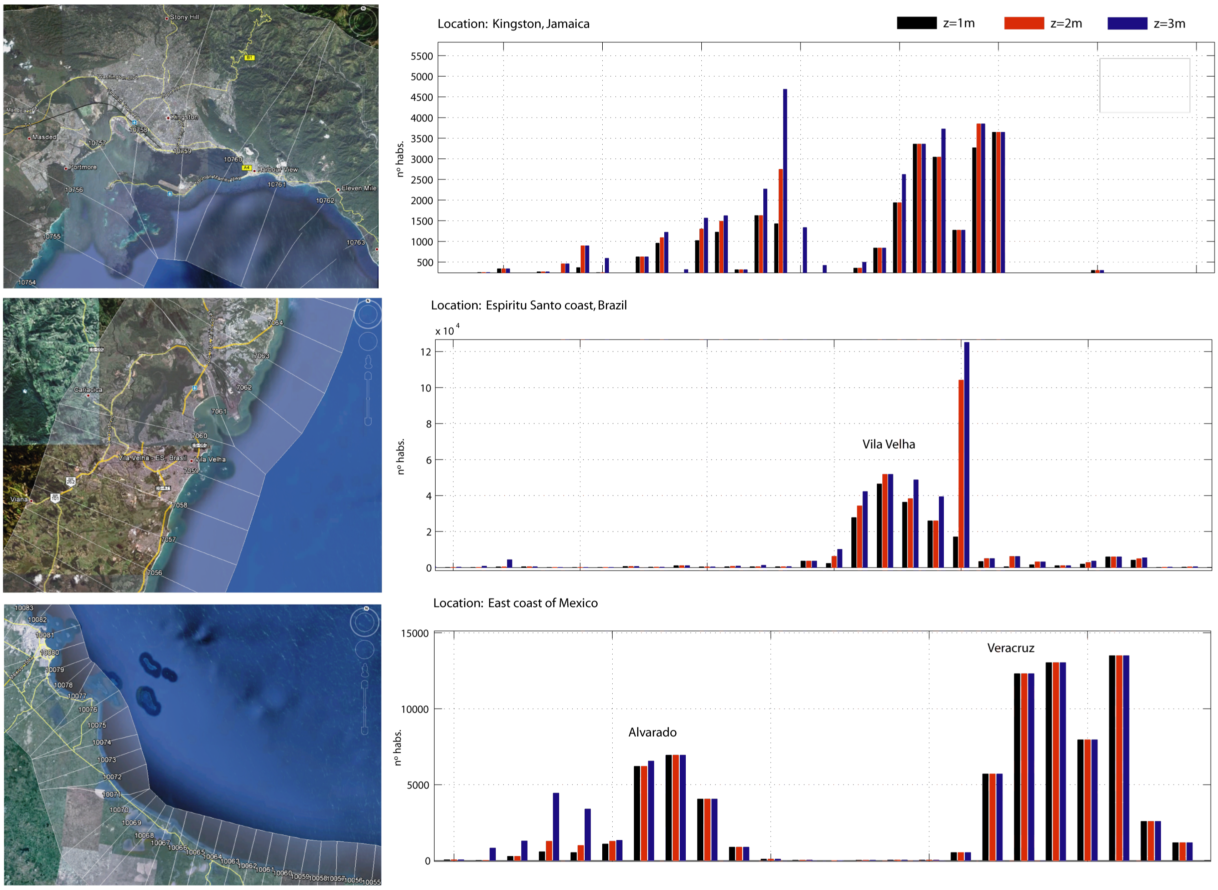

Figure 5.12: Number of people affected between 1 and 3 m at three urban regions in Latin America and the Caribbean. Satellite images taken from Google-Earth software ©.

are found in the Rio de la Plata area due to a combination of trends in the SLR and SS values (see trends results in section 5.2.4). The pacific coast of Mexico is another area prone to high trends, in the region of 6 mm/yr, while in the rest of the region flooding trends remain close to the SLR values, indicating that not significant contribution of the rest of components is found.

However, the trend in the location parameter is intense. Indeed, changes in the shape of the distribution are important to detect whether the probability of a certain value may vary accordingly. This can be seen in point 384 in Figure 5.13 where the probability associated with the higher values has increased along the period of study (a total of 58 years).

The changes in the extreme pdf imply changes for the values associated with certain return periods (T; i.e. the average recurrence interval over an extended period of time) with probability of exceedance of 1/T. Figure 5.14 depicts the 50-yr flooding level (a) and the change of this value from the first to the last decade in the study interval (b). The spatial variability of values is high. Larger levels, well over 5 m, concentrate in the southern Atlantic coast. These flooding levels must be taken with caution in the Caribbean area because hurricanes statistic is not properly included in it. The southern coast of Brazil and Uruguay (around a 40% of variation) along with

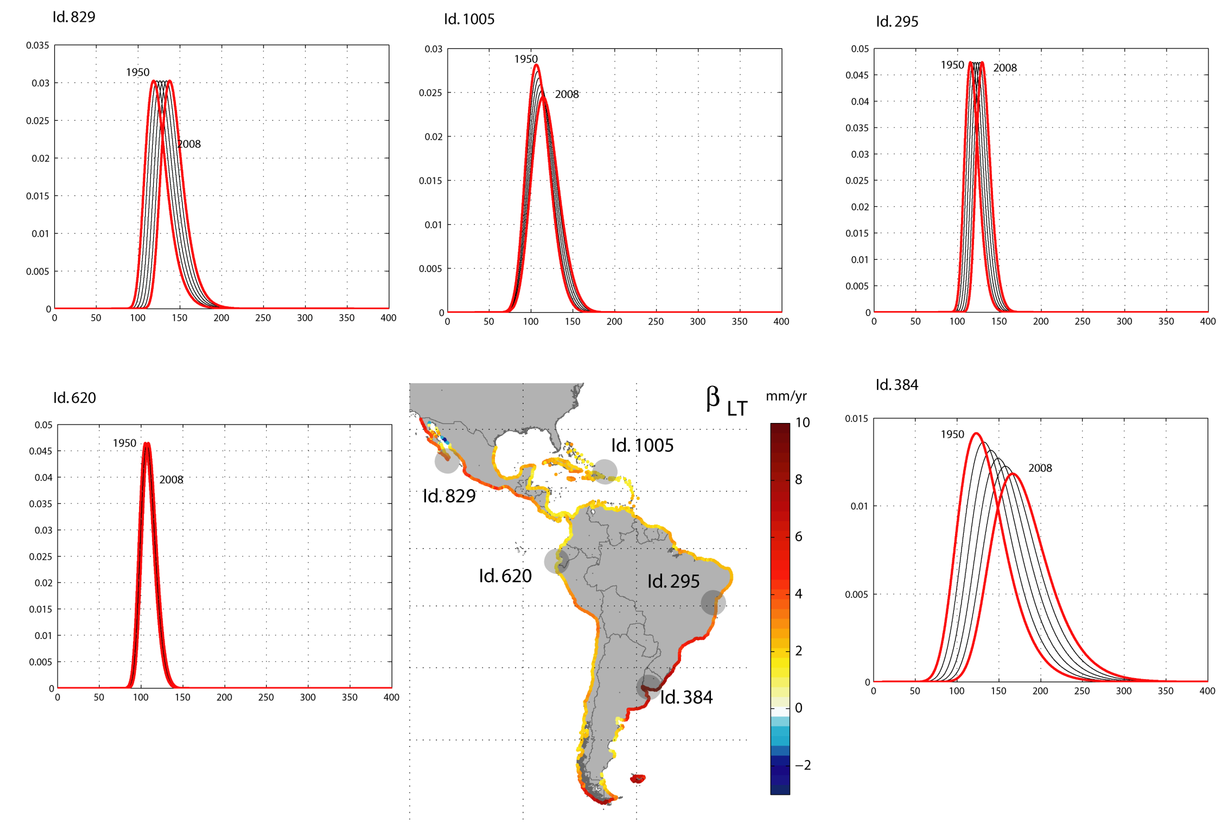

Figure 5.13: Trends of change in the flooding probability density functions at various points in LAC and change (mm/yr) in the mean distribution value at LAC coast.

certain areas of the Caribbean islands have undergone the largest change in the flooding level with return period of 50 years due to changes in the pdf of extreme flooding.

5.2.7 Erosion trends and scenarios

In analyzing SLR impacts, it is important to differentiate between flooding and erosion. Beach erosion is a process which is completely different from inundation or flooding. Erosion involves a movement of sands from the beach seaward, in a search for a restoration of balance to dissipate more energy due to wave breaking. Much of the sand is returned to the upper part of the beach profile by the long-period waves under normal sea-level conditions. This phenomenon shows that sea-level plays an important role in coastal erosion ([Zhang et al., 2004]). [Zhang et al., 2004] conclude that the agreement on application of Bruun's rule ([Bruun, 1962]) and the erosion trend observed on the eastern United States coasts indicates that it is caused by SLR. Other authors declare that Bruun's rule is not applicable generally as its hypotheses often fail on coasts; especially due to the limitation on the net longitudinal transport of sediment. While Zhang's analysis continues to be valid for ideal situations of sections of coast where there is no sediment input or output, thought must also be given to other effects on the balance of

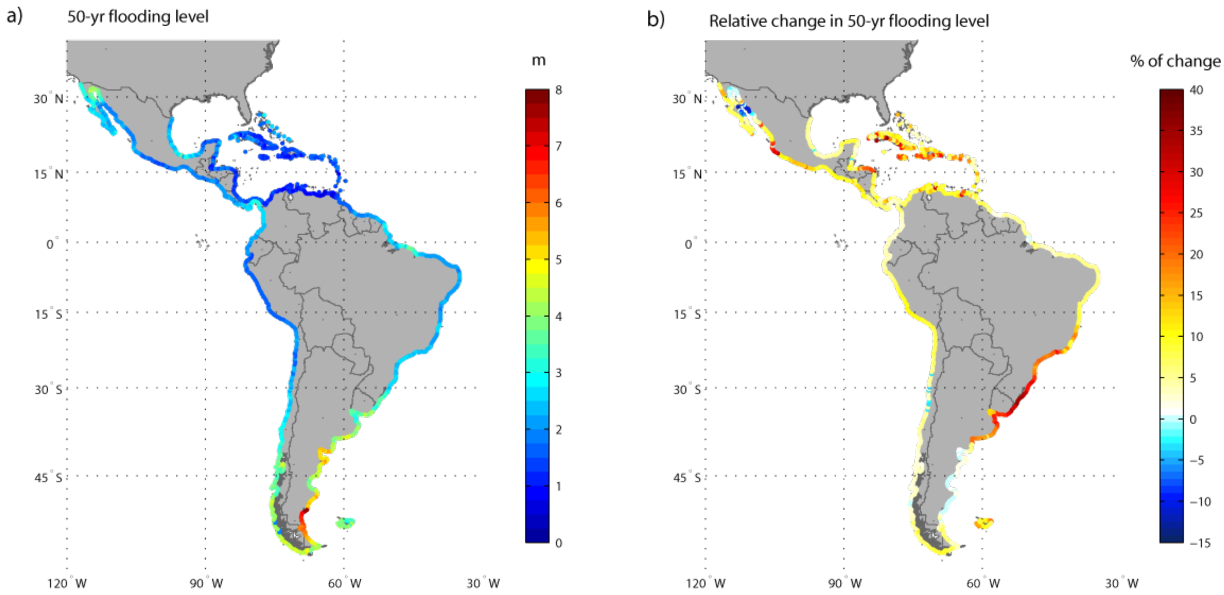

Figure 5.14: 50-years flooding height and relative change between the decades 1950-1960 and 1998-2008.

sediments on the coast ([Stive, 2004]).

On the scale of the diagnosis of the coastal impacts in LAC, an analysis based on Bruun's rule may be acceptable ([Nicholls, 1998]). Although studies of change on the coastline demand an analysis based on changes in the transport of sediment, or with other probabilistic solutions which also account for storm-related erosion (e.g., [Callaghan et al., 2008, Callaghan et al., 2009]). Figure 5.15 depicts the erosion rate based on Bruun´s rule for three representative diameters in the sand range.

According to long-term trends detected in the significant wave height exceeded 12 hours per year (H_{s12}), shown in Figure 5.16, there would likely be erosion induced by changes in wave intensity that can involve a larger magnitude than those expected from SLR. To account specifically for those changes, other approaches on storm-erosion are needed.

Although SLR would contribute to increasing beach erosion, in some areas anthropogenic effects have resulted in higher erosion rates, much greater than would naturally occur, mainly provoked by poor sand management practices at channel entrances and transversal coastal structures.

Concerning the changes in the wave climate, to obtain an estimate of erosion from changes in incident wave characteristics, a simplified model of the response of the pocket beaches to changes in the direction of the waves is analyzed. There are two hypotheses on which this analysis of the planform is based in the long-term: (i) the orthogonality of profile and planform (implying that the study can be made independently for each of them) and (ii) the different time-scale of the profile-plan processes. As a consequence of this different scale of processes, planform studies always assume that the beach profile has reached its equilibrium position, a hypothesis also

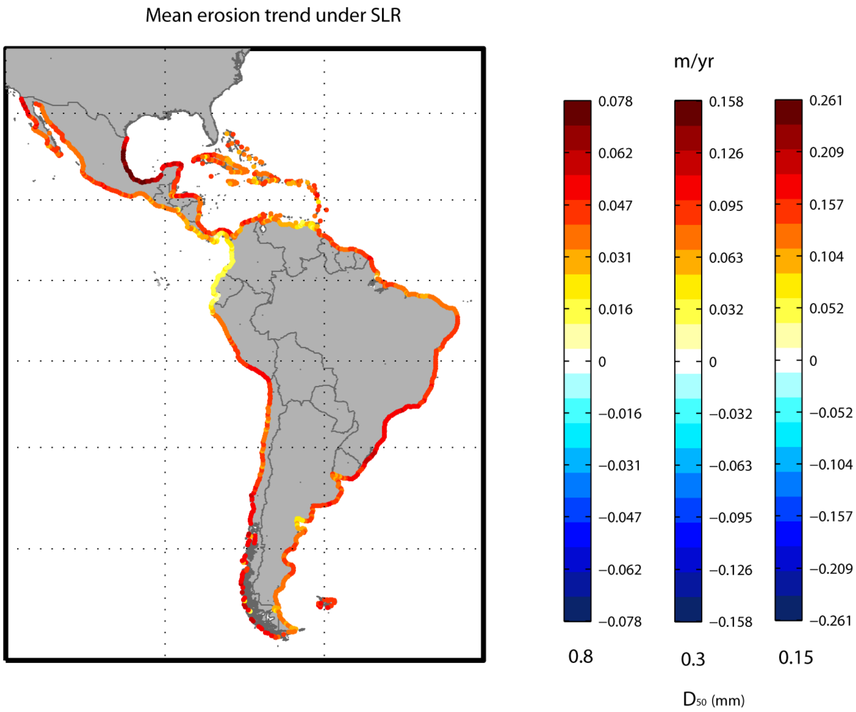

Figure 5.15: Long-term trend in beach erosion due to Sea-Level Rise (in application of Bruun's rule) for three representative sediments in the region of Latin America and the Caribbean.

admitted for application of Bruun's rule. Thus in the long-term evolution of a beach planform, the profile shape remains constant.

The latter means that pocket beaches are in a position of modal balance, with oscillations around the mean position. In general, such oscillations are weak except where the wave dominant energy direction is markedly seasonal. In any case, analysis of the potential impact of climate change on beach planform will be focused on the long-term effects, i.e. on the mean annual position.

The planform of these beaches is governed by the direction of the mean energy flux from the incident wave climate on the beach ([Hsu and Evans, 1989, González and Medina, 2001]). If this parameter is modified, the beach will rotate so that its planform will once more lie substantially orthogonal to the direction of the mean energy flow. This rotation will result in future erosion at one extreme and an advance at the opposite one, provided that sufficient sand is available. For this simplified performance model to be representative, the lateral limits of the beach must be able to contain the beach in the face of the advance, and that there is also no sand input from the sea outside or from the beach surroundings.

If this simplified behavior is assumed, a beach will change its orientation should the direction of the mean energy flow shift. Such change will be accompanied by an advance and retreat of the beach so that the volume of sand eroded will be equivalent to that deposited on the beach front.

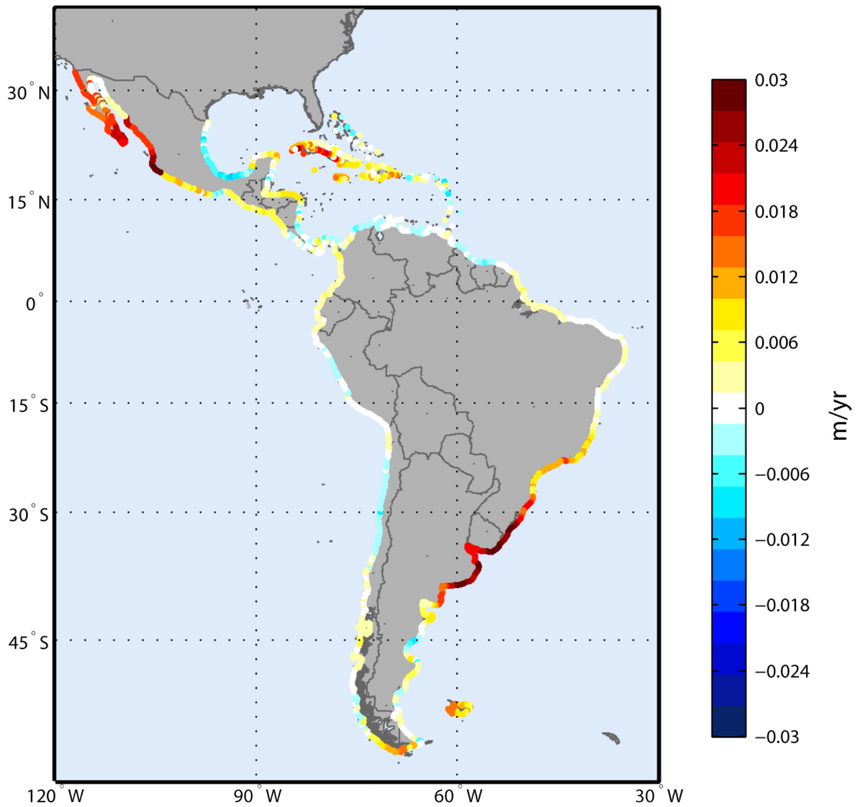

Figure 5.16: Long-term trend in the significant wave height averagely exceed 12 hours per year in the region of Latin America and the Caribbean. Computed from GOW reanalysis database.

Maximum beach retreat and advance will occur at the extreme points, and its value (RE_{max}) will depend approximately on the variation in the direction of the mean energy flux ($\delta\theta$) and the length of the beach (L), according to the equation:

$$RE_{max} = L/2 \cdot \tan(\delta\theta) \quad (5.2)$$

The trends obtained with this model for a theoretical pocket beach 1,000 m long driven by changes in the direction of the mean energy flux are shown in Figure 5.17. Baja California, southern Brazil and some Caribbean islands would be the regions most affected by this possible change.

Note that the actual impact would depend, among other factors, on the presence of the pocket beaches (see Figure 5.6) and their local characteristics. The risk analysis that follows will include this information.

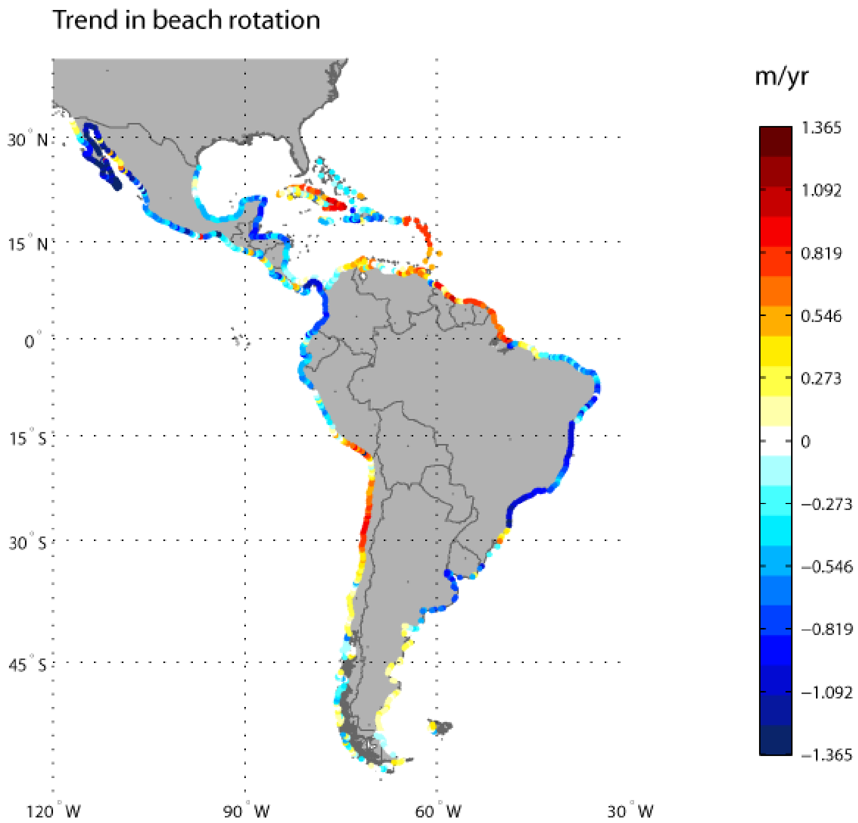

Figure 5.17: Trend of beach erosion following change in dominant energy flux direction (m/yr).

5.3 Environmental risk analysis

5.3.1 Flooding Risk

5.3.1.1 Flooding risk for coastal population

The exposure curves are defined by the area affected at each DTM topographic height. Analogously with the previous case, the vulnerability curves in each sector of study are determined by the data for resident population to each level. Figure 5.18 shows the population affected in the region by the 50-yr flooding, highlighting the region's inhabited coastal zones.

The assessment of the risk for the population is shown in Figure 5.19. In extrapolating trends, these results are obtained by integrating probability for each SLR levels and the number of persons below them, according to their spatial distribution at each study unit. The expected damage (i.e. number of inhabitants) is graded according to damage percentiles of 25, 50 and 75%. The results are shown on a single scale of ranges, for comparison with the consequences of an increase in current rates of change. It can be seen how, should current changes be maintained, the risk is very high for the urban zones of the Atlantic coast and the Caribbean islands. In a situation of 1 m SLR, very high risk extends to most of the Caribbean islands and the east coast

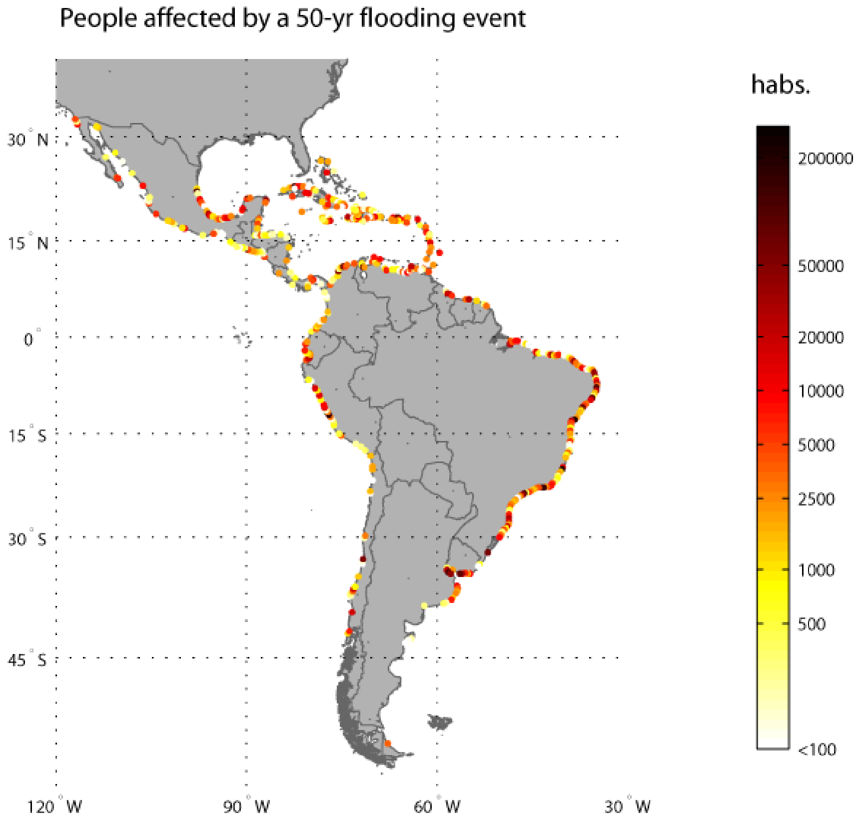

Figure 5.18: Number of people currently affected by a 50-year flooding event(population data reference in 2000).

of Brazil, Central America, Ecuador and Peru.

Figure 5.20 represents the risk of flooding from extreme events of rising sea-level, following integration of the agent, exposure and vulnerability components. The coasts most at risk are located in Brazil and Mexico, on both the Pacific and the Caribbean, and on the Caribbean islands. A large part of Peru and Ecuador are also at "very high risk" in the horizon to 2040, mainly due to urban agglomerations. Another hotspot is the area of influence of the Rio de la Plata, where urban density is high and large sea levels caused by extreme events occur.

To find an indicator of how the situation would change under a 1 m SLR scenario, the risk which would be associated with the statistic for flooding extremes with a mean sea-level 1 m above the current figure, uniformly for the whole region is obtained. Note that in this case the probability of occurrence of the hazard agent is not included in the risk analysis because the scenario is formulated a priori and homogeneously throughout the region. Both results are represented in ranges of damage for each situation and are not comparable because they identify locations of special risk. In this case, the coastal urban centers are the zones most affected.

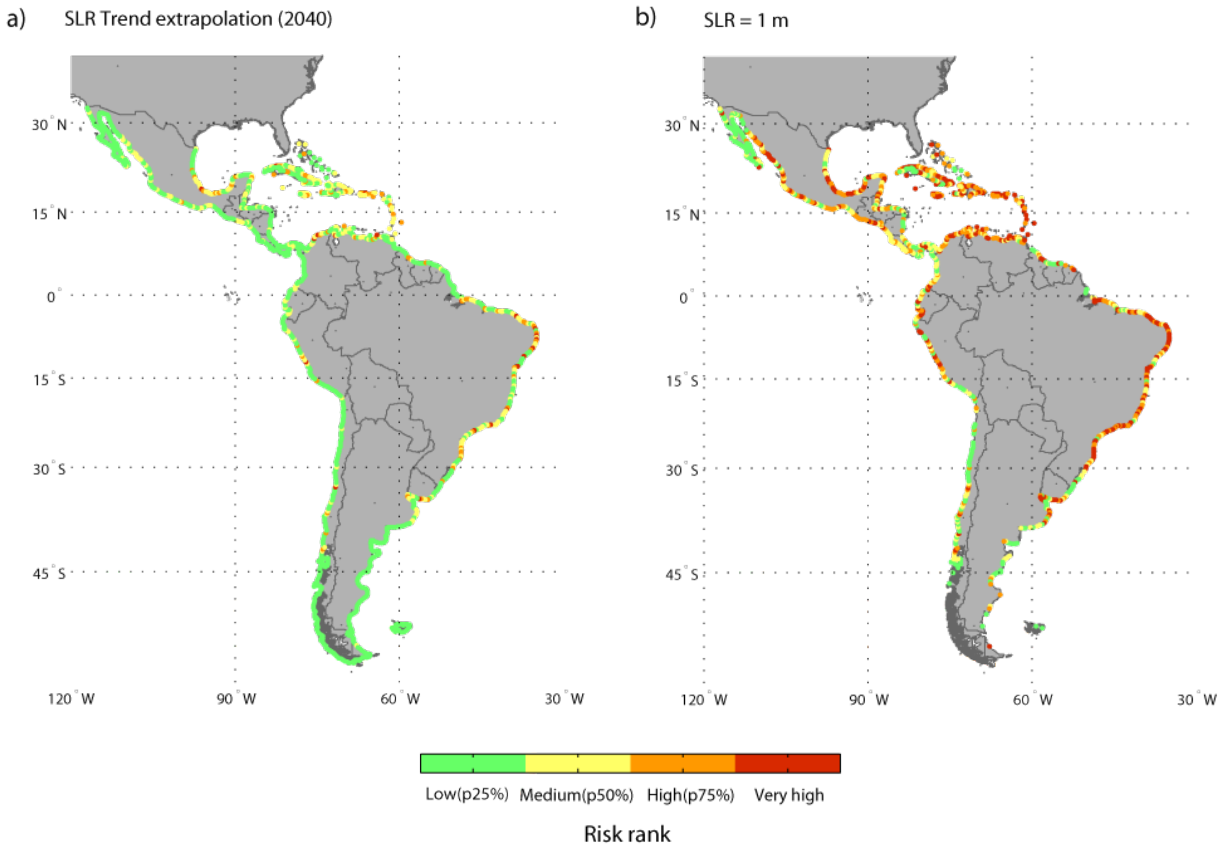

Figure 5.19: Levels of risk for the population associated with the extrapolation of Sea-Level Rise (SLR) past long-term trends to 2040 (a) and in a scenario of 1 m above current mean sea-level (b). The results are shown on a single scale of ranges, for comparison with the consequences of an increase in current rates of change.

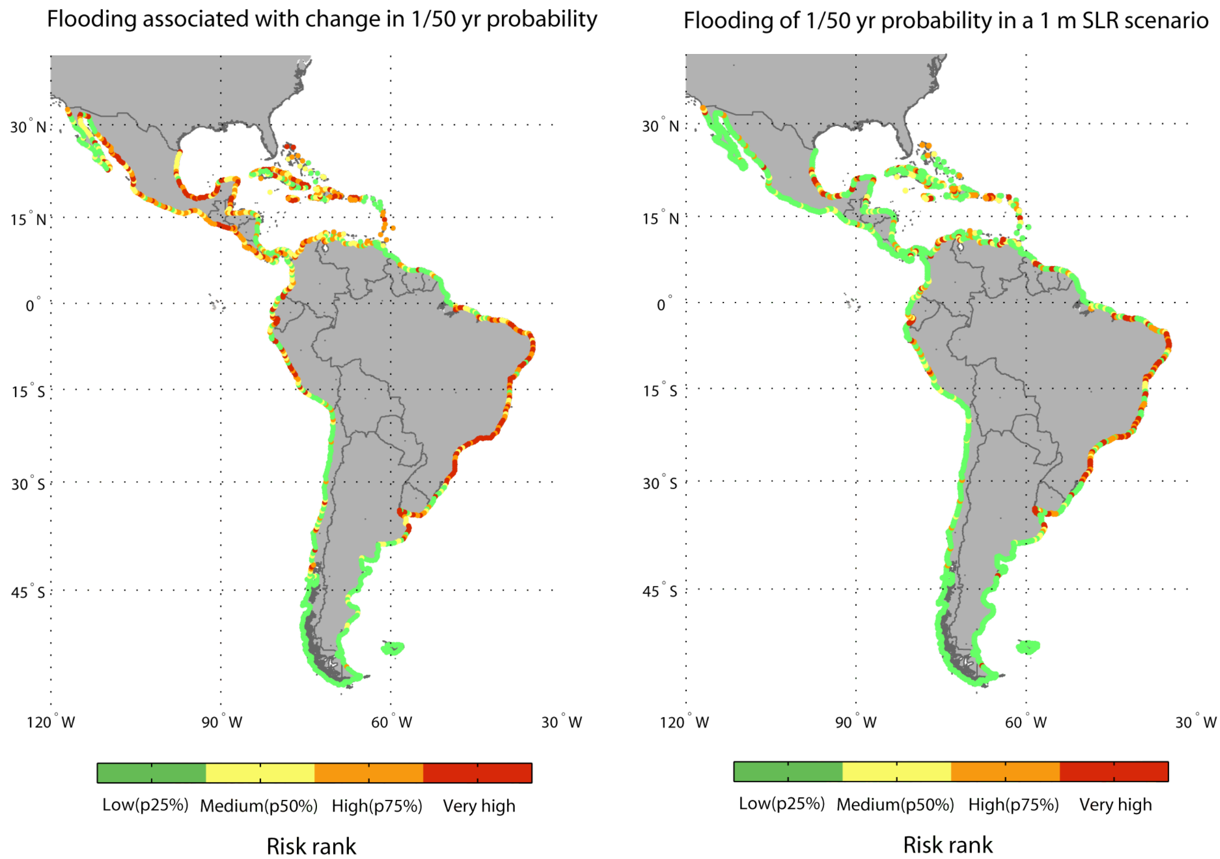

Figure 5.20: Risk levels for the population associated with flooding over a 50 year return period from extrapolation of the changes to 2040 detected in the past according to (a) changes in extremes probability density function and (b) 1 m above current mean sea-level.

5.3.1.2 Flooding risk for coastal roads and railways

In a manner similar to that for population, risks are studied for infrastructures. In this particular case, the vulnerability function is defined as the distribution by heights of the number of sections of infrastructures affected. No distinction is made between roads and railways, and both are dealt with jointly, although their relative importance and consequences may not be the same.

Figure 5.21 shows the results. The areas with highest risk are concentrated in very specific locations in southern Brazil, Rio de la Plata, Central America and the Northern Caribbean islands.

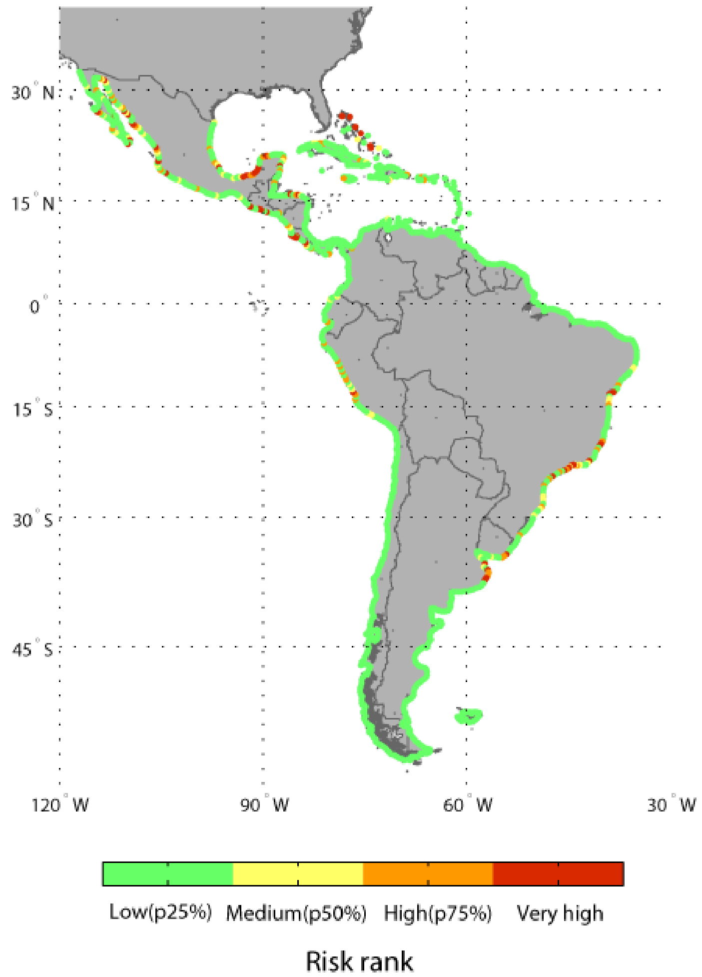

Figure 5.21: Risk levels for infrastructures (roads and rails) associated with 50-yr flooding event, by extrapolating to 2040 changes detected in the past extreme probability density functions.

5.3.2 Erosion risk

5.3.2.1 Erosion risk

For erosion risk assessment, the proposed methodology and global framework, introduced and described in Chapter 1, is here followed.

The hazard term is defined by the probability of reaching each level of erosion under SLR. Exposure term accounts for the beach length at each 5 km study unit. Note that if there is no beach, no risk should be expected as only sandy beaches erosion is being considered in here .

Vulnerability in this case is evaluated as the erosion expected relative to the total area of the beach, so that: $Vu = r/A_b$, where r is the erosion reached with a certain probability and A_b represents the beach surface area. Note that vulnerability increases when the erosion does. To identify the double function of sandy beaches, as coastal protection and as recreational resource, two different surface areas are considered: (1) only accounting for areas where urban frontlines were found, and (2) total available surface area, independently of adjacent inhabited areas. Results are shown below.

a) As coastal protection:

Considering just beaches on the maritime frontage of urban zones (i.e. urban beaches), Figure 5.22 shows the risk of erosion beaches from SLR by (a) extrapolating current tendencies and (b) for a 1 m scenario, consistent throughout the LAC region.

In this case, the vulnerability term is defined by the area eroded relative to that available on urban beaches. Greatest damage would occur on the coasts of Brazil, the Caribbean islands and the southern Caribbean coast.

Concerning the erosion induced by rotation of the beach planform, Figure 5.23 shows the results of risk for loss of beach surface considered as coastal protection, where only the areas with a significant proportion of pocket beaches and urban frontage are susceptible of such a change. The potential effects are mainly located in the south-east coast of the Caribbean and Brazil. Note that the south-western coast, despite presenting a high proportion of pocket beaches, lacks of adjacent population settlements and the risk is therefore low in that area. In areas with no beaches of such a type or negligible shifts, no risk is expected.

b) As potential beach resource:

Taking into consideration the current available beach area, irrespective of whether it is located on urbanized coasts, a beach can be studied as a resource, for example, for tourism. Using information registered by satellite imagery for each unit of study, the total beach area available at each unit is analyzed. With this information and the SLR erosion rates ([Losada et al., 2012]), the erosion damage for each SLR threshold can be integrated. The damages, in this case, particularly concentrate on the Caribbean coasts and islands where less beach area is available.

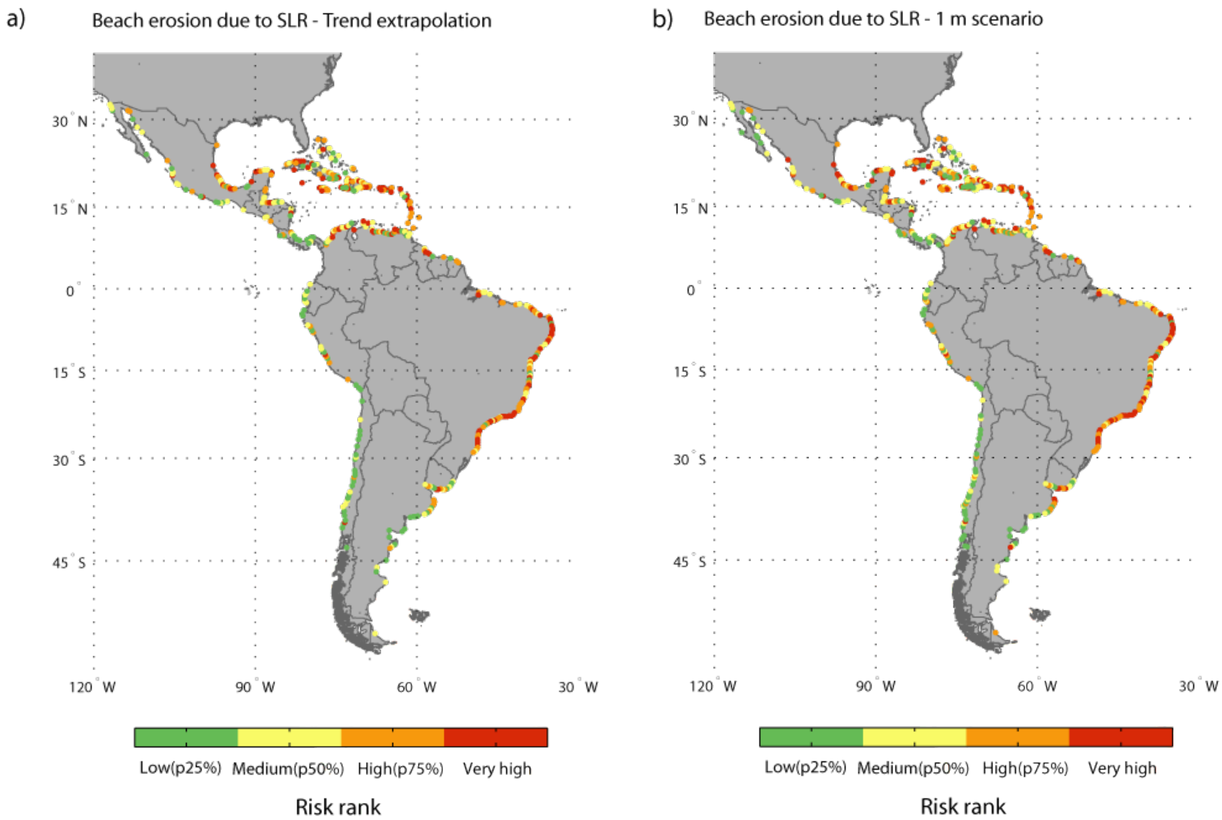

Figure 5.22: Risk levels for coastal city settlements from rising sea-level erosion of beaches conforming their urban coastal frontage by: (a) extrapolation of past changes to 2040 and (b) with 1 m above current mean sea-level.

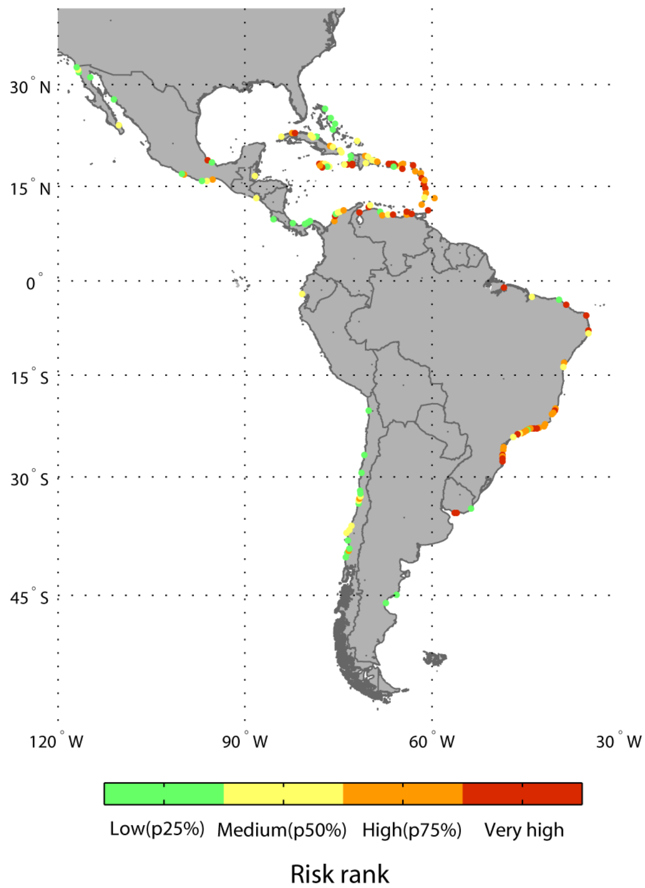

Figure 5.23: Risk levels for coastal urban settlements from beach planform rotation for pocket beaches conforming their urban coastal frontage, by extrapolation of past changes of the mean energy flux to 2040.

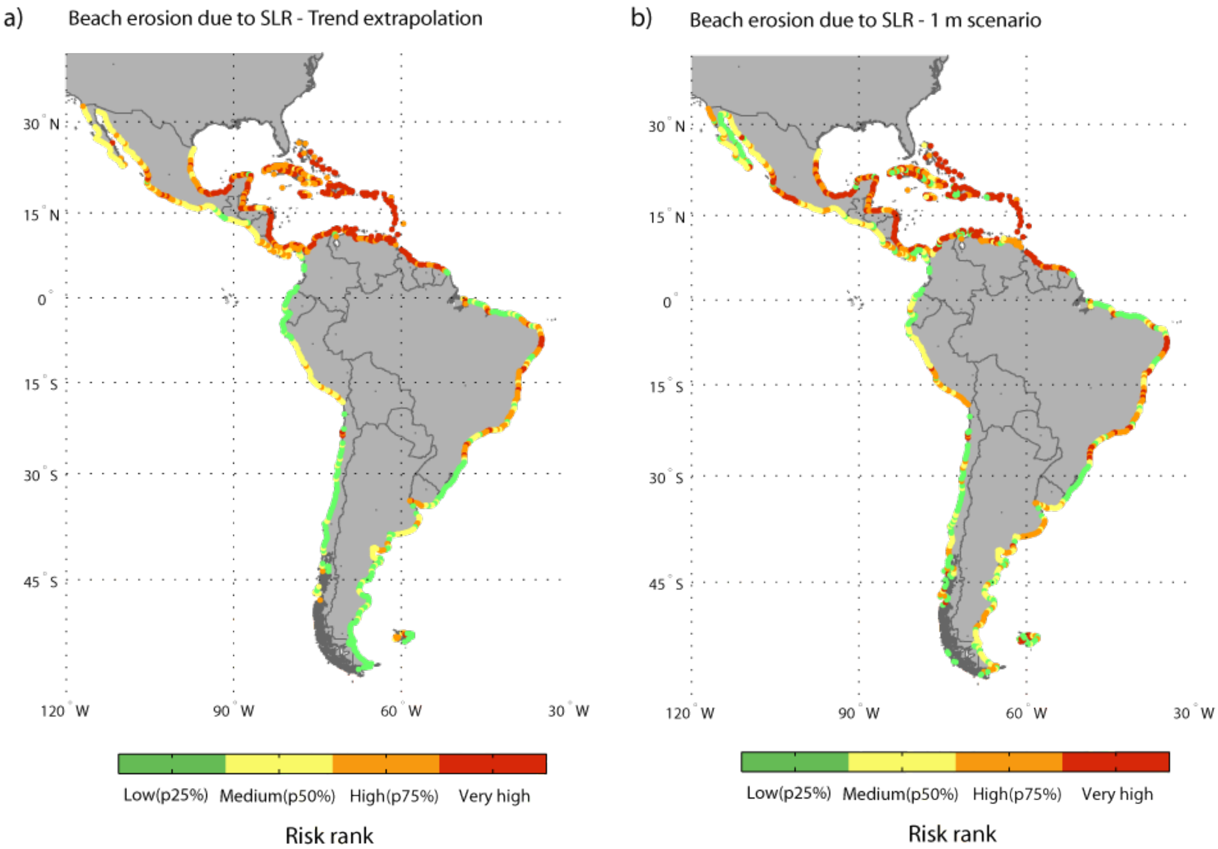

Figure 5.24: Risk levels for available beach resources (depending on beach area) for beach erosion from rising sea level by: (a) extrapolation of change tendencies to 2040 and (b) with 1 m above current mean sea-level.

5.4 Conclusions

An assessment of potential impacts on coastal areas has become increasingly important considering identified past changes in sea-levels, surges and waves. Being Latin America and the Caribbean a region of the world especially sensible to environmental changes and stresses, while a general development and population growth is also expected, a risk-based approach to coastal areas impacts assessment was necessary from a management perspective. Not only rising sea-levels are considered in the study but also the wave climate, tides and surges, in a combined manner. This ultimately resulted in the analysis of inundation from sea-level rise and coastal flooding due to extreme sea-levels, from the combination of tides, surges and wave set-up. Beach erosion was also studied from a simple relation with sea-level rise, although erosion rates were also identified from changes in the wave mean energy flux direction, with special focus on Baja California, southern Brazil and some Caribbean islands.

The risk methodology followed in the work is based on the analysis of the probability of occurrence of certain coastal hazards and their potential consequences, distinguishing the terms of exposure and vulnerability separately, but not considering the economic dimension of the problem. In particular the impacts of inundation, coastal flooding extreme events and beach erosion are addressed through an integrated risk-based approach which relies on the statistical analysis of both instrumental and numerical datasets for wave climate and sea-level components, distinguishing astronomic tide, storm surge and mean sea-level. For computation of trends, regression techniques were employed while for the specific study of extremes a non-stationary extreme model was required.

To allow the analysis of the vulnerability terms, a geospatial analysis was performed for several datasets, including: population density (GRUMP-CIESIN), land uses (Land cover and GlobCover), coastal typology and roads and railways (DCW). The coastline of the region was divided into 14,494 units of study where the different data were combined and integrated.

Results showed that largest inundation risks due to rising sea-levels concentrate in the urban areas of the Atlantic coast and the Caribbean islands. However, should a situation of 1 m of increase in mean water level occur, the areas at higher risk would be the Caribbean islands and the east coast of Brazil, alongside with Central America, Ecuador and Peru. These results further support the special concern that must be taken with El-Niño events in the Pacific coast when compared with sea-level rise past changes.

Temporary flooding events, from the combined action of tides and extreme sea-levels, due to effect of winds, pressure and waves, have also been taken into consideration. It has been shown to be a factor of the greatest relative importance in some coasts. Trends in the region of 10 mm/yr were found for the Rio de la Plata area from a combination of trends in sea-level rise and storm surges extremes. The pacific coast of Mexico also showed 6 mm/yr of change over the last decades. In the rest of the region, flooding trends remain close to sea-level rise rates.

The analysis was performed through a non-stationary extreme value model so that changes in the probability density functions were possible to be identified. The probability of certain values, associated with a given return period, seems to have varied accordingly. Larger changes in recurrence of extremes values concentrate in the southern Atlantic coast, although, from a relative increment point of view, southern coast of Brazil, Uruguay and certain areas of the Caribbean have undergone changes about a 30 and 40% during the last 6 decades in the 50-yr flooding event. Despite not considering hurricanes behavior adequately for the tropical areas in the present analysis, results seem to be revealing in those latitudes.

In terms of risk, the coasts at highest risk for coastal population are located in Brazil and Mexico and on the Caribbean islands. The main factor configuring these risks is the urban agglomerations. Another area of concern is the Rio de la Plata region due to concentration of population and strong trends in flooding levels. Considering roads and railways in the coastal areas, the zones of greatest risk are concentrated in highly specific locations in southern Brazil, Rio de la Plata, Central America and the Northern Caribbean islands. Whether these affections would present different relative importance and how it will affect the transport system for local communities is out of the scope of the present research, but an interesting factor for measuring the consequences in monetary terms.

In light of these results, pocket beaches in the region could have undergone erosion in line with changes in mean wave energy direction sustainedly during the last years and may remain in the near future. This combined with increases in sea-levels imply risks from coastal protection and available beach resource. Coasts of Brazil and the Caribbean present the highest risks in terms of coastal protection, while the Caribbean coasts are the most threatened areas in terms of beach resource losses.

Chapter 6

Conclusions and future research

"Don't judge each day by the harvest you reap but by the seeds that you plant"

Robert L. Stevenson, Scottish writer

6.1 General overview

This Thesis has addressed the study of the global wave climate and its temporal variability to determine some of the potential coastal and technological implications under a risk-based framework. Several steps were taken towards such an aim.

First of all, it was necessary to develop a new database of global wave data with adequate time span and sufficient quality along the continental coastal margins. Based on it, an analysis of wave climatology was performed with a planetary scope and facing different time scales, covering from the seasonal to the inter-annual and long-term changes.

Subsequent to the understanding of wave climatology and its variability, the problem of potential consequences for the human system was raised. It was intended to face the problem from a risk analysis perspective since changes by themselves do not provoke consequences. It is indeed the combination of the probability of hazards with the possible consequences on the system which would utterly lead to a successful diagnosis of the situation. For this, an integral methodology for risk assessment was adapted from the disaster risk state of art and applied to coastal specific problems.

From the myriad of potential effects of a changing climate, the work focused, in particular, on some of the technological and environmental effects of a changing wave climate. Specifically, one of the problems tackled was the implications for the wave energy technologies of changing wave energy resources and varying wave extremes, in terms of operations and survivability. For coastal zones, the aim fell on the study of erosion and coastal flooding in Latin America and the Caribbean, by way of example. Also, the impacts of the varying marine dynamics were combined with a deep analysis of the exposure and vulnerability of the coasts in the region.

Several advances and findings were found in the whole process which are outlined in this section.

6.2 Contributions

The present work was aimed at studying the temporal variability and the long-term changes in the global wave climate in order to provide a first insight into some coastal and technological risks which may derive from them. To reach that end, in a holistic approach, it was needed to develop an accurate wave dataset of enough time span and some other methods and tools to analyze the data and the temporal variability.

A global wave dataset (GOW) was firstly simulated with a planetary scope covering the period from 1948 to 2008 and corrected with altimeter data from 1992 to 2008. Tropical cyclones spurious data was statistically identified and rejected. The data was extensively validated with altimetry and buoy observations in order to assure the statistical correspondence with the wave conditions in different time scales. This dataset constitutes the basis for further analysis of the wave climate, its variability and its potential effects.

A description of the global climatology followed although with great similarities to other works. Special focus is given to the description of periods, important for wave energy study, and to the directional behavior of the wave climate. These last two features have been less attended in the current state of the art.

Concerning the variability of the wave climate, the variability of the wave heights, the mean energy flux direction and the wave power have been studied in relation to many of the most influencing climate patterns in the globe. From this analysis, consequences for coastal areas and an estimate of their mean contribution to the wave climate parameters has been inferred. The final conclusion is that rates of change and temporal variations in the wave climate are necessary to be considered somehow in the coastal hazard zones.

Subsequent to the wave climate study, the GOW reanalysis was used to perform two main tasks: (1) the evaluation of the global wave energy resources, describing its spatio-temporal variability throughout different scales; and (2) a risk analysis of the absorbed wave power for four offshore Wave Energy Converters with a twofold scope: (a) the impact of resources variation in a life-cycle and (b) the survivability risk from expected variations in the 100-yr wave height.

For the evaluation of the global wave energy resource, the GOW database was validated with buoy data in wave power levels for monthly and yearly scales. Results showed a good accordance at both time scales. The correction applied to the numerical hindcast was also checked in terms of wave energy estimates, revealing a considerable correction (over 40 %) along the continental margins.

There exists a considerable controversy on the figures of the global wave energy resource. In this work, a new method to assess the potential resource is proposed which should be more realistic since it takes into account the direction of the wave energy and the coastal alignment. The resource values, obtained from the GOW database on a hourly basis over the last six decades, were compared with the current state of the art. Long-term trends and influence of climate patterns were also investigated yielding to the conclusion that they are factors to account for in the wave energy studies.

Comprehensive information was provided in this work that may be useful in the wave energy field. Some examples are the wave power scatter diagrams or the frequency of occurrence of the combinations of wave heights and periods. They reflect the varying wave climate conditions and further confirms the need for a site-specific design of converters for each region.

With the aim of contributing to clarify what could be reasonably expected from several technologies at offshore depths, going beyond wave energy potential assessment, a risk-based method was proposed to consider the impact of the variability of the available resource on real devices. Unfortunately, since no detail information on matrix powers were available for different wave climate conditions, a method for the scaling of devices was proposed and successfully applied. The method was tested for four devices for which the risks from wave energy production and the structural survivability degree of the installation were studied through a life-cycle.

Other sort of consequences exist from a changing climate, many of them implying coastal impacts as research has recently shown. An assessment of the potential impacts on the coastal areas has become increasingly important observed changes in sea-level, surges and waves. In particular, Latin America and the Caribbean is a region of the world especially sensitive to environmental changes and stresses. A general development and population growth is also expected, so a risk-based first approach to coastal areas impacts assessment is necessary from a management perspective. In particular the impacts of inundation, coastal flooding associated with extreme events and beach erosion were addressed through an integrated risk-based approach which relies on the statistical analysis of both instrumental and numerical datasets for wave climate and sea-level components, including the astronomic tide, storm surges and mean sea-level. Beach erosion was addressed from a simple relationship with sea-level rise, although erosion rates were also identified from changes in the dominant direction of the wave energy.

The risk methodology followed in the work was based on the analysis of the probability of occurrence of certain coastal hazards and their potential consequences, distinguishing the terms of exposure and vulnerability separately, but not considering the economic dimension of the problem.

For computation of trends and probability of hazards, regression techniques were employed while for the specific study of the extremes, a non-stationary extreme model was required.

To allow for the analysis of the vulnerability terms, a geospatial analysis was performed for several datasets, including: population density, land uses, coastal typology and distribution of roads and railways. The coastline of the region was divided into 14,494 units of study where the different data were combined and integrated.

6.3 Results and conclusions

6.3.1 Wave modeling

- A wave hindcast was developed with the model Wavewatch III and driven by the NCEP/NCAR reanalysis winds and ice fields. The resolution was of 1.5° longitude x 1.0° latitude on a global domain, covering the period from 1948 to 2008.

- Due to discrepancies with wave measurements, numerical data were corrected through the application of a calibration method which used altimetry data from the period 1992-2008. It ultimately leaded to a remarkable correction in the statistic distribution of the dataset, specially noticeable for the continents coastal margins.

- Since the outliers due to tropical cyclones were not appropriately reproduced in the hindcast, because of a lack of resolution in the wind fields, the calibration of the dataset would be affected by its presence. Caution was therefore taken in the calibration step. Such spurious data were statistically identified and removed from the correction. Also the regions prone to outliers appearance in dataset were identified.

- A verification of the calibration method was performed, obtaining a correction based on the altimetry data from 1992 to 2005, while its effect was judged with the observations from the period 2006-2008. It confirmed a regionally varying correction, specially remarkable for high waves range and at the coastal regions.

- An exhaustive validation of the results was performed with altimeter and buoy measurements. The diagnostic statistics showed a fine agreement both in the scatter data and in the statistical distribution of wave heights, indicating that the new reanalysis reflects appropriately the wave characteristics identified by satellites from 1992 to 2008. The underlying assumption is that it would also reflect the statistics of previous periods.

- Taking all into account, the spatial and temporal coverage of the dataset and the statistic behavior obtained for the full range of wave heights, confirms that this new database is suitable for further global variability analysis of wave climatology.

6.3.2 Wave Climatology and its variability

- Concerning wave climatology, special emphasis was placed on its directional behavior, which was an original part of this work. In this respect, it was confirmed that during the austral winter the swell waves coming from the Southern Ocean dominate these areas provoking large shifts in the time series of the energy flux direction. This occurs due to the widening and strengthening of the storms in the SH and the weakening in the NH. This behavior is also reflected in the seasonal variations within the tropics.

- With regard to the long-term changes, results showed that not only the mean values are increasing but also the high tail of the H_s distribution values do in general terms. Moreover, trends for the 90^{th} percentile are more intense than for the mean values, at the same time showing a lower correlation with the climate indices.

- However, there are regions of the oceans where extreme values are increasing and mean conditions are not. Such are the cases of the Southern Atlantic or the Northwestern Pacific. Differences were also identified in the North Atlantic where no significant changes are obtained but for the northern area.

- Surprisingly, the trend pattern obtained for the available satellite period (1992-2008) significantly differs from that computed for the last six decades (1948-onwards). This fact indicates that longer time span in observations is needed to obtain meaningful trends of change in wave height parameters from satellite altimetry. As a consequence, trend patterns from this data source should be taken with caution so far.

- The analysis here developed also reveals that not only are the wave heights increasing but also the number of extreme events at several areas of the global ocean. Additionally, the proportional change in the extreme intensities is not uniform throughout the global ocean.

- The question of possible changes in the directional behavior of the dominant wave energy was here explored. Sustained changes in the storm activity at both hemispheres seem to be inducing large shifts in the mean energy flux direction, with a clockwise sense in the south and counter-clockwise in the north. Greater shifts are found in the mid Pacific with changes of more than 1 degree/yr. It is worth noting that the directional trends were obtained from a regression model for directional data which was specifically designed for this purpose in this Thesis owing to the lack of such modeling in this field.

- Inter-annual variability was studied by obtaining the correlation patterns with the most prominent climate indices. The Artic Oscillation and the Southern Annular Mode are the most influencing climate patterns in the Northern and Southern Hemisphere, respectively. The correlation was obtained for the mean wave heights and a high percentile (90%). Results showed that the influence is greater under mean conditions. The contribution of the presence of each climate pattern (i.e. per unit of standardized index) was also shown to be in the range of a 10% in large areas of the oceans, even exceeding a 25% in some regions in particular. The influence varies spatially and in magnitude within the year but the relative contribution is sustained in a great proportion.

- The inter-annual correlation patterns were also obtained for the anomaly of the mean energy flux direction obtaining clear evidences of shifts with some climate patterns. Southern Annular Mode controls the direction of wave energy in the Southern Hemisphere as already proved by previous research. However, the North Atlantic Oscillation, the Artic Oscillation and the Pacific North American Index seems to hold great influence on the Northern Hemisphere. This information constitutes a basis for further modeling on the inter-annual influence of beach rotation, coastal flooding and sediment transport variations on the global coasts.

- In the analysis of the results it was found that a global increase in the ocean wave power over the last decades may have occurred. In principle, such sustained change could be attributed to the numerical origin of the data or possible inhomogeneities. The former can not be discarded but the increase is strongly correlated with the Sea Surface Temperature. Results have been confirmed with satellite wave data in the available altimeter period (1992 onwards). The causes of this correlation and whether it enables an extrapolation into future of wave power based on variations in sea surface temperature needs further insight. Ocean and storm activity are indeed linked and, should this relationship be confirmed, wave energy could become an indirect measure of the climate change effect on storm activity.

6.3.3 Environmental and technological risks of a changing wave climate

The main conclusions from the technological risks study are listed below.

- The global offshore wave power is estimated in the region of 1 to 10 Twh (between 9,000 and 90,000 Twh/yr). A recent estimation was made in 32,000 Twh/yr considering all possible directions. In this work a new approach was developed, through a computation of the resource on a hourly basis in the period from 1948 to 2008 and taking also into consideration the direction of the energy and the coastal alignment. The global gross theoretical wave power was hence estimated approximately in 16,000 Twh/yr (corresponding with 1.8 Twh), being the standard deviation over 1,000 Twh/yr and the mean rate of long-term change of about 58 Twh/yr. This figure differs from previous estimations although when considering the full range of directions the figures were in close agreement with previous works.
- Only about a fraction of a 25 % of the theoretical resource is roughly considered as an indicator of possible technical absorption in the final converters.
- With respect to the spatial variability, the Southern Hemisphere showed a larger resource alongside with a lower variability. Meanwhile, the North-Atlantic, despite its large mean resource, revealed a large variance within the year. In general terms, the Northern Hemisphere evidenced a larger variability at high latitudes. Tropical areas are, however, more stable and, therefore, provide a small but sustained resource throughout the year of 15 to 20 kw/m. In other regions of the globe, this variability is also a matter for consideration in design and planning of wave farms. On a regional basis, it was also detected that the western borders of the continents present a higher potential and higher variability.
- From the correlation patterns with the most prominent climate indices, the most outstanding results were obtained for the Artic Oscillation, North-Atlantic Oscillation, East Atlantic and Pacific North American indices in the Northern Hemisphere, while the Southern Annular Mode and the Southern Oscillation Index are the dominant modes in the Southern Hemisphere.
- The mean contribution to wave power was also investigated. Although the effect of a climate index in the wave power may be larger in magnitude when the resource is highest (storm season), it has been revealed that during summer months, when the wave climate is milder, the presence of a certain climate pattern will affect in a higher degree. However, in the North Indian Ocean, a region with strong annual variability in the resource, the effect of the climate patterns is significantly remarkable in winter, when the variability range is

larger. In the light of these results, it was confirmed that natural variability should be a greater factor of concern for wave energy exploitation and design issues. Moreover, in some cases (like in the Southern Hemisphere with the SAM) inter-annual variability contribution are in the order of magnitude of the mean seasonality.

- Long-term trends were also addressed in this work. Especially remarkable were the trends found in the Southern Hemisphere, in the region of 1 kw/m/yr and sustained throughout the seasons. However, special caution must be taken regarding the fact that this area of the globe is the less reliable from the numerical atmospheric reanalysis; so it is for the wave reanalysis used in the analysis.

- In order to study the absorption of potential wave converters at a planetary scale, four devices were theoretically optimized for different wave climate conditions. Scaling of the four devices was based on Froude similitude so as each wave power matrix was transferred to different wave climate types. About an 85 % of theoretical wave power resource lied in the boundary of absorption (from combination of wave heights and periods) for all devices assuming the scaling procedure. Different behaviors were identified at different latitudes depending on the technology. The results, although a first estimate, demonstrated that different devices are prone to show different performance depending on the wave climate types. As a result, installation analysis should require a site-specific optimized design and comparison of technologies.

- The trends in the absorbed wave power time series were studied for each device. It was evidenced that should the past changes persist into the future, the different technologies would not show the same response, being some of them more affected than others. For a better assessment, this analysis should be extended to the study of changes in the combination of wave heights and periods, provided that these changes were somehow integrated in terms of the total absorbed wave power.

- Although varying spatially, the results for the survival risk indicator, based on the expected changes in the 100-yr significant wave height event, showed a generalized reduction of the so defined *security index*. It is ultimately indicating an increase of the structural risk. The former indicator could be related to design factors for future wave farms facilities.

Regarding the environmental risks of a changing climate, with the main focus on erosion and flooding impacts, it should be stressed that:

- Results show that largest inundation risks due to the rising sea-levels concentrate in the urban areas of the Atlantic coast and the Caribbean islands of the Latin America and the Caribbean region. However, should a situation of 1 m of increase in mean water level occur, the areas most at risk would be the Caribbean islands and the east coast of Brazil, together with Central America, Ecuador and Peru. The results further supported the special concern that must be taken with El-Niño events in the Pacific coast in comparison with sea-level rise observations, so far.

- Temporary flooding events, from the combined action of tides and increased sea-levels due to effect of winds, pressure and waves, have also been taken into consideration. It was confirmed as a factor of the greatest importance at some coasts. Trends in the region of 10 mm/yr were found for the Rio de la Plata area from a combination of trends in sea-level rise and storm surges. The pacific coast of Mexico also showed a 6 mm/yr rate of change over the last decades. In the rest of the region, flooding trends remain close to the sea-level rise rates.

- Changes in the probability density functions were identified through a non-stationary extreme value model. The probability of certain values (associated with a given return period) seems to have varied accordingly. Larger changes in the recurrence of extreme values concentrate in the southern Atlantic coast, although, from a relative point of view, southern coast of Brazil, Uruguay and certain areas of the Caribbean have undergone about 30 and 40% over the last 6 decades in the 50-yr flooding event. Despite not considering hurricanes behavior adequately for the tropical areas in the present analysis, results seem to be revealing in those latitudes.

- In terms of risk, the highest risk for coastal population was found in Brazil, Mexico and the Caribbean islands. The main factor originating these risks is urban agglomeration. Another area of concern is the Rio de la Plata region due to the concentration of population and strong trends in flooding levels.

- Considering roads and railways in the coastal areas, the zones of greatest risk are concentrated in scatter locations in southern Brazil, Rio de la Plata, Central America and the Northern Caribbean islands. Whether these affections would present different relative importance and how it may affect the transport system for local communities fell out of the scope of the present research, but it is an interesting factor to be addressed.

- In light of the results, pocket beaches in the region could have undergone erosion in line with changes in mean wave energy direction steadily during the last years and may remain in the near future. This, combined with increases in sea-levels, imply risks for coastal protection and the available beach resources. The coasts of Brazil and the Caribbean present the highest levels of risk in terms of coastal protection. Meanwhile, the Caribbean coast is the most threatened area in terms of available beach resource.

6.4 Future research

This Thesis constitutes a first step towards a further insight in different issues. These new challenges are described below.

In the area of **wave reanalysis** and modeling:

- To develop a reanalysis of higher resolution than GOW, of 0.5°, using the winds of NCEP/NCAR (Reanalysis I) and other forcings of higher resolution (CFSR), in order to obtain two datasets, one with longer time span and other with higher definition and quality, especially interesting for design purposes. The final scope of this task would be to provide accurate data for engineering design in offshore and coastal areas.

- To compare the two datasets of higher resolution and analyze the common period from 1979 onwards in terms of statistics behavior, variability, trends and other differences. In case that the most modern reanalyses are not updated in the future (to date finishing in 2010), the long-time span of the original results from NCEP/NCAR could be complemented or corrected based on the common period and its comparison.
- Future projections based on Global Circulation Models could be easily performed in a similar manner to the hindcast past data.
- Wave modeling based on NOAA-CIRES forcing for the period 1971-2008 could be helpful for an understanding of wave climate, although the quality of the results would be lower and similar to those obtained for the future projections.

Concerning the study of **wave climate and variability**, future research could address:

- The development of response models for climate indices and coastal impacts and dynamics. Some efforts have already been made in this regard for wave heights and sea-level anomaly for some of the publications already sent or under preparation which have resulted from this work (see [Reguero et al., 2012a]).
- Development of a new approach and framework for the consideration of the inter-annual variability and coastal risks in the coastal management practices. Since many areas are prone to be more affected by this scale variability rather than by the long-term changes, an insight into these problems would be more than worthy. Insurance efforts are already facing these problems in many areas of the world.

With regards to **risk analysis** and other related studies, advances may be taken in the following regards:

- Including the economic dimension in the risk analysis. Indirect affections should also be considered.
- Vulnerability terms should be a function of time and an insight into this matter would be an important advance. However, a main drawback is unfortunately imposed by the limited availability of data. Specific studies on vulnerability and exposure of detailed areas, from regional to urban scale, present enough entity by themselves as to be a topic of research. Many efforts are currently being invested in these issues globally.
- A more detailed study on coastal impacts such as erosion due to storm events and hurricanes should be made in specific areas identified from the diagnosis performed in this work. Higher resolution of data and specific models are available for such a challenge.
- An analysis of the safety degree of sea works such as vertical or rubble-mound breakwaters would be interesting, provided the design conditions (e.g., 500-yr significant wave height) have considerably varied in the last decades. This could be done through Hudson stability number and computing its changes in time and along the global coastline. A comparison

with current structures designs and with past failures would constitute a valuable validation.

- Works like [Mendelsohn et al., 2012], where socio-economic development is coupled with the past tropical cyclones damages, could also be extended to other coastal impacts like sea-level, non-hurricane flooding and adaptation. This matter is linked with the evolution of vulnerability with time, with damage even in the absence of changes in the hazards, and the economic dimension of the problem.
- Statistics based simulation techniques, such as previous experiences in USACE, could also be widely extended to coastal engineering practices for risk evaluation of projects.
- For Wave Energy Converters, an optimization of design based on an intensive and accurate knowledge (and forecast) of the wave climate, its spectral definition and the temporal variability in the resources is also ahead of us.
- One of the most prominent challenges would be introducing a risk-based decision framework for projects and programmes. Their implementation is being extended in engineering practices at several areas of the world, worth mentioning the USA, but such an approach is lacking in other regions. Introduction of a risk dimension, quantitatively and methodologically, would be a great advance and a very useful tool.

Appendix A

Statistical methods to study time variability

A.1 Introduction

This annex describes the methods and techniques used along the work for the analysis of the time variability in the global wave climate, focusing on their mathematical foundation. It first explains the basis of the study of temporal variability: inter-annual variability and long-term trends. Note that when the methods did not present enough entity to be included in this annex, or were case specific, their explanation is included in the corresponding chapter. However, this was not the rule.

Most of the techniques are well known in the discipline but an original contribution should be remarked since it constitutes a new approach for directional study of long-term trends. The circular regression model used for the directional variables was originally developed for this work, which is explained in section A.2.5.

A.2 Methods for the study of long-term trends, inter-annual variability and trend extrapolation

A.2.1 Introduction

A trend is generally taken to mean a (non-random) smooth function with a systematic, generally monotonic, variation in time series. The phenomenon of trend is ubiquitous in climate data. The simplest example case is a linear trend observed in many atmospheric time series, such as that in recent global surface temperature, which has become known as global warming.

The detection of long-term trends is affected by a number of factors, including the size of trend to be detected, the time span of available data, and the magnitude of variability and autocorrelation of the noise in the data ([Weatherhead et al., 1998]).The number of years of data necessary to define the trend depend on, among other factors, the size of the trend, the magnitude of the variance and the autocorrelation coefficient of the noise. As a result, some environmental variables allow an easier detection of trends (e.g., sea-level rise) than others because of their low variability and autocorrelation (e.g., wave direction or extremes). To this end, different models and techniques are needed, depending on: the variable to study, whether they are scalar or directional and the noise of the signal with respect to the size of the trend. The different techniques explored in the present work are explained hereafter.

Environmental time-series show greater variability than the long-term trends over the periods of several years, seasons or months. Large scale climatic patterns affect other related climate variables such as wave climatology or sea-levels. The study of these factors is necessary to determine the influence and quantitative contribution of the different time scales.

A.2.2 Linear regression

Regression analysis is a statistical technique which allows modeling the functional dependency between two variables and make predictions of one variable when other variables are known. It has been widely used in many different engineering, financial and science applications.

Linear regression also has an important application in the definition of trends, i.e. the long-term movement in time series data after other components have been accounted for. It tells whether a particular dataset has increased or decreased over a certain period of time. A trend line could simply be drawn by eye through a set of data points, but their position and slope is calculated more properly using statistical techniques like linear regression. Trend lines typically are straight lines, although some variations use higher degree polynomials depending on the degree of curvature desired.

This technique for trend detection is not valid in cases where other potential changes can affect the data (e.g. ENSO influence in time-series of sea-level rise), but is a simple and widely used approach. Researchers usually include several covariates in their regression analysis in an effort to remove factors that might produce spurious correlations.

Regression analysis consists in, based on data, calculating the regression coefficients based on the following assumptions:

1. There is a linear relationship between dependent and independent variables, as the scatter diagram indicates.
2. X observations are error free, but predictor variable Y has an error term ε which has zero mean and an unknown but constant variance σ^2 implying that the spread in data about the regression line is constant.
3. Errors are uncorrelated and normally distributed.

Either simple or multilinear, a linear regression analysis can be expressed as:

$$\boldsymbol{Y} = \boldsymbol{X}\boldsymbol{\beta} + \boldsymbol{\varepsilon}, \tag{A.1}$$

where $\boldsymbol{Y}$ contains n observations of the dependent variable, $\boldsymbol{X}$ is the design matrix of size $n \times (p+1)$ where x_{ij} is the observation of the ith regressor variable in the jth data set, $\boldsymbol{\beta}$ is the regression coefficients vector to be determined with p components, and $\boldsymbol{\varepsilon}$ are uncorrelated and identically distributed normal random variables with zero mean and unknown constant variance.

There are several methods to estimate the parameters. If the least-squares method is used to estimate the parameters the following problem is solved:

$$\underset{\boldsymbol{\beta}}{\text{Minimize}} \quad \mathrm{SS}_E = \boldsymbol{\varepsilon}^T\boldsymbol{\varepsilon} = (\boldsymbol{Y}-\boldsymbol{X\beta})^T(\boldsymbol{Y}-\boldsymbol{X\beta}) \ . \tag{A.2}$$

The $(1-\alpha)$ confidence interval for each parameter is equal to:

$$\begin{aligned} \beta_j^{\text{up}} &= \hat{\beta}_j + t_{(1-\alpha/2,n-p-1)}\hat{\sigma}_j, \ j=0,1,\ldots,p \\ \beta_j^{\text{lo}} &= \hat{\beta}_j - t_{(1-\alpha/2,n-p-1)}\hat{\sigma}_j, \ j=0,1,\ldots,p, \end{aligned} \tag{A.3}$$

where $t_{(1-\alpha/2,n-p-1)}$ is the Student's t-distribution $(1-\alpha/2)$ quantile with $n-p-1$ degrees of freedom and $\hat{\sigma}_j$ is the estimated standard deviation for parameter j:

$$\hat{\sigma}_j = \sqrt{\frac{\hat{\boldsymbol{\varepsilon}}^T\hat{\boldsymbol{\varepsilon}}}{n-p-1}\left[\left(\boldsymbol{X}^T\boldsymbol{X}\right)^{-1}\right]_{jj}}, \tag{A.4}$$

where $\left[\left(\boldsymbol{X}^T\boldsymbol{X}\right)^{-1}\right]_{jj}$ is the j-th diagonal element of the inverse matrix.

More details on statistic and probabilistic theory can be consulted in [Cox and Hinkley, 1974, Mukhopadhyay, 2000, Bickel and Doksum, 2000].

A.2.3 Heteroscedastic regression model

Consider the standard linear regression model

$$\boldsymbol{y} = \boldsymbol{X\beta} + \boldsymbol{\varepsilon}, \tag{A.5}$$

where $\boldsymbol{y} = (y_1, y_2, \ldots, y_n)^T$ is a $n \times 1$ response variable vector, $\boldsymbol{X}$ is a $n \times k$ matrix of predictor variables often called "design matrix", $\boldsymbol{\beta}$ is a $k \times 1$ vector of regression coefficients or parameters, and $\boldsymbol{\varepsilon} = (\varepsilon_1, \varepsilon_2, \ldots, \varepsilon_n)^T$ is a $n \times 1$ vector of random errors assumed to be jointly normally distributed random variables $\boldsymbol{\varepsilon} \sim N(\boldsymbol{0}, \sigma^2\boldsymbol{V})$, where $\sigma^2\boldsymbol{V}$ is a positive definite variance-covariance matrix.

Regression parameters $\boldsymbol{\beta}$ are usually estimated using the WLS method,

$$\underset{\boldsymbol{\beta}}{\text{Minimize}} \ \boldsymbol{\varepsilon}^T\boldsymbol{W}\boldsymbol{\varepsilon} = \underset{\boldsymbol{\beta}}{\text{Minimize}} \ (\boldsymbol{Y}-\boldsymbol{X\beta})^T\boldsymbol{W}(\boldsymbol{y}-\boldsymbol{X\beta}), \tag{A.6}$$

where $\boldsymbol{W} = \boldsymbol{V}^{-1}$. For model (A.5), WLS coincides with the maximum likelihood (ML) estimation method. Note that, for homoscedastic models, $\boldsymbol{W}$ corresponds to the identity matrix, i.e. $w_{ii} = 1;\ i = 1, \ldots, n;\ w_{ij} = 0;\ i, j = 1, \ldots, n$ and $i \neq j$, and (A.6) becomes the traditional least squares (LS) method.

When the homoscedastic assumption (constant variance) does not hold, it is often possible to transform the response variable to stabilize the variance by using certain transformations to the response variable. However, here a nonlinear heteroscedastic regression model is adopted.

An intrinsically (nonlinearizable) nonlinear regression model can be written as

$$y_i = f_\mu(x_i;\boldsymbol{\beta}) + \varepsilon_i; \quad i = 1, 2, \dots, n, \tag{A.7}$$

where the function f_μ is known and nonlinear in the parameter vector $\boldsymbol{\beta}$, and $\varepsilon_i; i = 1, \dots, n$ are jointly normally distributed $\boldsymbol{\varepsilon} \sim N(\mathbf{0}, \sigma^2\boldsymbol{V})$ errors as in model (A.5).

Like in (A.6), the standard NWLS method, for $\boldsymbol{W} = \boldsymbol{V}^{-1}$ diagonal, can be stated as

$$\underset{\boldsymbol{\beta}}{\text{Minimize}}\ \boldsymbol{\varepsilon}^T\boldsymbol{W}\boldsymbol{\varepsilon} = \underset{\boldsymbol{\beta}}{\text{Minimize}} \sum_{i=1}^{n} w_{ii}\left(y_i - f_\mu(x_i;\boldsymbol{\beta})\right)^2, \tag{A.8}$$

where n is the number of observations. Note that analogously to the linear case, nonlinear regression models can also be used including weights in the formulation.

For wave hindcast data, a simple scatter plot of hindcast versus instrumental data allows observing how the variance of the regression model changes over the regression function. Consequently, we consider a nonlinear heteroscedastic regression model in which the standard deviation σ_i of the ith error is a function of the predictor variable (x_i):

$$\sigma_i = f_\sigma(x_i;\boldsymbol{\theta}) = w_{ii}^{-1/2}, \tag{A.9}$$

where $\boldsymbol{\theta}$ is a new $s \times 1$ vector of coefficients or parameters. If the parameter vector $\boldsymbol{\theta}$ were known, estimation of the parameter vector $\boldsymbol{\beta}$ could be based on the NWLS method (A.8). However, the values of $\boldsymbol{\theta}$ are usually unknown, and can be estimated using maximum likelihood methods. Thus, assuming that random errors are uncorrelated and normally distributed random variables each with mean zero and standard deviation given by (A.9), the whole set of model parameters ($\boldsymbol{\beta}$ and $\boldsymbol{\theta}$) can be jointly estimated maximizing the log-likelihood function:

$$\ell(\boldsymbol{\beta},\boldsymbol{\theta}) = -\sum_{i=1}^{n}\log\left(f_\sigma(x_i;\boldsymbol{\theta})\right) - \frac{1}{2}\sum_{i=1}^{n}\left(\frac{y_i - f_\mu(x_i;\boldsymbol{\beta})}{f_\sigma(x_i;\boldsymbol{\theta})}\right)^2. \tag{A.10}$$

The estimates $\hat{\boldsymbol{\beta}}$ that maximize the log-likelihood function (A.10), and solve (A.8), allow calculating the residual vector $\hat{\boldsymbol{\varepsilon}}$, which is defined as:

$$\hat{\boldsymbol{\varepsilon}} = \boldsymbol{y} - f_\mu(\boldsymbol{x};\ \hat{\boldsymbol{\beta}}) . \tag{A.11}$$

The maximization of the log-likelihood function can be done using any of the available solvers. The algorithm here used has been the Trust Region Reflective Algorithm under Matlab software, also capable of dealing with upper and lower bounds through the function *fmincon*. For further details about the method, [Mínguez et al., 2011] can be consulted.

A.2.4 Trend-EOF analysis

In the last several decades, atmospheric scientists have contributed major efforts in climate data analysis to extract patterns from simulated and observed large gridded datasets. Various methods have been developed to find patterns of variability from the high-dimensional weather/climate system. Among these methods, Empirical Orthogonal Functions (EOFs) have been the most widely used in atmospheric science since the late 1940s (e.g., [Obukhov, 1947, Obukhov, 1960, Lorenz, 1956]; see also [Craddock, 1973] for a discussion of eigenanalysis in meteorology).

EOF technique relies on the identification of the Principal Components (PCs) of a dataset. The goal of principal component analysis is to identify the most meaningful basis to re-express a data set so that this new basis filters out the noise and reveal hidden structure.

Various trend detection methods exist in the literature. These methods are mainly devised for univariate time series. There is, however, no general method for gridded data, although EOFs and a few related methods have been used for that purpose.

However, EOFs are not precisely designed for trend detection. EOF analysis (e.g., [Lorenz, 1956]; [Obukhov, 1960]; [Kutzbach, 1967]) finds linear combination of the different variables of a gridded spatio-temporal field that successively maximizes variance subject to orthogonality constraints. The obtained linear combinations are the (uncorrelated) principal components (PCs) and the spatial (orthogonal) EOF patterns are the loadings of the PCs.

Given the importance of trends and because EOFs and closely related methods are unable, in general, to capture trends, Trend-EOF analysis was suggested by [Hannachi, 2007] as an alternative technique for the extraction of robust trend patterns from a space-time gridded dataset. The method consists of an eigen-analysis of the covariance matrix, similar to traditional EOFs, but takes the inverted ranks (the time positions of the sorted observations) instead of the direct observations. Since sequences of inverse ranks provide a robust measure of monotonicity, the maximization of the variance of a linear combination of inverse ranks corresponds to the maximization of monotonicity, yielding robust space-time trend patterns.

Let $X_i = \{x_1, x_2, ..., x_n\}$ be a time series, for times $t = \{t_1, t_2, ..., t_n\}$, of a geophysical variable at grid points $^{=}1, 2, ..., p$, thus configuring a data matrix of nxp values. To resolve the issue of trend, the concept of monotonicity was included. The solution is obtained by looking for a new transformation that gives a measure of monotonicity, so the original data are firstly sorted (e.g. in decreasing order.) Then the position in time of each value from the sorted series is used to constitute a new dataset, $Q_i = \{q_1, q_2, ..., q_n\}$, of time positions of sorted data (i.e. the inverse-ranks of the data). Inverse ranks in the matrix Q need to be weighted by the cosine of the corresponding latitude in order to correct for the non-uniform data distribution on the geographic grid.

To better understand the transformation, a simple illustration case is included. Let consider a simple time series for a certain location with five elements (time positions): $x = (0.4, 0, 0.2, 0.9, -0.3)$. The new transformed time series is obtained by sorting in order: $(-0.3, 0, 0.2, 0.4, 0.9)$. The new data would therefore be conformed of: $q = (5, 2, 3, 1, 4)$, which is a permutation of the original time series.

Then, maximum correlation between time positions of the sorted data identify times when the different time series are increasing (or decreasing) together. The leading modes based on this new correlation (or covariance) provide the answer to trends as is explained next. For further explanations, [Hannachi, 2007] can be consulted.

We require the following correlations (or covariances):

$$\rho(X_a, X_b) = cov(Q_a, Q_b) \tag{A.12}$$

for $a, b = 1, 2, ..., p$. Trend-EOFs and trend-PCs (TPCs) are then provided respectively by the 'EOFs' and the 'PCs' using the newly obtained covariance (or correlation) matrix:

$$\Gamma = [\rho(X_a, X_b)] = \frac{1}{n} \cdot Q^T \cdot H^T \cdot H \cdot Q \tag{A.13}$$

where $H = (I_n - \frac{1}{n} 1_n^T 1_n)$ is the centring operator, I_n the nxn identity matrix, and 1_n a column vector of length n containing only ones. So, if v is a eigenvector resulting from the eigen-decomposition above, the TPC (i.e. PC time series) in physical space is given by $w = HXv$, and the corresponding spatial pattern is composed of the regression coefficients between the TPC and the anomaly time series of the original field. The first TPC will maximize the total monotonicity, and will not be correlated with the second one, and, therefore will include the long-term trend if it exists ([Hannachi, 2007]; [Barbosa and Andersen, 2009]).

This technique presents several practical advantages that can be outlined ([Barbosa and Andersen, 2009]):

- Physical interpretability and continuity: as the total monotonicity is maximized for the whole domain the resultant long-term trend shows continuity along different locations and will not be affected by spurious data if existed.
- Separation of different trend patterns: because the second TPC maximizes the monotonicity but subjected to be uncorrelated with the first one (long-term trend), no residue is found in the other patterns.
- Inter-annual variations: this technique finds a long-term trend unaffected by inter-annual variations in the time series, like ENSO related data, which is particular useful for certain parts of the globe.
- Short time span: it is particularly useful for short time series, such as the ones based on satellite data.

A.2.5 Circular regression model

Data that describes directions, such as the mean wave directions, cannot be analyzed in the same manner as ordinary linear variables that measure, for example, size or quality. Standard statistical methods for linear responses cannot be applied because the variables are cyclical in nature, limited to 0 to 2π. Statisticians have developed special ways to analyze circular variables in earth sciences (e.g., [Mardia, 1972, Fisher, 1993, Mardia and Jupp, 2000]). The use of circular response models are also extent in other fields (see for example [Schmidt et al., 2009] with application in neuroscience). Here, a method based on iterative optimization is proposed to be used in the identification of long-term trends in circular variables.

The regression problem for a circular variable (i.e. wave directions) when varying in time (i.e. linear variable) is a complex task that cannot be addressed by linear regression analysis like in a linear-linear response. The linear variable, in this case time, can vary from an initial time reference, t_0, to an end date, t_n. However, the circular response is restricted to $[0, 2\pi]$ radians. The circular data are therefore bounded to a close space where the concept of origin is arbitrary or undefined. [Fisher and Lee, 1992] suggest that when the distribution of the circular variables are not too dispersed, the regression problem can be handled satisfactorily by transforming the data to continuous linear variables. This solution is adequate for most of the ocean basins owing to low variability in wave directions. However, it is not valid for a global analysis, especially at tropical latitudes where the range of variation is over 180° as is shown in chapter 3 for the seasonal behavior of the mean direction of wave energy. For this reason, a circular-linear regression is proposed, expressed as:

$$\theta = \beta_0 + \beta_1 \cdot t \tag{A.14}$$

where θ represents the circular data and β_i are the coefficients of the regression to be estimated. Note that the proposed regression model resembles a cylindrical response in time and it hence can be represented in cylindrical coordinates, as a circular response (i.e. polar axis) varying in time (i.e. z axis). As previously said, θ values range from 0 to 2π, and consequently for each value, θ_i, there are two options of distance to the regression line: $\theta_i - \widehat{\theta_i}$ and $2\pi - (\theta_i - \widehat{\theta_i})$. The basic difficulty lies on determining which is the minimum distance (i.e. residual) to the regression line (unknown and that needs to be determined). Figure A.1 illustrates the problem for two sample cases where the circular data and the regression line vary within the circle limits. The main objective is to minimize the square of residuals to the regression line, similarly to linear regression, but subjected to certain restrictions. This is expressed as:

$$\underset{\beta_0, \beta_1}{\text{Minimize}} \quad \sum_{i=1}^{n} f_i \cdot \epsilon_i^2$$

being

$$\epsilon_i = min(|2\pi - (\theta_i - \widehat{\theta_i})|, |\theta_i - \widehat{\theta_i}|); \forall i$$
$$\widehat{\theta_i} = \beta_0 + \beta_1 \cdot t_i; \forall i$$
$$\beta_{i,low} \leq \beta_i \leq \beta_{i,up}$$

where f_i represents possible relative weights that can be introduced in the optimization problem.

As graphically seen in the representation of the problem, the derivatives are not continual and the problem is not convex. Consequently, it needs an iterative method to be optimized. This has been performed through a parallelized optimization algorithm searching for local minima in a certain range of values for each parameter.

Once the optimum regression line is obtained, or equivalently, the minimum distances to the regression line defined, they are replaced in the original dataset and, this time, linear regression is used to compute the regression model, confidence intervals and rest of statistics, since the circular data values are not further restricted to $[0, 2\pi]$.

An application of the proposed model is shown in chapter 3 for detection of long-terms trends in the global mean wave energy direction. A cylindrical representation of the model can also be consulted therein.

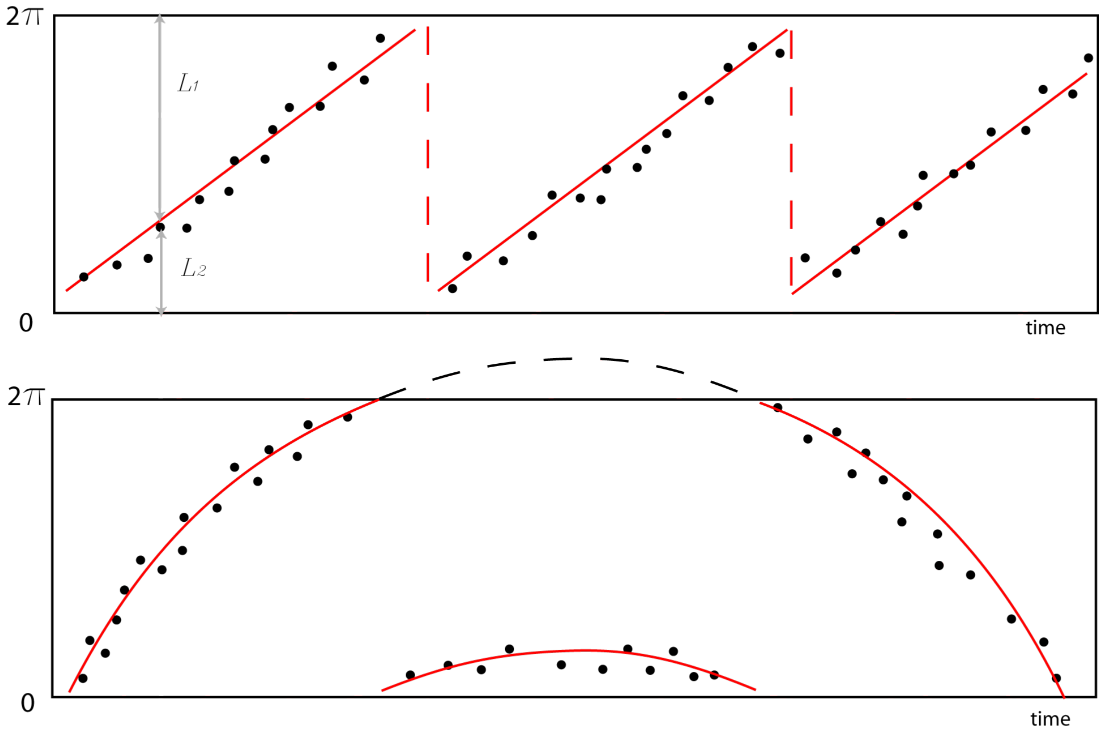

Figure A.1: Sketch of evolution in time of two circular variables, showing the non-continual regression line and the two possible circular lengths (L_1 and L_2) for each data value

A.2.6 Inter-annual variability

Climate variability refers to variations in the mean state and other statistics of the climate on spatial and temporal scales beyond individual weather events ([Solomon et al., 2007]). Many geophysical variables depend on large-scale changes in the atmosphere-ocean system, which are often represented by regional climate patterns expressed through different indices. This work is not intended to be limited to long-term trend analysis but the inter-annual variability is also explored.

To assess the influence of these climate patterns on wave climatology and sea-level variables, herein is proposed a regression model between each climate index time series and other climate variables (Y), as follows:

$$\frac{Y(t) - \mu_m}{\sigma_m} = \beta \frac{CI(t) - \mu_{CI}}{\sigma_{CI}} \tag{A.15}$$

where Y represents the monthly time series of each climate variable anomaly, after being de-trended and standardized to have unit variance and zero mean.

In a regression model, the correlation between two variables (Y and X) can be expressed as a function of the slope of the regression line and the standard deviations of the two variables ([Rodgers and Nicewander, 1988]). The relationship between correlation and regression can therefore be portrayed in:

$$r = \beta_{YX} \cdot (\sigma_X / \sigma_Y) \tag{A.16}$$

where β_{YX} is the slope of the regression line for predicting variable Y from X and σ denotes the standard deviation of each variable.

The regression model proposed above presents an useful characteristic. The standardized slope of the data (β) represents the Pearson's correlation coefficient between the climate index anomaly and the variable time series. From this relationship, the contribution per unit of the standardized climate index can also be studied for each variable by incorporating the corresponding monthly standard deviation.

In the following chapters different wave climate variables, like wave heights, directions or wave power, are related with inter-annual variability by these means.

A.2.7 Extreme value analysis

The study of extreme events and its temporal variability need to be addressed with a specific approach. Recent advances in the extreme value theory (see [Coles, 2001, Katz et al., 2002] as general references) allow modeling the natural variability of extreme events of environmental and geophysical variables. These methods introduce time-dependent variations within a certain time scale (year, season or month), improving our knowledge on some important processes which are time dependent. Additionally, a key issue is the possibility to construct regression models to show how the variables of interest may depend on other measured covariates such as the North Atlantic Oscillation or El Niño related events.

Several possible techniques have been used to characterize extreme events: high annual percentiles (e.g., [Woodworth and Blackman, 2004, Nicholls, 2011]), maxima in a block of time (e.g., [Araujo and Pugh, 2004, Méndez et al., 2007]), maxima of r-largest maxima method (e.g., [Guedes Soares and Scotto, 2004, Marcos et al., 2009]), and the peaks over a certain threshold

(POT; see [Goda, 2000, Zhang et al., 2009, Méndez et al., 2007]). Another possibility is to fit a distribution using monthly maxima (e.g. [Panchang and Li, 2006]). In general, these methods assume a homogeneous distribution for the extreme population data within a year. However, the hypothesis of homogeneity is not adequately satisfied, since the effects of seasonality are evident ([Holthuijsen, 2007]).

In an attempt to model the seasonal behavior of the maximum significant wave height within a year, [Carter and Challenor, 1981] proposed a month-to-month distribution, assuming that data are identically distributed within a given month and analyzing them separately. Subsequently, an annual distribution is obtained by combining the monthly distributions.

A similar analysis is performed by [Morton et al., 1997], applying a seasonal POT model to wind and significant wave height data. Recently, [Méndez et al., 2007] developed a time-dependent POT model for extreme significant wave height which considers the parameters of the distribution as functions of time (harmonics within a year, exponential long-term trend, climate indices as covariates, etc.). However, that work focuses on the definition of the higher extreme events of the year (values exceeding a given threshold) and disregards the extreme events within milder seasons, therefore being unable to model the entire variability within a year.

[Menéndez et al., 2009] and [Izaguirre et al., 2011] developed a time-dependent model based on the GEV distribution that accounts for seasonality and inter-annual variability of extreme monthly significant wave height. The non-stationary behavior is parameterized using functions of time (harmonic functions and covariates) for the parameters of the distribution. All these models try to reproduce the behavior of extreme value variables using sophisticated parameterizations.

To select the best parametrization and the corresponding optimal parameter estimates based on the Generalized Extreme Value (GEV) distribution the method proposed in [Mínguez, 2010]. The method minimizes the Akaike Information Criterion (AIC; [Akaike, 1974]), which establishes a compromise between obtaining a good fit and using a simple model. The main advantage of the method is that it converges monotonically to the final solution incorporating one single parameter at a time. The parameter at each iteration is included based on sensitivity analysis and/or perturbation techniques from the last solution obtained, thus reducing the number of different parameterizations tested drastically. Therefore, it it reduces considerably the computational time, providing analogous results as alternative methods.

A.2.7.1 Regression model based on time-dependent GEV distribution

The justification for using the GEV distribution is that it corresponds to the class of all possible limiting distributions for maxima. Moreover, the POT approach converges to the GEV distribution.

Time-dependent methods within a certain time scale, use time series of block maxima for successive periods (x_t), which are called maxima series, where x_t is the selected maxima for a given period (e.g., month) t.

Therefore, monthly maxima series (MMS) X_t of the variable for month t follows a GEV distribution with time-dependent location parameter μ_t, scale parameter ψ_t, and shape parameter

ξ_t, with probability density function (PDF) given by:

$$g(x_t;\mu_t,\psi_t,\xi_t)=\begin{cases}\dfrac{\exp\left\{-\left[\xi_t\dfrac{(x_t-\mu_t)}{\psi_t}+1\right]_+^{-1/\xi_t}\right\}}{\psi_t\left[\xi_t\dfrac{(x_t-\mu_t)}{\psi_t}+1\right]_+^{1+\dfrac{1}{\xi_t}}}; & \xi_t\neq 0,\\[2ex] \dfrac{\exp\left\{\dfrac{\mu_t-x_t}{\psi_t}-\exp\left(\dfrac{\mu_t-x_t}{\psi_t}\right)\right\}}{\psi_t}; & \xi_t=0,\end{cases}$$

where $[a]_+ = \max(0,a)$, and the support is $x_t \le \mu_t - \psi_t/\xi_t$ if $\xi_t < 0$ (Weibull), $x_t \ge \mu_t - \psi_t/\xi_t$ if $\xi_t > 0$ (Fréchet), or $-\infty < x_t < \infty$ if $\xi_t = 0$ (Gumbel).

Note that we consider X_t as the random variable associated with the maximum at time t, and x_t a particular instance, value or data of the corresponding random variable. The corresponding cumulative distribution function is then given by:

$$F(x_t;\mu_t,\psi_t,\xi_t)=\begin{cases}\exp\left\{-\left[\xi_t\dfrac{(x_t-\mu_t)}{\psi_t}\right)\right\}; & \xi_t\neq 0,\\[2ex] \exp\left\{\dfrac{\mu_t-x_t}{\psi_t}-\exp\left(\dfrac{\mu_t-x_t}{\psi_t}\right)\right\}; & \xi_t=0,\end{cases}$$

The GEV distribution includes three distribution families corresponding to the different types of the tail behavior: Gumbel family, the case $\xi_t = 0$; Fréchet distribution, with $\xi_t > 0$; and Weibull family, with $\xi_t < 0$ and a bounded tail.

To introduce seasonality, possible long-term trends and the influence of different covariates, the model proposed by [Menéndez et al., 2009] is extended as follows:

$$\mu_t = \beta_0 + \sum_{i=1}^{P_\mu}\left[\beta_{2i-1}\cos(iwt)+\beta_{2i}\sin(iwt)\right] + \beta_{\mathrm{LT}}t + \sum_{k=1}^{Q_\mu}\beta_k^{\mathrm{co}}n_{k,t} \quad (A.17)$$

$$\log(\psi_t) = \alpha_0 + \sum_{i=1}^{P_\psi}\left[\alpha_{2i-1}\cos(iwt)+\alpha_{2i}\sin(iwt)\right] + \alpha_{\mathrm{LT}}t + \sum_{k=1}^{Q_\psi}\alpha_k^{\mathrm{co}}n_{k,t} \quad (A.18)$$

$$\xi_t = \gamma_0 + \sum_{i=1}^{P_\xi}\left[\gamma_{2i-1}\cos(iwt)+\gamma_{2i}\sin(iwt)\right], \quad (A.19)$$

where t is given in years, $\log(\psi_t)$ ensures positiveness of the scale parameter ($\psi_t > 0$), β_0, α_0, and γ_0 are mean values, β_i, α_i, and γ_i are the amplitudes of harmonics considered in the model, $w = 2\pi/T$ is the angular frequency, T is one year, and P_μ, P_ψ and P_ξ are the number of sinusoidal harmonics to be considered within the year, associated with the location, scale and shape parameters, respectively. Note that it is possible to consider the effects of long-term trends and covariate influences for both location and scale parameters, through the coefficients β_{LT}, α_{LT}, β_k^{co}; $k = 1, \ldots, Q_\mu$ and α_k^{co}; $k = 1, \ldots, Q_\psi$, where Q_μ and Q_ψ are the number of covariates considered (e.g., climate indices, monthly mean sea level pressure principal components, etc.) for location and scale parameters, respectively. $n_{k,t}$ is the value of covariate k at time t. It is assumed that long-term and covariate components related to the shape parameter are negligible, nevertheless, it could be incorporated easily in the methodology. In conclusion, the model is complex enough to account for seasonality, covariates and long-term trends.

Note that the distribution present time-dependent parameters (μ_t, ξ_t and ψ_t). This implies that the properties of the statistical distribution change in time and, as a result, the probability of a certain extreme value may vary within a year, in several years or along decades (i.e. if the long-term trend is significant).

For non-stationary or time-dependent GEV, the calculation of time-dependent return-level quantiles $q_{t,T}$ associated with a return period R (in years) can be carried out as:

$$q_{t,R} = \begin{cases} \mu_t - \frac{\psi_t}{\xi_t}\left[1 - \left(-\log\left(1 - \dfrac{1}{T}\right)\right)^{-\xi_t}\right], & \text{if } \xi_t \neq 0, \\ \\ \mu_t - \psi_t \log\left(-\log\left(1 - \dfrac{1}{T}\right)\right), & \text{if } \xi_t = 0. \end{cases} \tag{A.20}$$

Confidence intervals are obtained, assuming approximate normality for the maximum likelihood estimators, using the delta method ([Rice, 1994]).

The estimation of the return quantile q_R for a certain year t is obtained by solving:

$$1 - 1/T = \begin{cases} \exp[-\int_{t_i}^{t_i+L}(1 + \xi_t \frac{q_T - \mu_t}{\psi_t})]_+^{-1/\xi_t} dt] & \text{if } \xi_t \neq 0, \\ \\ \exp[-\int_{t_i}^{t_i+L}(\exp(\frac{\mu_t - q_T}{\psi_t})]dt], & \text{if } \xi_t = 0. \end{cases} \tag{A.21}$$

where L corresponds to one year.

For any model including a certain number of model parameters P_μ, P_ψ, P_ξ, Q_μ, and Q_ψ represented by the following parameter vector:

$$\boldsymbol{\theta} = (\beta_0, \beta_i, \beta_{\mathrm{LT}}, \beta_k^{\mathrm{co}}, \alpha_0, \alpha_i, \alpha_{\mathrm{LT}}, \alpha_k^{\mathrm{co}}, \gamma_0, \gamma_i), \tag{A.22}$$

and for n_d observations of monthly maxima x_t occurring at time t, model parameters are estimated using the method of maximum likelihood (see details in [Mínguez, 2010]).

Based on [Menéndez et al., 2009], the quality of the model is determined using the Akaike Information Criterion (AIC, [Akaike, 1974]), which establishes a compromise between obtaining a good fit and keeping the model as simple as possible. The best model is, therefore, selected based on minimizing the following objective function:

$$\underset{\boldsymbol{\theta}}{\text{Minimize}} \quad \text{AIC} = -2\ell^*(\boldsymbol{x}, \boldsymbol{t}; \boldsymbol{\theta}) + 2n_p \tag{A.23}$$

where $\ell^*(\boldsymbol{x}, \boldsymbol{t}; \boldsymbol{\theta})$ is the maximum log-likelihood optimal objective function for given parameters $\boldsymbol{\theta}$, and n_p is the number of parameters (harmonics, trends and/or covariates) included in $\boldsymbol{\theta}$. The term $-2\ell^*(\boldsymbol{x}, \boldsymbol{t}; \boldsymbol{\theta})$ measures the goodness of fit, while the number of parameters n_p favors the simplicity of the model. The automatic model selection is computed following the algorithm developed by [Mínguez, 2010].

Bibliography

[ABP, 2008] ABP (2008). Atlas of uk marine renewable energy resources. Technical report, ABP Marine Environmental Research limited, www.abpmer.co.uk.

[Adger, 2006] Adger, W. (2006). Vulnerability. *Global Environmental Change*, 16:268–28.

[Akaike, 1974] Akaike, H. (1974). A new look at the statistical model identification. *IEEE Transactions on Automatic Control*, (19):716–723.

[Alexandersson et al., 2000] Alexandersson, H., Tuomenvirta, H., Schmith, T., and Iden, K. (2000). Trends of storms in nw europe derived from an updated pressure data set. *Climate Research*, 14:71–73.

[Alheit and Bakun, 2010] Alheit, J. and Bakun, A. (2010). Population synchronies within and between ocean basins: apparent teleconnections and implications as to physical–biological linkage mechanisms. *Journal of Marine Systems*, 79(3):267–285.

[Allan and Komar, 2000] Allan, J. and Komar, P. (2000). Are ocean wave heights increasing in the eastern north pacific. *Eos, Transactions, American Geophysics Union*, 81:561–566.

[Allan and Komar, 2006] Allan, J. and Komar, P. (2006). Climate controls on us west coast erosion processes. *Journal of Coastal Research*, 22(3):511–529.

[Alves and Young, 2004] Alves, G. and Young, I. (2004). On estimating extreme wave heights using combined geosat, topex/poseidon and ers-1 altimeter data. *Applied Ocean Research*, 25(4):167–186.

[Alves, 2006] Alves, J. (2006). Numerical modeling of ocean swell contributions to the global wind-wave climate. *Ocean Modelling*, 11:98–122.

[Andrews et al., 2006] Andrews, E. D., Antweiler, R., Neiman, P., and Ralph, F. (2006). Influence of ENSO on Flood Frequency along the California Coast. *The Wave Energy Resource*, 17:337–348.

[Angelis-Dimakis et al., 2010] Angelis-Dimakis, A., Biberacher, M., Dominguez, J., Fiorese, G., Gadocha, S., Gnansounou, E., Guariso, G., Kartalidis, A., Panichelli, L., and Pinedo, I. (2010). Methods and tools to evaluate the availability of renewable energy sources. *Renewable and Sustainable Energy Reviews*, 15(2):1182–1200.

[Araujo and Pugh, 2004] Araujo, I. B. and Pugh, D. T. (2004). Sea levels at newlyn 1915-2005: Analysis of trends for future flooding risks. *Journal of Coastal Research*, 24(4C):203–212.

[Ardalan and Hashemi-Farahani, 2007] Ardalan, A. and Hashemi-Farahani, H. (2007). A harmonic approach to global ocean tide analysis based on topex/poseidon satellite. *Marine Geophysical Research*, 28:235–255.

[Babarit et al., 2012] Babarit, A., Halsb, J., Muliawanb, M., Kurniawanb, A., Moanb, T., and Krokstadc, J. (2012). Numerical benchmarking study of a selection of wave energy converters. *Renewable Energy*, 41:44–63.

[Bacon and Carter, 1991] Bacon, S. and Carter, D. (1991). Wave climate changes in the north atlantic and north sea. *International Journal of Climatology*, 11(5):545–558.

[Barbosa and Andersen, 2009] Barbosa, S. M. and Andersen, O. B. (2009). Trend patterns in global sea surface temperature. *International Journal of Climatology*, 2055(January):2049–2055.

[Barnett et al., 2006] Barnett, C., Hossell, C., Perry, M., Procter, C., and Hughes, G. (2006). Patterns of climate change across scotland. Sniffer project cc03, Scotland & Northern Island Forum for Environmental Research.

[Barnston and Livezey, 1987] Barnston, A. and Livezey, R. (1987). Influence of enso on Flood Frequency along the california coast. *Monthly Weather Review*, 115:1083–1126.

[Barstow, 1996] Barstow, S. (1996). World wave atlas. *Monthly Weather Review*, 4:24–35.

[Barstow et al., 2008] Barstow, S., Gunnar, M., Mollison, D., and Cruz, J. (2008). *Ocean wave energy*, chapter 4. The Wave Energy Resource, pages 93–132. Berlin: Springer.

[Bartholome and Belward, 2005] Bartholome, E. and Belward, A. (2005). Glc2000: A new approach to global land cover mapping from earth observation data. *International Journal of Remote Sensing*, 263(93):1959–1977.

[Bender, 2010] Bender, M.A., K. T. T. R. S. J. V. G. G. S. H. I. (2010). Modeled impact of anthropogenic warming on the frequency of intense atlantic hurricanes. *Science*, 327:454–458.

[Bengtsson et al., 2004] Bengtsson, L., Hagemann, S., and Hodges, K. (2004). Can climate trends be calculated from reanalysis data? *Journal of Geophysical Research*, (109).

[Bengtsson et al., 2006] Bengtsson, L., Hodges, K., and Roeckner, E. (2006). Storm tracks and climate change. *Journal of Climate*, 19:3518–3543.

[Bickel and Doksum, 2000] Bickel, P. J. and Doksum, K. A. (2000). *Mathematical Statistics: Basic Ideas and Selected Topics: Vol. I.* Prentice Hall, New York, second edition.

[Bird, 1985] Bird, E. (1985). *Coastline Changes: A Global Review.* Wiley and Sons.

[Bird, 2000] Bird, E. (2000). *Coastal Geomorphology: An Introduction.* Wiley and Sons, UK.

[Birkmann, 2006] Birkmann, J. (2006). *Measuring Vulnerability to Natural Hazards: Towards disaster Resilient Societies*. United Nations University.

[Booij et al., 1999] Booij, N., Ris, R., and Holthuijsen, L. (1999). A third generation wave model for coastal region, i: Model description and validation. *Journal of Geophysical Research*, 104:769–7666.

[Bruun, 1962] Bruun, P. (1962). Sea-level rise as a cause of shore erosion. *Journal of Waterways Harbors Division - American Society of Civil Engineers*, 88:117–130.

[Caires and Sterl, 2003] Caires, S. and Sterl, A. (2003). Validation of ocean wind and wave data using triple collocation. *Journal of Geophysical Research*, 108:3098, doi: 10.1029/2002JC001491.

[Caires and Sterl, 2005a] Caires, S. and Sterl, A. (2005a). 100-year return value estimates for ocean wind speed and significant wave height from the era-40 data. *Journal of Climate*, 18:1032–1048.

[Caires and Sterl, 2005b] Caires, S. and Sterl, A. (2005b). A new non-parametric method to correct model data: Application to significant wave height from the ERA-40 reanalysis. *Journal of Atmospheric and Oceanic Technology*, 22:443–459.

[Caires et al., 2004a] Caires, S., Sterl, A., Bidlot, J., Graham, N., and Swail, V. (2004a). Intercomparison of different wind-wave reanalyses. *Journal of Climate*, 17(10):1893–1913.

[Caires et al., 2004b] Caires, S., Sterl, A., Komen, G., and Swail, V. (2004b). The web-based knmi/era-40 global wave climatology atlas. *Bulletin of the World Meteorological Organization*, 53(2):142–146.

[Callaghan et al., 2008] Callaghan, D., Nielsen, P., Short, a., and Ranasinghe, R. (2008). Statistical simulation of wave climate and extreme beach erosion. *Coastal Engineering*, 55(5):375–390.

[Callaghan et al., 2009] Callaghan, D., Roshanka, R., and Andrew, S. (2009). Quantifying the storm erosion hazard for coastal planning. *Coastal Engineering*, 56(1):90–93.

[Camus et al., 2011] Camus, P., Mendez, F., and Medina, R. (2011). A hybrid efficient method to downscale wave climate to coastal areas. *Coastal Engineering*, doi: 10.1016/j.coastaleng.2011.05.007.

[Carnell and Senior, 2002] Carnell, R. and Senior, C. (2002). An assessment of measures of storminess: simulated changes in northern hemi- sphere winter due to increasing co2. *Climate Dynamics*, 12:467–476.

[Carter and Challenor, 1981] Carter, D. and Challenor, P. (1981). Estimating return values of environmental variables. *Quart. J. Roy. Meteor. Soc.*, 107:259–266.

[Carter and Draper, 1988] Carter, D. and Draper, L. (1988). Has the north-east atlantic become rougher? *Nature*, 332:494.

[Carter et al., 1994] Carter, T., Parry, M., Harasawa, H., and Nishioka, S. (1994). Ipcc technical guidelines for assessing climate change impacts and adaptations. Technical report, IPCC. Department of Geography, University College London, UK and the Center for Global Environmental Research, National Institute for Environmental Studies, Japan.

[Cavaleri et al., 2007] Cavaleri, L., Alves, J., Ardhuin, F., Babanin, A., Banner, M., Belibassakis, K., Benoit, M., Donelan, M., Groeneweg, J., Herbers, T., Hwang, P., Janssen, P. A. E. M., Janssen, T., Lavrenov, I. V., Magne, R., Monbaliu, J., Onorato, M., Polnikov, V., Resio, D., Rogers, W. E., Sheremet, A., McKee Smith, J., Tolman, H. L., van Vledder, G., Wolf, J., and Young, I. (2007). Wave modelling. The state of the art. *Progress in Oceanography*, 75(4):603–674.

[Cavaleri and Sclavo, 2006] Cavaleri, L. and Sclavo, M. (2006). The calibration of wind and wave model data in the mediterranean sea. *Coastal Engineering*, 53:613–627.

[Cazenave, 2008] Cazenave, A., L. A. L. W. (2008). Present-day sea level rise: A synthesis. *Oceanography. C.R. Geoscience*, 340:761–770.

[CEI-RMSL, 1987] CEI-RMSL (1987). *Responding to Changes in Sea Level: Engineering Implications*. Committee on Engineering Implications of Changes in Relative Mean Sea Level. Marine Board, National Research Council.

[CEPAL, 2012a] CEPAL (2012a). *Impactos del Cambio Climático en las costas de ALyC*. Efectos del Cambio Climático en la Costa de América Latina y el Caribe. CEPAL-ONU.

[CEPAL, 2012b] CEPAL (2012b). *Vulnerabilidad y exposición de las costas de ALyC frente al Cambio Climático*. Efectos del Cambio Climático en la Costa de América Latina y el Caribe. CEPAL-ONU.

[CEPAL, 2012c] CEPAL (2012c). *Vulnerabilidad y exposición de las costas de ALyC frente al Cambio Climático*. Efectos del Cambio Climático en la Costa de América Latina y el Caribe. CEPAL-ONU.

[Chelliah and Ropelewski, 2000] Chelliah, M. and Ropelewski, C. (2000). Reanalyses- based tropospheric temperature estimates: Uncertainties in the context of global climate change detection. *Journal of Climate*, 131:3187–3205.

[Chen et al., 2004] Chen, G., Bi, S.-W., and Ezraty, R. (2004). Global structure of extreme wind and wave climate derived from topex altimeter data. *International Journal of Remote Sensing*, 25(5):1005–1018.

[Ching-Piao et al., 2012] Ching-Piao, T., Ching-Her, H., Chien, H., and Hao-Yuan, C. (2012). Study on the wave climate variation to the renewable wave energy assessment. *Renewable Energy*, (38):50–61.

[Church and White, 2011] Church, J. and White, N. (2011). Sea-level rise from the late 19th to the early 21st century. *Surveys in Geophysics*, 32:585–602.

[Church et al., 2004] Church, J., White, N., Coleman, R., Lambeck, K., and Mitrovica, J. (2004). Estimates of the regional distribution of sea-level rise over the 1950 to 2000 period. *Journal of Climate*, 17:2609–2625.

[Church et al., 2010] Church, J., Woodworth, P., Aarup, T., and Wilson, S. (2010). *Understanding Sea Level Rise and Vulnerability.* Wiley UK.

[CIESIN, 2005] CIESIN (2005). *Gridded Population of the World and the Global Rural-Urban Mapping Project.* Center for International Earth Science Information Network (CIESIN), Columbia University.

[Coburn et al., 1991] Coburn, A., Spence, R., and Pomonis (1991). *Vulnerability and Risk Assessment.* Disaster Management Training Programme (DMTP) UNDRO/UNDP, Geneva.

[Coles, 2001] Coles, S. (2001). *An Introduction to Statistical Modelling of Extreme Values.* Springer, London.

[Collins et al., 2010] Collins, M., An, S., Cai, W., Ganachaud, A., Guilyardi, E., Jin, F., Jochum, M., Lengaigne, M., Power, S., Timmermann, A., Vecci, G., and Wittenberg, A. (2010). The impact of global warming on the tropical pacific ocean and el niño. *Nature Geoscience*, 3:391–397.

[Compo et al., 2011] Compo, G., Whitaker, J., Sardeshmukh, P., Matsui, N., Allan, R., Yin, X., Gleason, B., Vose, R., Rutledge, G., Bessemoulin, P., Brannimann, S., Brunet, M., Crouthamel, R., Grant, A., Groisman, P., Jones, P., Kruk, M., Kruger, A., Marshall, G., Maugeri, M., Mok, H., Nordli, A., Ross, T., Trigo, R., Wang, X., Woodruff, S., and Worley, S. (2011). The twentieth century reanalysis project. *Quarterly Journal of the Royal Meteorological Society*, 137(654):1–28.

[Cornett, 2008] Cornett, A. (2008). A global wave energy resource assessment. *Renewable Energy*, pages 1–9.

[Cotton, 1998] Cotton, P. (1998). A feasibility study for a global satellite buoy intercalibration experiment. Consultation Report 26 26, Southampton Oceanography Centre, Southampton Oceanography Centre, Southampton, UK, 73.

[Cox and Swail, 2001] Cox, A. and Swail, V. (2001). A global wave hindcast over the period 1958-1997: Validation and climate assessment. *Journal of Geophysical Research*, 106(C2):2313–2329.

[Cox and Hinkley, 1974] Cox, D. and Hinkley, D. (1974). *Theoretical Statistics.* Chapman and Hall, London.

[Craddock, 1973] Craddock, J. (1973). Problems and prospects for eigenvector analysis in meteorology. *Statistician*, 22:133–145.

[CRES, 2003] CRES (2003). Final report of the european thematic network on wave energy. Technical report, Centre for Renewables Energy Sources.

[Cruz, 2008] Cruz, J. (2008). *Ocean Wave Energy.* Heidelberg: Springer.

[Davison and Smith, 1990] Davison, A. and Smith, R. (1990). Models of exceedances over high thresholds (with discussion). *Journal of the Royal Statistical Society. Series B*, 52:393–442.

[De Santis et al., 2012] De Santis, A., Qamili, E., Spada, G., and Gasperini, P. (2012). Geomagnetic south atlantic anomaly and global sea level rise: A direct connection?. *Journal of Atmospheric and Solar-Terrestrial Physics*, 74:129–135.

[Dean and Dalrymple, 1991] Dean, R. and Dalrymple, R. (1991). *Water Wave Mechanics for Engineers and Scientists*. Advanced Series on Ocean Engineering. World Scientific.

[Dee et al., 2011] Dee, D., Uppala, S., Simmons, A., Berrisford, P., Poli, P., Kobayashi, S., Andrae, U., Balmaseda, M., Balsamo, G., Bauer, P., Bechtold, P., Beljaars, A. C. M., van de Berg, L., Bidlot, J., Bormann, N., C., D., R., D., Fuentes, M., Geer, A., Haimberger, L., Healy, S., Hersbach, H., Holm, E., Isaksen, L., Kallberg, P., Kohler, M., Matricardi, M., McNally, A., Monge-Sanz, B., Morcrette, J., Park, B., Peubey, C., de Rosnay, P., Tavolato, C., Thepart, J., and Vitart, F. (2011). The era-interim reanalysis: configuration and performance of the data assimilation system. *Quarterly Journal of the Royal Meteorological Society*, pages 553–597.

[Dijkstra, 2006] Dijkstra, H. (2006). The enso phenomenon: theory and mechanisms. *Advances in Geosciences*, 6(3):3–15.

[Dodet et al., 2010] Dodet, G., Bertin, X., and Taborda, R. (2010). Wave climate variability in the north-east atlantic ocean over the last six decades. *Ocean Modelling*, 31(120-131).

[Dodman, 2009] Dodman, D. (2009). *Population Dynamics and Climate Change*, chapter Urban Form, Greenhouse Gas Emissions and Climate Vulnerability. UNFPA-IIED.

[Dodman and Satterthwaite, 2009] Dodman, D. and Satterthwaite, D. (2009). *Assessing the Costs of Adaptation to Climate Change; A Review of the UNFCCC and Other Recent Estimates.*, chapter The Costs of Adapting Infrastructure to Climate Change., pages 73–89. IIED and Grantham Institute.

[Douglas, 1992] Douglas, B. (1992). Global sea level acceleration. *Journal of Geophysical Research*, 97(C8):12699–12706.

[Dunnett and JS., 2009] Dunnett, D. and JS., W. (2009). Electricity generation from wave power in canada. *Renewable Energy*, 34:179–95.

[ECLAC, 2011] ECLAC (2011). *Statistical yearbook for Latin America and the Caribbean*. United Nations Publication.

[Egbert and Erofeeva, 2002] Egbert, G. and Erofeeva, S. (2002). Efficient inverse modeling of barotropic ocean tides. *Journal of Atmospheric and Oceanic Technology*, 19:183–204.

[Emanuel, 2005] Emanuel, K. (2005). Increasing destructiveness of tropical cyclones over the past 30 years. *Nature*, 436:686–688.

[Enfield and Mayer, 1997] Enfield, D. and Mayer, D. (1997). Tropical atlantic sea surface temperature variability and its relation to el niño-southern oscillation. *Journal of Geophysical Research*, 102(C1):929–945.

[ESBI, 2005] ESBI (2005). Accessible wave energy resource atlas, ireland: 2005. Technical report, Environmental service - Marine Institute/Sustainable Energy.

[Falcao, 2010] Falcao, A. (2010). Wave energy utilization: A review of the technologies. *Renewable and Sustainable Energy Reviews*, 14:899–918.

[Falnes and Lovseth, 1991] Falnes, J. and Lovseth, J. (1991). Ocean wave energy. *Energy policy*, 19(8):768–775.

[Farr et al., 2007] Farr, T., Rosen, P., Caro, E., Crippen, R., Duren, R., Hensley, S., Kobrick, M., Paller, M., Rodriguez, E., Roth, L., Seal, D., Shaffer, S., Shimada, J., Umland, J., Werner, M., Oskin, M., Burbank, D., and Alsdorf, D. (2007). The shuttle radar topography mission. *Review of Geophysics*, 45(RG2004):33pp.

[Feng et al., 2006] Feng, H., Vandermark, D., Quilfen, Y., Chapron, B., and Beckley, B. (2006). Assessment of wind-forcing impact on a global wind-wave model using the topex altimeter. *Ocean Engineering*, 33(11-12):1431–1461.

[Fiore et al., 2009] Fiore, M., D'Onofrio, E., Pousa, J., Schnack, E., and Bertola, G. (2009). Storm surges and coastal impacts at mar del plata, argentina. *Continental Shelf Research*, 29(14):1643–1649.

[Fisher, 1993] Fisher, N. (1993). *Statistical Analysis of Circular data.* Cambridge Univ. Press.

[Fisher and Lee, 1992] Fisher, N. and Lee, A. (1992). Regression model for an angular response. *Climate Dynamics*, 48:665–667.

[Flather and Williams, 2000] Flather, R. and Williams, J. (2000). *Climate change effects on storm surges: methodologies and results*, pages 66–78. Climate Scenarios for Water-related and Coastal Impact. Norwich:CRU, ECLAT-2 Workshop Report, No 3.

[Folley and Whittaker, 2009] Folley, M. and Whittaker, T. (2009). Analysis of the nearshore wave energy resource. *Renewable Energy*, 34(7):1709–1715.

[Füssel, 2007] Füssel, H. (2007). Vulnerability: A generally applicable conceptual framework for climate change research. *Global Environmental Change*, 17:155–167.

[Geng and Sugi, 2003] Geng, Q. and Sugi, M. (2003). Possible change of extratropical cyclone activity due to enhanced greenhouse gases and sulfate aerosols - study with a high-resolution agcm. *Journal of Climate*, 16:2262–2274.

[Glickman, 2000] Glickman, T. (2000). *Glossary of Meteorology.* 2nd Edition. American Meteorological Society.

[Goda, 2000] Goda, Y. (2000). *Random Seas and Design of Maritime Structures.*, volume 15 of *Advanced Series on Ocean Engineering*, page 443. World Scientific.

[Goldenberg et al., 2001] Goldenberg, S. B., Landsea, C. W., Mestas-Nuñez, A. M., and Gray, W. M. (2001). The recent increase in atlantic hurricane activity: Causes and implications. *Science*, 293:474–479.

[González and Medina, 2001] González, M. and Medina, R. (2001). On the application of static equilibrium bay formulations to natural and man-made beaches. *Coastal Engineering,*, 43:209–225.

[Goodwin, 2005] Goodwin, I. (2005). A mid-shelf, mean wave direction climatology for south-eastern Australia, and it's relationship to the El-Niño - Southern Oscillation since 1878. *International Journal of Climatology*, 25:1715–1729.

[Gower, 2002] Gower, J. (2002). Temperature, wind and wave climatologies, and trends from marine meterological buoys in the north-east pacific. *Journal of Climate*, 15:3709–3718.

[Graham and Diaz, 2001] Graham, N. and Diaz, H. (2001). Evidence for intersification of north pacific winter cyclones since 1948. *Bulletin of the American Meteorology Society*, pages 1869–1893.

[Gray et al., 2010] Gray, L. J., Beer, J., Geller, M., Haigh, J., Lockwood, M., Matthes, K., Cubasch, U., Fleitmann, D., Harrison, G., Hood, L., Luterbacher, J., Meehl, G., Shindell, D., van Geel, B., and White, W. (2010). Solar influences on climate. *Review of Geophysics*, 48(RG4001):53.

[Group, 1998] Group, T. W. (1998). Changing waves and storms in the northeast atlantic? *Bulletin of the American Meteorology Society*, 79:741–760.

[Guedes Soares and Scotto, 2004] Guedes Soares, C. and Scotto, M. (2004). Application of the r-largest order statistics for long-term predictions of significant wave height. *Coastal Engineering*, 51:387–394.

[Guilyardi et al., 2009] Guilyardi, E., Wittenberg, A., Fedorov, A., Collins, M., Wang, C., Capotondi, A., van Oldenborgh, G., and Stockdale, T. (2009). Understanting El Niño in ocean-atmosphere general circulation models: progress and challenges. *Bulletin of the American Meteorological Society*, 90:325–340.

[Gulev and Grigorieva, 2004] Gulev, S. and Grigorieva, V. (2004). Last century changes in ocean wind wave height from global visual wave data. *Geophysical Research Letters*, 31(L24302).

[Gulev and Grigorieva, 2006] Gulev, S. and Grigorieva, V. (2006). Variability of the winter wind waves and swell in the north atlantic and north pacific as revealed by the voluntary observing ship data. *Journal of Climate*, 19:5667–5685.

[Gulev and Hasse, 1999] Gulev, S. and Hasse, L. (1999). Changes of wind waves in the north atlantic over the last 30 years. *International Journal of Climatology*, 19:1091–1117.

[Gulev et al., 2001] Gulev, S., Zolina, O., and Grigoriev, S. (2001). Extratropical cyclone variability in the northern hemisphere winter from the ncep/ncar reanalysis data. *Climate Dynamics*, 17:795–809.

[Hannachi, 2007] Hannachi, A. (2007). Pattern hunting in climate : a new method for finding trends in gridded climate data. *International Journal of Climatology*, 15(July 2006):1–15.

[Hanson et al., 2009] Hanson, J., Tracy, B., Tolman, H., and Scott, R. (2009). Pacific hindcast performance of three numerical wave models. *Journal of Atmospheric and Oceanic Technology*, 26:1614–1633.

[Hardoy and Lankao, 2011] Hardoy, J. and Lankao, P. (2011). Latin america cities and climate change: challenges and options to mitigation and adaptation responses. *Current opinion in Environmental sustainability*, 3:158–163.

[Hardoy and Pandiella, 2009] Hardoy, J. and Pandiella, G. (2009). Urban poverty and vulnerability to climate change in latin america. *Environment and Urbanization*, 21(1):203–224.

[Harley et al., 2010] Harley, M., Turner, I., Short, A., and Ranasinghe, R. (2010). Interannual variability and controls of the sydney wave climate. *International Journal of Climatology*, 30:1322–1335.

[Harrison and Wallace, 2005] Harrison, G. and Wallace, a. (2005). Climate sensitivity of marine energy. *Renewable Energy*, 30(12):1801–1817.

[Harvey, 1996] Harvey, N. (1996). The significance of coastal processes for management of the river murray estuary. *Australian Geographical Studies*, 34(1):45–57.

[Hasselman et al., 1998] Hasselman, S., Hasselman, K., Janssen, P. A. E. M., Komen, G. T., Bertotti, L., Lionello, P., Guillaume, A., Cardone, V. C., Greewood, J. A., Reistad, M., Zambresky, L., and Ewing, J. A. (1998). The WAM model: a third generation ocean wave prediction model. *Journal of Physical Oceanography*, 18(12):1775–1810.

[Hemer et al., 2007] Hemer, M., Church, J., and Hunter, J. (2007). Waves and climate change on the australian coast. *Journal of Coastal Research*, 50:432–437.

[Hemer et al., 2010] Hemer, M., Church, J., and Hunter, J. (2010). Variability and trends in the directional wave climate of the southern hemisphere wave climate of the southern hemisphere. *International Journal of Climatology*, 30:475–491.

[Hemer et al., 2006] Hemer, M., Church, J., Swail, V., and Wang, X. (2006). Coordinated global wave climate projections. *Atmosphere-Ocean Interactions*, 2:185–218.

[Hemer et al., 2008] Hemer, M., Simmonds, I., and Keay, K. (2008). A classification of wave generation characteristics during large wave events on the southern australian margin. *Continental Shelf Research*, 28:634–652.

[Henfridsson et al., 2007] Henfridsson, U., Neimane, V., Strand, K., Kapper, R., Bernhoff, H., Danielsson, O., Leijon, M., Sundberg, J., Thorburn, K., and Ericsson, E. (2007). Wave energy potential in the Baltic Sea and the Danish part of the North Sea, with reflections on the Skagerrak. *Renewable Energy*, 32(12):2069–2084.

[Hepner and Davis, 2004] Hepner, T. and Davis, R. (2004). Effect of el niño (1997-98) on beaches of the peninsular gulf coast of florida. *Journal of Coastal Research*, 20(3):776–791.

[Holthuijsen, 2007] Holthuijsen, L. (2007). *Waves in Oceanic and Coastal Waters*. Cambridge University Press.

[Horel and Wallace, 1981] Horel, J. and Wallace, J. (1981). Planetary-scale atmospheric phenomena associated with the southern oscillation. *Monthly Weather Review*, 109:813–829.

[Horton et al., 2008] Horton, R., Herweijer, C., Rosenzweig, C., Liu, J., Gornitz, V., and Ruane, A. (2008). Sea level rise projections for current generation CGCMs based on the semi-empirical method. *Geophysical Research Letters*, 35(2):1–5.

[Hou et al., 2003] Hou, B., Frakes, L., Alley, N., and Heithersay, P. (2003). Evolution of beach placer shorelines and heavy mineral deposition in the eastern eucla basin, south australia. *Australian Journal of Earth Sciences*, 50(6):955–965.

[Houston and Dean, 2011] Houston, J. and Dean, R. (2011). Sea-level acceleration based on us tide gauges and extensions of previous global-gauge analyses. *Journal of Coastal Research*, 27(3):2409–417.

[Hsu and Evans, 1989] Hsu, J. and Evans, C. (1989). Parabolic bay shapes and aplications. *Proc., Institution of Civil Engineers*, 87:556 – 570.

[Hulme et al., 2002] Hulme, M., Jenkins, G., Lu, X., Turnpenny, J., Mitchell, T., Jones, R., Lowe, J., Murphy, J., Hassell, D., Boorman, P., McDonald, R., and Hill, S. (2002). Climate change scenarios for the united kingdom. Technical report, UKCIP Scientific Report.

[IDAE, 2010] IDAE (2010). Evaluation of wave energy potential in spain. Technical report, IHCantabria - IDAE (Instituto para la diversificicación y ahorro de la Energía - Spanish Government).

[IEA, 2009] IEA, . (2009). Energy statistics of non-oecd countries. Technical report, International Energy Agency.

[Inatsu and Hoskins, 2004] Inatsu, M. and Hoskins, B. (2004). The zonal asymmetry of the southern hemisphere winter storm track. *Journal of Climate*, 17:488—4892.

[Inatsu et al., 2002] Inatsu, M., Mukougawa, M., and Xie, S. (2002). Tropical and extratropical sst effects on the midlatitude storm track. *Journal of Meteorology Society, Japan*, pages 1069–1076.

[IPCC, 2007a] IPCC (2007a). *Climate Change 2007: Synthesis Report. Contribution of Working Groups I, II and III to the Fourth Assessment Report of the Intergovernmental Panel on Climate Change.* Cambridge University Press, Cambridge, United Kingdom and New York, NY, USA.

[IPCC, 2007b] IPCC (2007b). *Contribution of Working Group II to the Fourth Assessment Report of the Intergovernmental Panel on Climate Change, 2007.* Cambridge University Press, Cambridge, United Kingdom and New York, NY, USA.

[Isaacs and Seymour, 1973] Isaacs, J. and Seymour, R. (1973). The ocean as a power resource. *International Journal of Environmental Studies*, 4(3):201–205.

[Izadparast and Niedzwecki, 2011] Izadparast, A. and Niedzwecki, J. (2011). Estimating the potential of ocean wave power resources. *Ocean Engineering*, 38:177–185.

[Izaguirre et al., 2011] Izaguirre, C., Mendez, F., Menendez, M., and Losada, I. (2011). Global extreme wave height variability based on satellite data. *Geophysical Research Letters*, 38(L10607).

[Jacobson, 2009] Jacobson, M. (2009). Review of solutions to global warming, air pollution, and energy security. *Energy and Environmental Science*, 2.

[Jevrejeva et al., 2010] Jevrejeva, S., Moore, J., and Grinsted, A. (2010). How will sea level respond to changes in natural and anthropogenic forcings by 2100? *Geophysical Research Letters*, 37(7):1–5.

[Kalnay et al., 1996] Kalnay, E., Kanamitsu, M., Cistler, R., Collins, W., Deaven, D., Gandin, L., Iredell, M., Saha, S., White, G., Woolen, J., Zhu, Y., Chelliah, M., Ebisuzaki, W., Higgins, W., Janowiak, J., Mo, K., Ropelewski, C., Wang, J., Leetma, A., Reynolds, R., Jenne, R., and Joseph, D. (1996). The ncep/ncar reanalysis project. *Bulletin of the American Meteorology Society*, 77:437–471.

[Kanamitsu et al., 2002] Kanamitsu, M., Ebisuzaki, W., Woollen, J., Yang, S., Hnilo, J., Fiorino, M., and Potter, G. (2002). Ncep doe amip-ii reanalysis (r-2). *Bulletin of American Meteorology Society*, 83:1631–1643.

[Katz et al., 2002] Katz, R., Parlange, M., and Naveau, P. (2002). Statistics of extremes in hydrology. *Advances in water resources*, 25:1287–1304.

[Katz, 1988] Katz, R. W. (1988). Use of cross correlations in the search for teleconnections. *Journal of Climate*, (8):241–253.

[Knutson et al., 2010] Knutson, T., McBride, J., Chan, J., Emanuel, K., Holland, G., Landsea, C., Held, I., Kossin, J., Srivastava, A., and Sugi, M. (2010). Tropical cyclones and climate change. *Nature*, 3:157–163.

[Knutson et al., 2008] Knutson, T., Sirutis, J., Garner, S., Gabriel, A., and Held, I. (2008). Simulated reduction in atlantic hurricane frequency under twenty-first-century warming conditions. *Nature Geoscience*, 1:359 – 364.

[Komar et al., 2000] Komar, P., Allan, J., Guillermo, M., Marra, J., and Ruggiero, P. (2000). El Niño and La Niña : erosion processes and impacts. *Coastal Engineering*, pages 2414–2427.

[Komen et al., 1994] Komen, G., Cavaleri, L., Domelan, M., Hasselmann, K., Hasselmann, S., and Janssen, P. (1994). *Dynamics and Modeling of Ocean Waves*. Cambridge University Press.

[Konyaev, 1990] Konyaev, K. V. (1990). *Spectral analysis of physical oceanographic data*, volume 81 of *Russian Translation Series*. A.A. Balkema.

[Krogstad and Barstow, 1999] Krogstad, H. and Barstow, S. (1999). Satellite wave measurements for coastal engineering applications. *Coastal Engineering*, 37:283–307.

[Kutzbach, 1967] Kutzbach, J. (1967). Empirical eigenvectors of sea-level pressure, surface temperature and precipitation complexes over north america. *Journal of Applied Meteorology*, 6:791–802.

[Kyte et al., 2006] Kyte, E., Quartly, G., Srokosz, M., and Tsimplis, M. (2006). Interannual variations in precipitation: The effect of the north atlantic and southern oscillations as seen in a satellite precipitation data set and in models. *Journal of Geophysical Research*, 111(D24).

[Lambert and Fyfe, 2006] Lambert, S. and Fyfe, J. (2006). Changes in winter cyclone frequencies and strengths simulated in enhanced greenhouse warming experiments: results from the models participating in the ipcc diagnostic exercise. *Climate Dynamics*, 26:713–728.

[Landsea et al., 2006] Landsea, C., Harper, B., Hoarau, K., and Knaff, J. (2006). Can we detect trends in extreme tropical cyclones? *Science*, 313:452–454.

[Larkin and Harrison, 2001] Larkin, N. and Harrison, D. (2001). ENSO warm (El Niño) and cold (La Niña) event life cycles: ocean surface anomaly patterns, their symmetries, asymmetries, and implications. *Journal of climate*, 15:1118–1140.

[Leckebusch et al., 2006] Leckebusch, G., Koffi, B., Ulbrich, U., Pinto, J., Spangehl, T., and Zacharias, S. (2006). Analysis of frequency and intensity of european winter storm events from a multi-model perspective, at synoptic and reginonal scales. *Climate Research*, 31:59–74.

[Leckebusch and Ulbrich, 2004] Leckebusch, G. and Ulbrich, U. (2004). On the relationship between cyclones and extreme windstorm events over europe under climate change. *Global and Planetary Change*, 44:181–193.

[Lenee-Bluhm et al., 2011] Lenee-Bluhm, P., Paasch, R., and Özkan-Haller, H. (2011). Characterizing the wave energy resource of the us pacific northwest. *Renewable Energy*, 36:2106–2119.

[Lewis et al., 2011] Lewis, A., Estefen, S., Huckerby, W., Musial, W., Pontes, T., and Torres-Martinez, J. (2011). *Special Report on Renewable Energy Sources and Climate Change Mitigation*, chapter Ocean energy. Cambridge University Press, United Kingdom and New York.

[Lionello et al., 2002] Lionello, P., Dalan, F., and Elvini, E. (2002). Cyclones in the mediterranean region: the present and the doubled co2 climate scenarios. *Climate Research*, 22:147–159.

[Lionello and Sanna, 2005] Lionello, P. and Sanna, A. (2005). Mediterranean wave climate variability and its link with nao and indian monsoon. *Climate Dynamics*, 25:611–623.

[Loeptien et al., 2008] Loeptien, U., Zolina, O., Gulev, S., Latif, M., and Soloviov, V. (2008). Cyclone life cycle characteristics over the northern hemisphere in coupled GCMs. *Climate Dynamics*, 315:507–532.

[Longuet-Higgins, 1970] Longuet-Higgins, M. (1970). Longshore currents generated by obliquely incident sea waves. *Journal of Geophysical Research*, 75(33):6778–6789.

[Lorenz, 1956] Lorenz, E. (1956). Empirical orthogonal functions and statistical weather prediction. technical report, statistical forecast project report 1. Technical Report 49, Department of Meteorology, MIT.

[Losada et al., 2012] Losada, I., Reguero, B., Mendez, F., Castanedo, S., Abascal, A., and Minguez, R. (2012). Long-term changes in sea-level components in latin america and the caribbean. *submitted to Global and Planetary Change*.

[Luceño et al., 2006] Luceño, A., Menendez, M., and Mendez, F. (2006). The effect of temporal dependence on the estimation of the frequency of extreme ocean climate events. *Proceedings of the Royal Society*, 462:1683–1697.

[Mackay et al., 2010] Mackay, E., Bahaj, A., and Challenor, P. (2010). Uncertainty in wave energy resource assessment. part 2. variability and predictability. *Renewable Energy*, 35:1809–1819.

[Magrin et al., 2007] Magrin, G., G.C., G., Cruz, C., Gimenez, J., Moreno, A., Nagy, G., Nobre, C., and Villamizar, A. (2007). *Climate Change 2007: Impacts, Adaptation and Vulnerability. Contribution of Working Group II to the Fourth Assessment Report of the Intergovernmental Panel on Climate Change*, chapter Latin America., pages 581–615. Cambridge Univ. Press.

[Mann and Emanuel, 2006] Mann, M. and Emanuel, K. (2006). Atlantic hurricane trends linked to climate change. *EOS, Transactions, American Geophysical Union*, 87(24):233–244.

[Mantua et al., 1997] Mantua, N., Hare, S., Zhang, Y., Wallace, J., and Francis, C. (1997). A pacific interdecadal climate oscillation with impacts on salmon production. *Bulletin of the American Meteorological Society*, 78:1069–1079.

[Marcos et al., 2009] Marcos, M., Tsimplis, M., and Shaw, A. (2009). Sea level extremes in the southern europe. *Journal of Geophysical Research*, 114(C01007).

[Mardia, 1972] Mardia, K. (1972). *Statistics of Directional Data*. Academic Press.

[Mardia and Jupp, 2000] Mardia, K. and Jupp, P. (2000). *Directional Statistics*. Wiley UK.

[Marshall, 2003] Marshall, G. (2003). Trends in the southern annular mode from observations and reanalyses. *Journal of Climate*, 16:4134–4143.

[Martine, 2009] Martine, G. (2009). *Population dynamics and policies in the context of global climate change*, pages 9–30. UNFPA-IIED.

[Masselink and Pattiaratchi, 2001] Masselink, G. and Pattiaratchi, C. (2001). Seasonal changes in beach morphology along the sheltered coastline of perth, western australia. *Marine geology*, 172:243–263.

[McCabe et al., 2001] McCabe, G., Clark, M., and Serreze, M. (2001). Trends in northern hemisphere surface cyclone frequency and intensity. *Journal of Climate*, 14:2763–2768.

[McCarthy et al., 2001] McCarthy, J., Canziani, O., Leary, N., Dokken, D., and White, K. E. (2001). *Climate Change 2001: Impacts, Adaptation, and Vulnerability: Contribution of Working Group II to the Third Assessment Report of the Intergovernmental Panel on Climate Change*. Cambridge University Press, Cambridge, United Kingdom and New York, NY, USA.

[McGranahan and Anderson, 2007] McGranahan, Gordon, D. B. and Anderson, B. (2007). The rising tide: assessing the risks of climate change and human settlements in low-elevation coastal zones. *Environment and Urbanization*, 19(1):17–37.

[Meehl et al., 2007] Meehl, G., Stocker, T., Collins, W., Friedlingstein, P., Gaye, A., Gregory, J., Kitoh, A., Knutti, R., Murphy, J., Noda, A., Raper, S., Watterson, I., Weaver, A., and Zhao, Z.-C. (2007). *Global climate projections*, chapter Global climate projections, pages 747–846. Cambridge Univ. Press, New York.

[Mendelsohn et al., 2012] Mendelsohn, R., Emanuel, K., Chonobayashi, S., and Bakkensen, L. (2012). The impact of climate change on global tropical cyclone damage. *Nature Climate Change*, (15):1–5.

[Méndez et al., 2007] Méndez, F., Menéndez, M., Luceño, A., and Losada, I. (2007). Estimation of the long-term variability of extreme significant wave height using a time-dependent peak over threshold (pot) model. *Journal of Geophysical Research*, 111(C09024).

[Menéndez et al., 2009] Menéndez, M., Méndez, F., Izaguirre, C., Luceño, A., and Losada, I. (2009). The influence of seasonality on estimating return values of significant wave height. *Coastal Engineering*, 56:211–219.

[Menendez et al., 2008] Menendez, M., Mendez, F., Losada, I., and Graham, N. (2008). Variability of extreme wave heights in the northeast pacific ocean based on buoy measurements. *Geophysical Research Letters*, 35(L22607).

[Merrifield, 2009] Merrifield, M. A., S. T. M. G. T. M. (2009). An anomalous recent acceleration of global sea level rise. *Journal of Climate*, 22:5772–5781.

[Michael, 2007] Michael, J. (2007). Episodic flooding and the cost of sea-level rise. *Ecological Economics*, 63(1):149–159.

[Miller et al., 2006] Miller, R., Schmidt, G., and Shindell, D. (2006). Forced variations of annular modes in the 20th century ipcc ar4 simulations. *Journal of Geophysical Research*, 111(D18101).

[Mínguez, 2010] Mínguez, R., M. F. I. C. M. M. L. I. (2010). Pseudo-optimal parameter selection of non-stationary generalized extreme value models for environmental variables. *Environmental Modelling & Software*, 25:1592–1607.

[Mínguez et al., 2011] Mínguez, R., Espejo, A., Tomás, A., Méndez, F. J., and Losada, I. J. (2011). Directional calibration of wave reanalysis databases using instrumental data. *Journal of Atmospheric and Oceanic Technology.* . doi: 10.1175/JTECH-D-11-00008.1.

[Mínguez et al., 2012] Mínguez, R., Reguero, B. G., Luceño, A., and Méndez, F. J. (2012). Regression models for outlier identification (hurricanes and typhoons) in wave hindcast databases. *Journal of Atmospheric and Oceanic Technology.*

[Mollison, 1986] Mollison, D. (1986). *Hydrodynamics of ocean wave-energy utilization*, chapter Wave Climate and the Wave Power Resource, pages 133–156. Springer.

[Mollison et al., 1976] Mollison, D., Buneman, O., and Salter, S. (1976). Wave power availability in the ne atlantic. *Nature*, 263:223–226.

[Mori et al., 2010] Mori, N., Yasuda, T., Mase, H., Tom, T., and Oku, Y. (2010). Projection of extreme wave climate under global warming. *Hydrological Research Letters*, 4:14–19.

[Mork et al., 2010] Mork, G., Barstow, S., Kabuth, A., and Pontes, T. (2010). Assessing the global wave energy potential. In ASME, editor, *Proceedings of OMAE2010*, number 20473. 29th International Conference on Ocean, Offshore Mechanics and Artic Engineering.

[Morton et al., 1997] Morton, I. D., Bowers, J., and Mould, G. (1997). Estimating return period wave heights and wind speeds using a seasonal point process model. *Coastal Engineering*, 31:305–326.

[Mukhopadhyay, 2000] Mukhopadhyay, N. (2000). *Probability and Statistical Inference.* Marcel Dekker, New York.

[Myrhaug et al., 2009a] Myrhaug, D., Leira, B., and Holm, H. (2009a). Wave power statistics for individual waves. *Applied Ocean Research*, 31(4):246–250.

[Myrhaug et al., 2009b] Myrhaug, D., Leira, B., and Holm, H. (2009b). Wave power statistics for sea-states. In *Proceedings of the 28th International Conference on Ocean, Offshore and Arctic Engineering, Honolulu, USA*. OMAE09-79132.

[Nicholls, 1998] Nicholls, R. (1998). Assessing erosion of sandy beaches due to sea-level rise. *Engineering Geology Special Publications*, 15:71–76.

[Nicholls, 2004] Nicholls, R. (2004). Coastal flooding and wetland loss in the 21st century: changes under the sres climate and socio-economic scenarios. *Global Environmental Change*, 14(1):69–86.

[Nicholls, 2011] Nicholls, R. (2011). Planning for the impacts of sea level rise. *Oceanography*, 24(2):144–157.

[Nicholls and Cazenave, 2010] Nicholls, R. and Cazenave, A. (2010). Sea level rise and its impact on coastal zones. *Science*, (328):1517–1520.

[Nicholls et al., 2007] Nicholls, R., Wong, P., Burkett, V., Codignotto, J., Hay, J., McLean, R., Ragoonaden, S., and Woodroffe, C. (2007). *Climate Change 2007: Impacts, Adaptation and Vulnerability. Contribution ofWorking Group II to the Fourth Assessment Report of the Intergovernmental Panel on Climate Change*, chapter 6 Coastal systems and low-lying areas, pages 315–356. Cambridge University Press.

[NOAA, 2006] NOAA, N. G. D. C. (2006). Etopo2v2 global gridded 2-minute database.

[Obukhov, 1947] Obukhov, A. (1947). Statistically homogeneous fields on a sphere. *Uspekhi Matematicheskikh Nauk*, 22:196–198.

[Obukhov, 1960] Obukhov, A. (1960). The statistically orthogonal expansion of empirical functions. bulletin. *Bulletin of the Academy of Sciences of the USSR. Geophysics Series (English Transl.) 1:*, 1:288–291.

[Onogi et al., 2007] Onogi, K., Tsutsui, J., Koide, H., Sakamoto, M., Kobayashi, S., Hatsushika, H., Matsumoto, T., Yamazaki, N., Kamahori, H., Takahashi, K., Kadokura, S., Wada, K., Kato, K., Oyama, R., Ose, T., Mannoji, N., and Taira, N. (2007). The jra-25 reanalysis. *J. Meteor. Soc. Japan*, 85:369–432.

[Osborn, 2004] Osborn, T. (2004). Simulating the winter north atlantic oscillation: the roles of internal variability and greenhouse gas forcing. *Climate Dynamics*, 22(6–7):605–623.

[Panchang and Li, 2006] Panchang, V. and Li, D. (2006). Large waves in the gulf of mexico caused by hurricane ivan. *Bulletin of American Meteorology Society*, pages 481–489.

[Penland and Matrosova, 1998] Penland, C. and Matrosova, L. (1998). Prediction of tropical atlantic sea surface temperatures using linear inverse modeling. *Journal of Climate*, 110:483–496.

[Pfeffer et al., 2008] Pfeffer, W. T., Harper, J. T., and O'Neel, S. (2008). Kinematic constraints on glacier contributions to 21st-century sea-level rise. *Science (New York, N.Y.)*, 321(5894):1340–3.

[Philander, 1982] Philander, S. (1982). *El Niño, La Niña and the Southern Oscillation.* Academic Press.

[Pilar et al., 2008] Pilar, P., Guedes Soares, S., and Carretero, J. (2008). 44-year wave hindcast for the north east atlantic european coast. *Coastal Engineering*, 55(11):861–871.

[Pinto et al., 2007] Pinto, J., Ulbrich, U., Leckebusch, G., Spangeh, T., Reyers, M., and Zacharias, S. (2007). Changes in storm track and cyclone activity in three sres ensemble experiments with the echam5/mpi-om gcm. *Climate Dynamics*, 29:195–210.

[Pontes et al., 2002] Pontes, M., Cavaleri, L., and Mollison, D. (2002). Ocean waves: energy resource assessment. *Marine Technology Society Journal*, 36:42–51.

[Pontes et al., 2005] Pontes, M., R., A., and H., O. P. (2005). A nearshore wave energy atlas for portugal. *Journal of Offshore Mechanics and Arctic Engineering*, 127:249–255.

[Power et al., 1999] Power, S., Casey, T., Folland, C., Colman, A., and Mehta, V. (1999). Interdecadal modulation of the impact of enso on australia. *Clymate Dynamics*, 15:319–324.

[Rahmstorf, 2007] Rahmstorf, S. (2007). A semi-empirical approach to projecting future sea-level rise. *Science (New York, N.Y.)*, 315(5810):368–70.

[Rahmstorf and Vermeer, 2011] Rahmstorf, S. and Vermeer, M. (2011). Discussion of: Houston, j.r., and dean, r.g., 2011. sea-level acceleration based on u.s. tide-gauges and extensions of previous global-gauge analyses. journal of coastal research, 27(3), 409-417. *Journal of Coastal Research*, 274(3):784–787.

[Ranasinghe et al., 2004] Ranasinghe, R., McLoughlin, R., Short, A., and Symonds, G. (2004). The southern oscillation index, wave climate, and beach rotation. *Marine Geology*, 204:273–287.

[Rasmusson and Carpenter, 1982] Rasmusson, E. and Carpenter, T. (1982). Variations in tropical sea surface temperature and surface winds fields associated with the southern oscillation/el niño. *Monthly Weather Review*, 110:354–384.

[Reguero et al., 2011] Reguero, B., Abascal, A., Menéndez, M., Castanedo, S., Méndez, F., Medina, R., and Losada, I. (2011). Gow y gos: Reanálisis de oleaje y marea meteorológica en la costa española. In *Libro de resúmenes de las XI Jornadas de costas y puertos, Las Palmas de Gran Canaria.*

[Reguero et al., 2012a] Reguero, B., Méndez, F., and Losada, I. (2012a). Variability of multivariate wave climate in latin america and the caribbean. *Global and Planetary Change (in press).*

[Reguero et al., 2012b] Reguero, B., Menendez, M., Mendez, F., Minguez, R., and Losada, I. (2012b). A global ocean wave (gow) calibrated reanalysis from 1948 onwards. *Coastal Engineering*, (65):38–55.

[Rice, 1994] Rice, J. (1994). *Mathematical Statistics and Data Analysis.* Duxbury Pr.

[Rienecker et al., 2011] Rienecker, M., Suarez, M., Gelaro, R., Todling, R., Bacmeister, J., Liu, E., Bosilovich, M., Schubert, S., Takacs, L., Kim, G.-K., Bloom, S., Chen, J., Collins, D. amd Conaty, A., Silva, A., and Coauthors (2011). Merra - nasa's modern-era retrospective analysis for research and applications. *Journal of Climate*, 24:3624–3648.

[Rignott, 2011] Rignott, E., V. I. v. d. B. M. M. A. L. J. (2011). Acceleration of the contribution of the greenland and antarctic ice sheets to sea level rise. *Geophysical Research Letters*, page L05503.

[Rodgers and Nicewander, 1988] Rodgers, J. and Nicewander, W. (1988). Thirteen ways to look at the correlation coefficient. *The American Statistician*, 42(1):59–66.

[Ryan et al., 1999] Ryan, H., Gibbons, H., Hendley, J., and Stauffer, P. (1999). El Niño Sea-Level rise wreaks havoc in California's San Francisco bay Region. *U.S. Geological Survey - Fact Sheet 175-99.*

[Saha and Coauthors, 2010] Saha, S. and Coauthors (2010). The ncep climate forecast system reanalysis. *American Meteorology Society Bulletin*, 91:1015–1057.

[Saji et al., 1999] Saji, N., Goswami, B., Vinayachandran, P., and Yamagata, T. (1999). A dipole mode in the tropical indian ocean. *Nature*, 401:360–363.

[Sarachik and Cane, 2010] Sarachik, E. and Cane, M. (2010). *The El Niño-Southern Oscillation Phenomenon.* Cambridge University Pres.

[Satterthwaite et al., 2009] Satterthwaite, D., Huq, S., Reid, H., Pelling, M., and Lankao, P. (2009). Adapting to climate change in urban areas; the possibilities and constraints in low and middle-income nations. Human Settlements Discussion Paper Series, Climate Change and Cities 1, IIED.

[Schmidt et al., 2009] Schmidt, R., Diba, K., Leibold, C., Schmitz, D., Buzsaki, G., and Kempter, R. (2009). Single-trial phase precession in the hippocampus. *The Journal of Neuroscience*, 21:13232–13241.

[Schneggenburger et al., 1997] Schneggenburger, C., Günther, H., and Rosenthal, W. (1997). Shallow water wave modelling with nonlinear dissipation. *German Journal of Hydrography*, 49(2/3):431–444.

[Schneiderbauer and Ehrlich, 2004] Schneiderbauer, S. and Ehrlich, D. (2004). *Risk, hazard and people´s vulnerability to natural hazards: A review of definitions, concepts and data*. European Comission - Joint Research Center (EC-JCR).

[Schwing, 2011] Schwing, F. (2011). Climate change, teleconnections patterns, and regional processes forcing marine populations in the pacific. *Journal of Marine Systems*, 79:245–257.

[Seager et al., 2003] Seager, R., Harnik, N., Kushnir, Y., Robinson, W., and Miller, J. (2003). Mechanisms of hemispherically symmetric climate variability. *Journal of Climate*, 16:2960–2978.

[Seager et al., 2010] Seager, R., Naika, N., Ting, M., Cane, M., Harnikb, N., and Kushnira, Y. (2010). Adjustment of the atmospheric circulation to tropical pacific sst anomalies: Variability of transient eddy propagation in the pacific–north america sector. *Quart. J. Roy. Meteor. Soc.*

[Semedo et al., 2011a] Semedo, A., Beherens, A., Bengtsson, L., Günther, H., Sterl, A., and Weisse, R. (2011a). *Impact of a warmer climate on the global wave field.* 12th International Workshop on Wave Hindcasting and Forecasting And 3rd Coastal Hazard Symposium.

[Semedo et al., 2011b] Semedo, A., Suselj, K., Rutgersson, A., and Sterl, A. (2011b). A global view on the wind sea and swell climate and variability from era-40. *Journal of Climate*, 24:1461–1479.

[Shchepetkin and MacWilliams, 2003] Shchepetkin, A. and MacWilliams, J. (2003). A method for computing horizontal pressure-gradient force in an oceanic model with a nonaligned vertical coordinate. *Journal of Geophysical Research*, 108 (C3):3090.

[Short et al., 1995a] Short, A., Cowell, P., Cadee, M., Hall, W., and Van Dijke, B. (1995a). Beach rotation and possible relation to the southern oscillation. pages 329–334, National Tidal Facility, Adelaide.

[Short et al., 1995b] Short, A., Trembanis, A., and Turner, I. (1995b). Beach oscillation, rotation and the southern oscillation, narrabean beach, australia. In ASCE, editor, *Proceedings of the 27th International Coastal Engineering Conference*, pages 2439–2452, Sydney.

[Smith, 2001] Smith, R. (2001). Environmental statistics. Technical report, Department of Statistics. University of North Carolina, Chapel Hill.

[Smolka, 2008] Smolka, M. (2008). *The new global frontier: urbanization, poverty and environment in the 21st century.*, chapter Informality and Poverty in Latin American Urban Policies, pages 99–114. Earthscan.

[Solomon and Forbes, 1999] Solomon, S. and Forbes, D. (1999). Coastal hazards and associated management issues on south pacific islands. *Ocean and Coastal Management*, 42:523–554.

[Solomon et al., 2007] Solomon, S., Qin, D., Manning, M., Chen, Z., Marquis, M., Averyt, K., Tignor, M., and Miller, H. e. (2007). *Climate Change 2007: the physical science basis. Contribution of Working Group I to the Fourth Assessment Report of the Intergovernmental Panel on Climate Change.* Cambridge University Press, New York.

[Sterl, 2004] Sterl, A. (2004). On the (in)homogeneity of reanalysis products. *Journal of Climate*, 17:3866–3873.

[Sterl and Caires, 2005] Sterl, A. and Caires, S. (2005). Climatology, variability and extrema of ocean waves: The web-based knmi/era-40 wave atlas. *International Journal of Climatology*, 25(On the (in)homogeneity of reanalysis products):963–997.

[Sterl et al., 1998] Sterl, A., Komen, G., and Cotton, P. (1998). Fifteen years of global wave hindcasts using winds from the european centre for medium-range weather forecast reanalysis: Validating the reanalyzed winds and assessing the wave climate. *Journal of Geophysical Research*, 103(C3):5477–5492.

[Stive, 2004] Stive, M. (2004). How important is global warming for coastal erosion? *Climatic Change*, 64(1):27–39.

[Swail and Cox, 2000] Swail, V. and Cox, A. (2000). On the use of ncep/ncar reanalysis surface marine wind fields for a long-term north atlantic wave hindcast. *Journal of Atmospheric and Oceanic Technology*, 17:532–545.

[Terray et al., 2004] Terray, L., Demory, M.-E., Déqué, M., de Coetlogon, G., and Maisonnave, E. (2004). Simulation of late-21st century changes in wintertime atmospheric circulation over europe due to anthropogenic causes. *Journal of Climate*, 17:4630–4635.

[Teske, 2010] Teske, S. (2010). *Energy Revolution.* Greenpeace International European Renewable Energy Council (EREC).

[Thorpe, 1992] Thorpe, T. (1992). A review of wave energy. Technical Report R-72. Vols 1 and 2, ETSU for the UK Government.

[Thorpe, 1999] Thorpe, T. (1999). A brief review of wave energy. Technical Report R-102. Vols 1 and 2, ETSU for the UK Government.

[Tolman, 1989] Tolman, H. (1989). The numerical model wavewatch: a third generation model for the hindcasting of wind waves on tides in shelf seas. Communications on Hydraulic and Geotechnical Engineering 89-2, Delft Univ. of Techn.

[Tolman, 1992] Tolman, H. (1992). Effects of numerics on the physics in a third-generation wind-wave model. *Journal of Physical Oceanography*, 22:1095–1111.

[Tolman, 2002a] Tolman, H. (2002a). User manual and system documentation of wavewatch-iii version 2.22. *NOAA/NWS/NCEP Technical Note.*

[Tolman, 2002b] Tolman, H. (2002b). Validation of wavewatch iii version 1.15 for a global domain. *NOAA/NWS/NCEP/OMB Technical Note*, (213):33.

[Tolman, 2009] Tolman, H. (2009). User manual and system documentation of wavewatch-iii version 3.14. *NOAA/NWS/NCEP Technical Note*, (276):194.

[Tolman et al., 2002] Tolman, H., Balasubramaniyan, B., Burroughs, L., Chalikov, D., Chao, Y., Chen, H., and Gerald, V. (2002). Development and implementation of wind generated ocean surface wave models at ncep. *Weather and Forecasting*, 17:311–333.

[Tolman and Chalikov, 1996] Tolman, H. and Chalikov, D. (1996). Source terms in a third-generation wind wave model. *Journal of Physical Oceanography*, 26:2497–2518.

[Tomás et al., 2008] Tomás, A., Méndez, F. J., and Losada, I. J. (2008). A method for spatial calibration of wave hindcast data bases. *Continental Shelf Research*, 28:391–398 ISSN 0278–4343.

[Tompkins et al., 2005] Tompkins, E., Nicholson-Cole, S., Hurlston, L., Boyd, E., Hodge, G., Clarke, J., Gray, G., Trotz, N., and Varlack, L. (2005). *Surviving Climate Change in Small Islands - A Guide Book*. Tyndall Centre for Climate Change Research.

[Trenberth, 1991] Trenberth, K. (1991). Storm tracks in the southern hemisphere. *Journal of Atmospheric Sciences*, 48(19):2159–2178.

[Tsimplis et al., 2005] Tsimplis, M., Woolf, D., Osborn, T., Wakelin, S., Woodworth, P., Wolf, J., Flather, R., Blackman, D., Shaw, A., Pert, F., Challenor, P., and Yan, Z. (2005). Towards a vulnerability assessment of the uk and northern european coasts: the role of regional climate variability. *Philosophical Transactions of the Royal Society: Mathematical, Physical & Engineering Sciences*, 363(1831):1329–1358.

[Ulbrich et al., 2009] Ulbrich, U., G.C., L., and J.G., P. (2009). Extra-tropical cyclones in the present and future climate: a review. *Theorical and Applied Climatology*, 96:117–131.

[Uppala et al., 2005] Uppala, S., Kallberg, P., Simmons, A., Andrae, U., da Costa, Bechtold, V., Fiorino, M., Gibson, J., Haseler, J., Hernández, A., and Kelly, G. (2005). The era-40 reanalysis. *Quarterly Journal of the Royal Meteorological Society*, 131:2961–3012.

[USACE, 2002] USACE (2002). *Coastal Engineering Manual*. U.S. Army Corps of Engineers, Washington, D.C., engineer manual 1110-2-1100 (6 vol.) edition.

[USACE, 2011a] USACE (2011a). *Coastal storm risk management*. Number IWR Report 2011-R-09. US Army Corps of Engineers - Institute for Water Resources.

[USACE, 2011b] USACE (2011b). *Sea-level change considerations for civil works programs*. Number Circular No. 1165-2-212. US Army of Engineers.

[USC, 1996] USC (1996). Risk-based analysis for flood damage reduction studies. Manual 1110-2-1619, US Army Corps of Engineers - Department of the army.

[Vecchi et al., 2008] Vecchi, G., Swanson, K., and Soden, B. (2008). Whither hurricane activity? *Science*, 322:687–689.

[Vermeer and Rahmstorf, 2009] Vermeer, M. and Rahmstorf, S. (2009). Global sea level linked to global temperature. *Proceedings of the National Academy of Sciences of the United States of America (PNAS)*, 106(51):21527–32.

[Vincent and Soille, 1991] Vincent, L. and Soille, P. (1991). Watersheds in digital spaces: An efficient algorithm based on immersion simulations. *IEEE Transactions of Pattern Analysis and Machine Intelligence*, 13:583–598.

[Wallace and Gutzler, 1981] Wallace, J. and Gutzler, D. (1981). Teleconections in the geopotential height field during the northern hemisphere winter. *Monthly Weather Review*, 109:784–812.

[Walsh et al., 2012] Walsh, K., McInnes, K., and McBride, J. (2012). The impact of global warming on the tropical Pacific Ocean and El Niño. *Global and Planetary Change*, 80-81:149–164.

[Wang et al., 2009] Wang, C., Song, Z., Qiao, F., and Dong, S. (2009). What signals are removed and retained by using an anomaly field in climatic research? *International Journal of Climatology*, 2009:7.

[Wang and Swail, 2001] Wang, X. and Swail, V. (2001). Changes of extreme wave heights in northern hemisphere oceans and related atmospheric circulation regimes. *Journal of Climate*, 14(10):2204–2221.

[Wang and Swail, 2002] Wang, X. and Swail, V. (2002). Trends of atlantic wave extremes as simulated in a 40-yr wave hindcast using kinematically reanalyzed wind fields. *Journal of Climate*, 15:1020–2035.

[Wang et al., 2006] Wang, X., Swail, V., and Zwiers, F. (2006). Climatology and changes of extra-tropical cyclone activity: comparison of era-40 with ncep/ncar reanalysis for 1958-2001. *Journal of Climate*, 19:3145–3166.

[Wang et al., 2008] Wang, X., Swail, V., Zwiers, F., Zhang, X., and Feng, Y. (2008). Trends and variability of storminess in the northeast atlantic region, 1874–2007. *Climate Dynamics*, 33:1179–1195.

[Wang et al., 2011] Wang, X., Wan, H., Zwiers, F., Swail, V., Compo, G., Allan, R., Vose, R., Jourdain, S., and Yin, X. (2011). Trends and low-frequency variability of storminess over western europe, 1878-2007. *Climate Dynamics*.

[Weatherhead et al., 1998] Weatherhead, E., Reinsel, C., Tiao, G., Meng, X., Choi, D., Cheang, W., Keller, T., DeLuisi, J., Wuebbles, D., Kerr, J., Miller, A., Oltmans, S., and Frederick, J. (1998). Factors affecting the detection of trends: Statistical considerations and applications to environmental data. *Journal of Geophysical Research*, 103(D14):17149–17161.

[Webster et al., 2005] Webster, P., Holland, G. J., Curry, J., and Chang, H. (2005). Changes in tropical cyclone number, duration, and intensity, in warming environment. *Science*, 309:1844–1846.

[WEC, 2010] WEC (2010). 2010 survey of energy resources. Technical report, World Energy Council.

[Weisse and Von Storch, 2010] Weisse, R. and Von Storch, H. (2010). *Marine Climate and Climate Change - Storms, Wind Waves and Storm Surges.* Springer, ISBN 978-3-540-25316-7 Springer-Verlag Berlin Heidelber New York.

[West et al., 2001] West, J., Small, M., and Dowlatabadi, H. (2001). Storms, investor decisions, and the economic impacts of sea level rise. *Climatic Change*, 48:317–342.

[Wilson and Beyene, 2007] Wilson, J. and Beyene, A. (2007). California wave energy resource evaluation. *Journal of Coastal Research*, 23(3):679–90.

[Wolf and Woolf, 2006] Wolf, J. and Woolf, D. (2006). Waves and climate change in the north-east atlantic. *Geophysical Research Letters*, 33:L06604.

[Woodworth et al., 2009] Woodworth, P., White, N., Jevrejeva, S., Holgate, S., Church, J., and Gehrels, W. (2009). Evidence for the accelerations of sea level on multi-decade and century timescales. *International Journal of Climatology*, 29:777–789.

[Woodworth and Blackman, 2004] Woodworth, P. L. and Blackman, D. L. (2004). Evidence for systematic changes in extreme high waters since the mid-1970s. *Journal of Climate*, 172:1190–1197.

[Woolf and Challenor, 2002] Woolf, D. and Challenor, P. G. (2002). Variability and predictability of the north atlantic wave climate. *Journal of Geophysical Research*, 107(C10):3145.

[Woth, 2005] Woth, K. (2005). North sea storm surge statistics based on projections in a warmer climate: How important are the driving gcm and the chosen emission scenario? *Geophysical Research Letters*, 32(22):L22708.

[Yin, 2005] Yin, J. (2005). A consistent poleward shift of the storm tracks in simulations of the 21st century climate. *Geophysical Research Letters*, 32(L18701).

[Yohe et al., 1999] Yohe, G., Neumann, J., and Marshall, P. (1999). *The economic damage induced by sea level rise in the United States.* The Impact of Climate Change on the United States Economy. Cambridge University Press.

[Young, 1999] Young, I. (1999). Seasonal variability of the global ocean wind and wave climate. *International Journal of Climatology*, 19:931–950.

[Young et al., 2011] Young, I., Zieger, S., and Babanin, A. (2011). Global trends in wind speed and wave height. *Science*, 332(6028):451–455.

[Zhang et al., 2004] Zhang, K., Douglas, B., and Leatherman, S. (2004). Global warming and coastal erosion. *Climatic Change*, 64(1/2):41–58.

[Zhang et al., 2009] Zhang, K., Douglas, B., and Leatherman, S. (2009). Twentieth-century storm activity along the u.s. east coast. *Journal of Climate*, 13:1748–1761.